All ETDs from UAB

UAB Theses & Dissertations

2017

Autophagy in mitochondrial quality control and proteotoxicity in neurons

Matthew Redmann
University of Alabama at Birmingham

Follow this and additional works at: https://digitalcommons.library.uab.edu/etd-collection

AUTOPHAGY IN MITOCHONDRIAL QUALITY CONTROL AND
PROTEOTOXICTY IN NEURONS

by

MATTHEW REDMANN

JIANHUA ZHANG, COMMITTEE CHAIR
JAMES COLLAWN
ANITA HJELMELAND
ADAM WENDE
TALENE YACOUBIAN

A DISSERTATION

Submitted to the graduate faculty of The University of Alabama at Birmingham,
in partial fulfillment for the requirements for the degree of
Doctor of Philosophy

BIRMINGHAM, ALABAMA

2017

AUTOPHAGY IN MITOCHONDRIAL QUALITY CONTROL AND
PROTEOTOXICTY IN NEURONS

MATTHEW REDMANN

CELL, MOLECULAR, AND DEVELOPMENTAL BIOLOGY

ABSTRACT

Parkinson's disease (PD) is the 2nd most common neurodegenerative disorder
with aging as a significant risk factor. Sharing with aging brains, postmortem PD brains
exhibit cellular deficits including autophagic dysfunction, mitochondrial dysfunction, and
intracellular protein aggregates of alpha-synuclein. This dissertation will focus on the
interplay between these key disease features. To that end, we coupled primary cortical
neuronal cultures from either rats or mice with Seahorse extracellular flux, metabolomics
and biochemical techniques.

Autophagy is an important cell recycling program responsible for the clearance of
damaged proteins and organelles. Bafilomycin A1 and chloroquine are compounds that
inhibit autophagy by targeting the lysosome. Since it is now clear that mitochondrial
quality control is dependent on autophagy, we determined whether these compounds
could modify cellular bioenergetics. As expected, both bafilomycin and chloroquine
significantly increased the autophagosome marker LC3-II. Under these conditions, we
found that they significantly inhibited parameters of mitochondrial function and increased
mtDNA damage without inducing cell death. Associated with these mitochondrial
deficits, we also observed significant alterations in TCA cycle intermediates, indicating a
significant role of autophagy in cellular metabolic programs.

Beyond the importance of autophagy for mitochondrial quality, we further
investigated the interplay between protein aggregation and autophagy in a PD model.

Exposure to aSyn pre-formed fibrils (PFFs) has been shown to induce aggregation of endogenous aSyn resulting in cell death that is exacerbated by autophagy induction through either starvation or inhibition of mTOR by rapamycin. Since mTOR inhibition may also inhibit protein synthesis, and starvation by itself can be detrimental to neuronal survival, we investigated the effects of autophagy induction by a starvation and mTOR-independent method, using trehalose. We observed that on exposure to PFFs, there was increased abundance of pS129-aSyn aggregates and cell death. Trehalose alone increased LC3-II levels, consistent with increased autophagosome levels, that remained elevated with PFF exposure. Interestingly, trehalose alone increased cell viability over a 14-day time course and was also able to restore cell viability to control levels, but PFFs still exhibited toxic effects on the cells.

Together, these data provide essential information regarding the interplay of autophagy, mitochondrial function and protein aggregation in PD.

DEDICATION

Let us never forget that intellectual freedom and curiosity, beyond those imbued by the ivory walls of academia, are paramount to a healthy society and a healthy mind. And while this work represents the tiniest of bricks in the wall of human knowledge, I would like it to be a dedication to those in human history whom have not had the luxury as I, to investigate the truth of nature and marvel at its grandness. To those whom have had to belay the truth under oppression by religion, government, or ideology.

ACKNOWLEDGEMENTS

The road to the completion of this document, a dissertation, has been long and fraught with challenges and obstacles that have, at times, felt entirely unsurmountable. I have put more effort into achieving this goal than any other task to date, but as the clichéd but ever relevant phrase scrawled down in the 17th century by the English poet John Donne denotes, "No man is an island." And in that vein, I have many to thank for making these unsurmountable aims realized.

To Jess, my amazing fiancé and very soon to be wife, who is undoubtedly happy that I proposed before writing this so she could have her pronoun "upgraded" from girlfriend. You have steadfastly supported me throughout these tumultuous five years, helped me study, spent all night in lab with me to get data, and encouraged me when all I wanted to do was quit. It is fair to say, I would not be writing this if it were not for you and I look forward to spending the rest of our lives together.

To my brother, we have shared many memories and many milestones in life. You have always been a role model and inspired me to do the hard thing. And have reminded me that to grow and to accomplish something new, you must do things you've never done. I will always be thankful that I have you in my corner.

To my mother, whom has, over nearly the last 30 years as of this writing, drove me to a level of insanity only rivaled by Creutzfeldt–Jakob disease, but has always had my best interest at heart. I will always be grateful for the sacrifices you made.

To my undergraduate research mentor, Dr. Kris Curran, I have never properly thanked you for taking a chance on a young 22-year-old college student who perhaps spent a little too much time in places other than the library. But I have always appreciated that you fueled my love of science, taught me to do the work and believed in me when I didn't know how to myself.

To my mentor Jianhua, you have always encouraged me to try new experiments, attend conferences, network and expand my scientific horizons. And while we have disagreed from time to time over the years, you have nonetheless allowed me to make forays into the various aspects of science and business that aren't always available to graduate students and I am thankful for that. And to Victor who has always had an open door to discuss my data and who has pushed and pulled me into doing the experiments to complete the scientific story; and no doubt to his lab as well, which is comprised of fantastic people and scientists.

To my committee members Drs. Jim Collawn, Anita Hjelmeland, Adam Wende, and Talene Yacoubian, you have guided my scientific curiosities, encouraged me to think critically, and have constructively criticized both my over ambitious experimental goals and my "novel" interpretations of data.

And to those whom I have not mentioned, my many friends, colleagues, and lab mates who have kept me moving forward and have always had an open ear for a pessimistic soul much as myself. You know who you are, you are not forgotten and I thank you all as well.

TABLE OF CONTENTS

LIST OF TABLES

LIST OF FIGURES

INHIBITION OF AUTOPHAGY WITH BAFILOMYCIN AND CHLOROQUINE
DECREASES MITOCHONDRIAL QUALITY AND BIOENERGETIC FUNCTION IN
PRIMARY NEURONS

LIST OF ABBREVIATIONS

3MA	3-Methyladenine
ADP	Adenosine diphosphate
AKG	Alpha-Ketoglutarate
AraC	Cytosine arabinoside
aSyn	α-synuclein
ATG	Autophagy-related genes
ATP	Adenosine triphosphate
BSA	Bovine serum albumin
CI	Complex I (NADH dehydrogenase)
CII	Complex II (Succinate dehydrogenase)
CIII	Complex III (Cytochrome bc$_1$ complex)
CIV	Complex IV (Cytochrome C oxidase)
CMA	Chaperone mediated autophagy
Con	Control
CQ	Chloroquine
CV	Complex V (ATP synthase)
DIV	Days *in vitro*
DMSO	Dimethyl sulfoxide
DNA	Deoxyribonucleic acid
E. coli.	Escherichia coli
E18	Embryonic day 18
E64	Trans-epoxysuccinyl-L-leucylamido(4-guanidino)butane

FBS	Fetal bovine serum
GAPDH	Glyceraldehyde 3-phosphate dehydrogenase
GFAP	Glial fibrillary acidic protein
GRAS	Generally regarded as safe
HBSS	Hanks balanced salt solution
HMW	High molecular weight
HNE	4-Hydroxynonenal
HSC70	Heat shock cognate 70
HSP104	Heat shock protein 104
HSP90	Heat-shock protein 90
ICC	Immunocytochemistry
KO	Knockout
LAMP1	Lysosomal associated membrane protein 1
LAMP2A	Lysosomal associated membrane protein 2A
LC3	Microtubule-associated proteins 1 light chain 3
LRRK2	Leucine-rich repeat kinase 2
MAP2	Microtubule-associated protein 2
MFN1/2	Mitofusins 1/2
MPP+	1-methyl-4-phenylpyridinium
MPTP	1-methyl-4-phenyl-1,2,3,6-tetrahydropyridine
mtDNA	Mitochondrial DNA
MTLT	MitoTracker / LysoTracker
mTOR	Mammalian target of rapamycin
MTT	3-(4, 5-dimethylthiazolyl-2)-2, 5-diphenyltetrazolium bromide)
NBA	Neurobasal A medium
NBM	Neurobasal medium
nDNA	Nuclear DNA
Nrf2	Nuclear factor (erythroid-derived 2)-like 2

O	Oligomycin
OCR	Oxygen consumption rate
P/M	Pyruvate / Malate
P0-3	Postnatal day 0-3
p62	Sequestosome 1 (p62)
p-aSyn	Phosphorylated-α-synuclein
PARL	Presenilin associated rhomboid-like protease
PBS	Phosphate buffered saline
PCR	Polymerase chain reaction
PD	Parkinson's disease
Pen/Strep	Penicillin / Streptomycin
PFFs	Pre-formed fibrils
PI3KIII	Phosphoinositol-3-kinase class III
PINK1	PTEN induced putative kinase
PLL	Poly-L-Lysine
PMP	Plasma membrane permeabilizer
Pon S	Ponceau S
p-S129	Phosphorylated Serine 129
PVDF	Polyvinylidene difluoride
R	Rotenone
RIPA	Radioimmunoprecipitation assay buffer
RNA	Ribonucleic acid
SDS-PAGE	Sodium dodecyl sulfate polyacrylamide gel electrophoresis
siRNA	Small interfering RNA
SNAP29	Synaptosomal-associated protein 29
SNCA	Alpha-synuclein gene
STX17	Syntaxin 17
TCA	Tricarboxylic Acid cycle

TFEB	Transcription factor EB
TIM	Translocase of the inner (mitochondrial) membrane
TMPD	N,N,N′,N′-Tetramethyl-p-phenylenediamine
TOM	Translocase of the outer (mitochondrial) membrane
Tre	Trehalose
TX-100	Triton X-100
UPS	Ubiquitin proteasome system
USFDA	United States Food and Drug Administration
VAMP7/8	Vesicle-associated membrane protein 7/8
VDAC	Voltage dependent anion channel
WT	Wildtype
XF	Extracellular flux

MITOPHAGY MECHANISMS AND ROLE IN HUMAN DISEASE

by

MATTHEW REDMANN, MATTHEW DODSON, MICHAEL BOYER-GUITTAUT,
VICTOR DARLEY-USMAR, AND JIANHUA ZHANG

CHAPTER 1

INTRODUCTION

PARKINSON'S DISEASE

Clinical symptoms

Parkinson's disease (PD) was first scientifically documented by the British

physician James Parkinson in 1817 and is the second most common neurodegenerative

disorder, surpassed only by Alzheimer's disease [1, 2]. PD shares many commonalities

with other prevalent neurodegenerative diseases as well, such as dementia with Lewy

bodies and multiple systems atrophy [3, 4]. Diagnosis is based primarily on clinical

symptoms and as of current no test, biomarkers, or early means of detection exist. Signs

and symptoms used clinically to diagnose PD are tremor, bradykinesia, impaired posture,

postural instability, and reduced arm swing when walking [5]. Reduction in olfactory

sensing or an increase in constipation may predate the onset of motor symptoms by years.

These symptoms, however, are not inherently specific to PD and thus are not typically

used for diagnosis, but studies are currently underway to investigate using loss of smell

as an early indicator [6-9].

Pathology

Pathologically, the disease is characterized by the progressive and currently

unstoppable loss of dopaminergic neurons in the substantia nigra pars compacta. In

healthy brains, neurotransmission from dopaminergic neurons in the substantia nigra to

the striatum plays an important role in motor coordination. As the neurons succumb to cellular stress and toxicity, this neurotransmission is increasingly diminished and becomes insufficient for proper motor movement. Current therapies focus primarily on restoring the level of the neurotransmitter, dopamine, in the striatum. This is accomplished in a few ways. Carbidopa/levodopa combination is a standard treatment that increases dopamine in the brain while controlling for peripheral increases [10-12]. Additionally, dopamine agonists can be added or dopamine breakdown can be slowed by monoamine oxidase B inhibitors, thus extending synaptic levels [13]. And while there have been advances in reducing side effects and fine-tuning of treatments, the essence of these therapies remains unchanged since Levodopa was first administered in the 1960's [14-17]. Key cellular features of PD are highlighted in **Figure 1** and are discussed further below.

Protein accumulation

There is a clear correlation between the remaining neurons presenting with proteinaceous intracellular inclusion and those patients diagnosed with PD. These inclusions were first observed in the early 1900's by Fritz Lewy and are termed Lewy bodies and Lewy neurites, depending on their cellular location. The composition of these aggregates would remain unknown until the 1990's when alpha-synuclein (aSyn) was discovered as the principle component of Lewy bodies [18]. The exact role of aSyn remains unknown but in yeast aSyn has been shown to interact with lipid membranes and *in vitro* studies have shown that aSyn has an amphipathic helical region that suggests a role in vesicle trafficking or membrane stability [19-22]. One defining feature in PD

brains is that aSyn becomes hyper-phosphorylated at serine 129. The role of this

phosphorylation isn't apparent despite its constant occurrence in Lewy bodies [23]. aSyn

knockout animals exhibit minimal functional differences from wildtype which may be

due to the existence of aSyn homologues, beta and gamma-synuclein. Interestingly,

when all three synucleins are knocked out, the mice exhibit aberrations in synaptic

function, age related neurodegeneration and premature death [24-26].
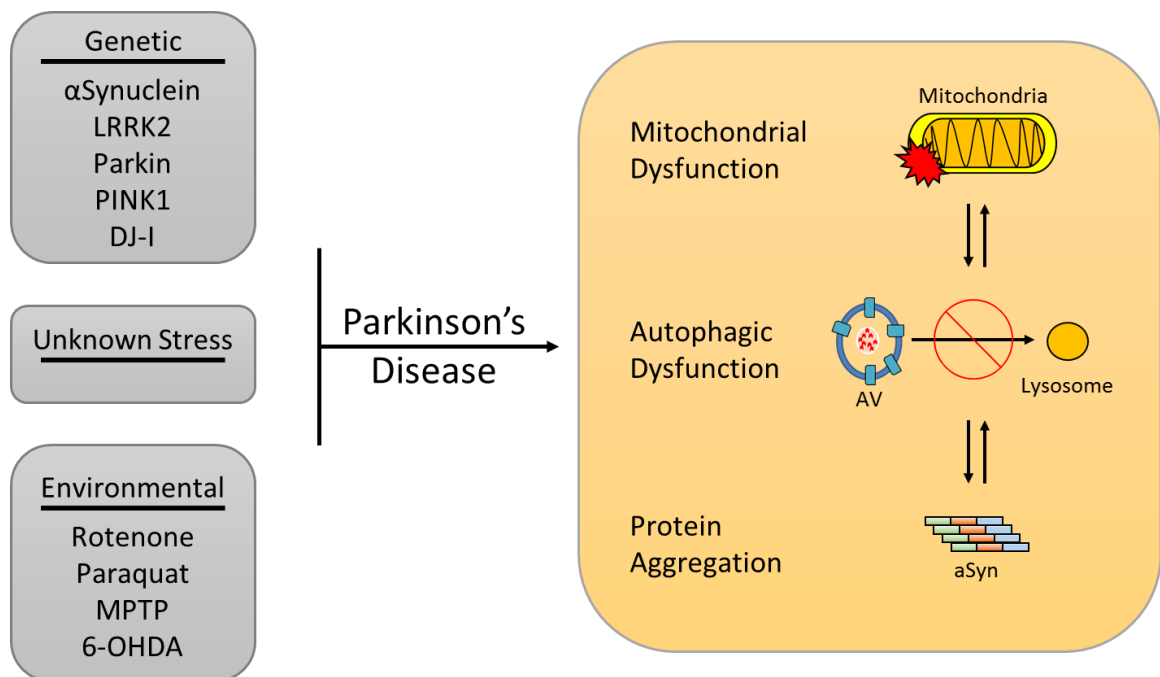
Figure 1: Parkinson's disease (PD) is a multi-factorial disease with genetic, environmental and unknown causes. Neurons that are affected by PD exhibit an interplay between mitochondrial dysfunction, autophagic dysfunction, and protein aggregation pathologies.

Whether aSyn aggregates at large or a subset of these aggregations are protective

against or deleterious towards neuronal survival is still unclear. It is postulated that the

oligomeric species and not the monomeric or large aggregates are responsible for cell

death [27, 28]. Nonetheless, *in vivo* mouse neurons containing aSyn inclusions induced

by pre-formed fibrils selectively degenerate compared to neighboring neurons free of

inclusions [29]. These aggregations also typically stain positive for ubiquitin and p62,

key protein degradation markers suggesting defects in pathways responsible for protein

turnover [30, 31].

aSyn has also been found to be able to leave the cell and spread pathology

elsewhere. This was first hypothesized by Braak and colleagues in 2003, suggesting that

PD pathology begins in the brain stem and progresses to higher regions of the brain [32].

It was later postulated that Lewy pathology may spread from the enteric system [33].

Striking evidence for intercellular transfer of aSyn came from post-mortem autopsies of

patients that received stem-cell transplants, whose nascent neuronal transplants exhibited

Lewy body pathology [34]. These observations have been further substantiated in cell

culture models where aSyn can be released from the cell and accumulate in the media

[35, 36].

Genetics

A small percentage of PD cases are linked to genetic causes, the most prevalent

mutations are those changes in alpha-synuclein (*SNCA)* and leucine-rich repeat kinase 2

(*LRRK2)*. In the case of *SNCA*, a duplication or triplication can increase risk and age of

disease onset [37, 38]. There are currently five known point mutations in aSyn: A53T,

A30P, E46K, H50Q, and G51D [39-43] and aSyn phosphorylation at Ser 129 has been

shown associated with Lewy bodies [44, 45] (**Figure 2**). In LRRK2, there are currently

six known mutations out of twenty that have been found to be pathogenic, with the most common disease-causing mutation being G2019S [46].

Unlike aSyn and LRRK2, where their exact functions are unknown, *PARK7* (DJ-1), *PARK2* (Parkin) and *PARK6* (PINK1) are responsible for maintenance of mitochondrial quality which provided genetic evidence of mitochondrial impairment in the disease [47-50]. Indeed, mitochondrial dysfunction has been reported in lymphoblasts carrying DJ-1 mutations [51], fibroblasts carrying PINK1 mutations [52], and induced pluripotent stem cell (iPSC)-derived neurons carrying PARKIN mutations [53].

Monogenic forms of PD, meaning a singular gene is accountable, account for 30% of familial PD and 3-5% of total PD cases, of which idiopathic forms predominate [54]. In addition to genetics, it has been postulated that environmental stress plays a role. This hypothesis has been supported by evidence in which pesticide exposure causes increased risk of PD and are described further below in their relationships to mitochondrial dysfunction [55-57].

Figure 2: The structure of aSyn is comprised of three main regions. The amphipathic region contains all 5 known point mutations in aSyn and is thought to be responsible for aSyn's interactions with membranes. The non-amyloid-β component (NAC) region of aSyn, named from being originally isolated from Alzheimer's disease amyloid plaques is an inherently hydrophobic region and is largely thought to be indispensable for aSyn aggregation. The acidic C-terminal tail is where serine 129 is located, the primary site of aSyn phosphorylation.

Involvement of dysfunctional mitochondria

Besides the above mentioned genetic evidence suggesting that mitochondrial dysfunction is directly involved in PD pathogenesis, there are epidemiological studies indicating mitochondrial dysfunction may be involved in PD as well [58-60].

Mitochondria fulfill essential roles for neurons by producing ATP through oxidative phosphorylation. When mitochondria accumulate damage they are unable to meet the energy requirements of the cell. Failing mitochondria were first implicated in PD when it was observed in the postmortem brains of PD patients that mitochondrial complex I activity was diminished [61, 62].

Pesticides that target mitochondria have been associated with increased risk of developing PD [63]. Furthermore, animal models using these chemicals exhibit neurodegeneration with PD-like symptoms. These neurotoxin models have played a critical role in investigating features of PD. Compounds like rotenone, paraquat, MPTP, and 6-hydroxydopamine have been found to induce dopaminergic neuron loss in mouse, rat and primate models through inhibition of mitochondrial complexes and production of reactive species [64].

Linking aSyn pathogenic mechanisms to mitochondrial dysfunction has been studies indicating that aSyn has a mitochondrial targeting sequence and once in the mitochondria can interact with the inner mitochondrial membrane, inhibit complex I and induce ROS production [65, 66]. Interestingly, aSyn knockout mice have been reported to be resistant to MPTP toxicity by down regulating dopamine transporters [67, 68]. Cumulatively, these models have demonstrated that protein accumulation, mitochondrial dysfunction and associated oxidative stress manifest in PD and suggest that clearing

7

damaged protein, mitochondria and reactive species damage may be beneficial in mitigating cellular pathology [69].

AUTOPHAGY

Autophagy is the process of recycling cellular content in which a double membraned vesicle, the autophagosome, delivers its cargo to the lysosome. This evolutionary conserved process was first observed in the 1950's by ultrastructural studies. The principle organelle that is responsible for degradation of cellular contents was termed the lysosome [70, 71]. The process of "self-eating" was soon after named "autophagy" to describe the process of the cell digesting its own cytoplasm and organelles. Double membraned vesicles filled with electron dense contents were soon after termed autophagosomes [72].

Regulation of autophagy

It has been estimated that the body turns over almost its entire complement of cellular proteins every 1-2 months [73-75]. Distinct but integrated pathways dispose of the cell's unwanted materials in order to regulate the amount of intracellular protein and to recycle proteins that are no longer needed, no longer functional, or during cellular stress such as starvation [76].

Lysosomal dependent autophagy can be sub-divided into 3 types: micro-autophagy, chaperone mediated autophagy (CMA) and macro-autophagy. Micro-autophagy involves the engulfment of the cytoplasm directly into a lysosomal compartment. The regulation of this process is still not well understood [77, 78].

CMA works through the delivery of cargo to the lysosome by specific

chaperones. Heat shock cognate 70 (HSC70) and heat shock protein 90 (HSP90) are able

to recognize a KFERQ motif on target proteins and bring them to the lysosome. Once at

the lysosome, these proteins are delivered through the lysosomal protein, lysosome-

associated membrane protein 2 (LAMP2A). Both aSyn and LRRK2 have been observed

to be degraded by CMA, but it is also clear that modified or mutated forms of aSyn seem

to resist degradation by CMA and "clog" the pathway that prevents degradation of other

substrates [79, 80].

Compensation between CMA and macro-autophagy (henceforth referred to as

autophagy) has been observed, in a cell model expressing mutant tau and when CMA

fails to remove aggregates, autophagy is able to be up-regulated to assist in tau clearance

[81]. Autophagosomes have been found to accumulate in PD brains and autophagic

failure can exacerbate the extracellular release of aSyn, and once released its uptake by

neighboring cells further propagates the disease [82, 83]. A complex signaling system is

involved in modulating the initiation, elongation and completion steps of autophagy

(**Figure 3**). The mammalian target of rapamycin (mTOR) allows for signal integration of

cellular nutrient sensing pathways [84]. When nutrient supply is ample, mTOR is

phosphorylated and is in its active state, resulting in the suppression of autophagy and the

activation of pro-growth translation factors p70S6K and 4E-BP1 by phosphorylation.

When nutrients are scarce, mTOR is dephosphorylated and inactivated, leading to the

dephosphorylation and inactivation of p70S6K and 4E-BP1 which in turn suppresses

protein translation. Simultaneously, autophagy becomes active as the Beclin/VPS34

complex is allowed to begin autophagosome initiation. During the autophagosome

maturation process, cytosolic LC3-I is lipidated and converted to LC3-II and is

incorporated into the autophagosome membrane. LC3-II can therefore be used as a

marker of autophagosome levels as it is typically only present in autophagosomes. Fusion

of autophagosomes with lysosomes is mediated by STX17, SNAP29, and VAMP7/8 [85].

Once delivered, the cargo is degraded by the lysosome. Inhibition of mTOR by

rapamycin can induce autophagy and has been shown effective in reducing PD like

symptoms in chemical models and aSyn overexpression models of PD [86, 87].
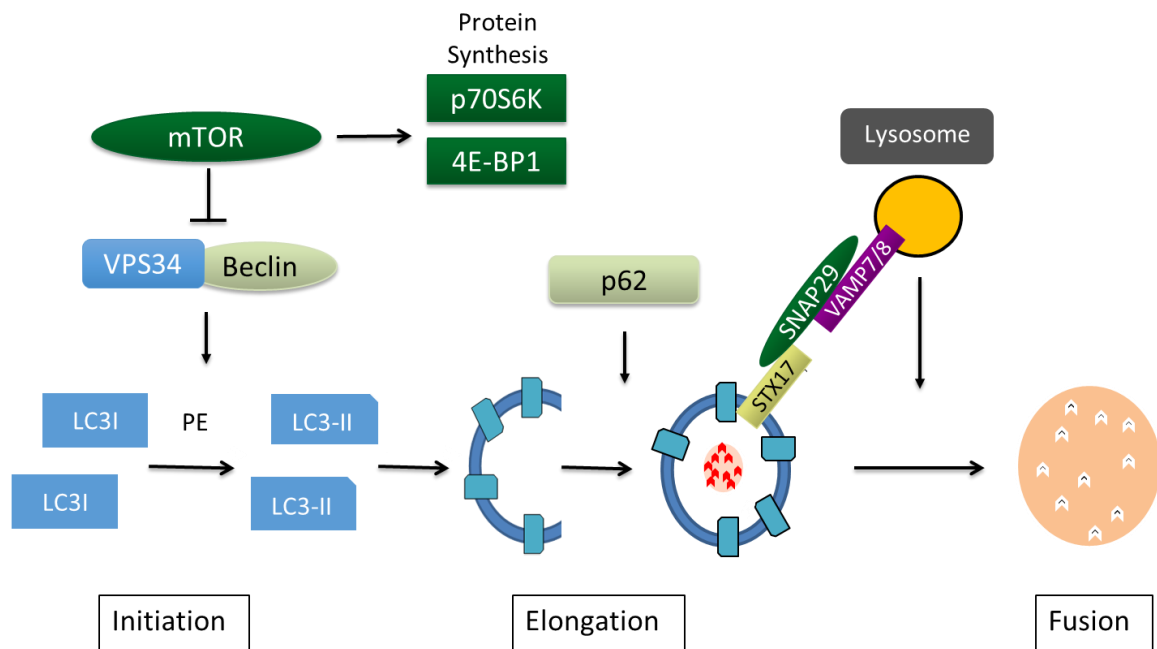
Figure 3: Overview of the autophagy lysosomal pathway. This pathway consists of three key steps. Autophagy initiation is controlled by mTOR. When mTOR is active it represses autophagy and activates protein synthesis through p70S6K and 4E-BP1. When inactive, the Beclin/VPS34 complex allows for autophagosome formation through the conversion of LC3-I to LC3-II. Elongation of autophagosomes is accompanied with sequestration of cargo and the closure of the double membraned autophagosome. p62 assists the delivery of cargo to the autophagosome. The final fusion step, where the autophagosome fuses with the lysosome, is mediated by STX17, SNAP29 and VAMP7/8.

The autophagy substrate and scaffold protein p62 plays a crucial function linking the autophagosome/lysosome machinery to other cell degradation pathways and co-stains with aSyn in PD [88]. The scaffold protein has several domains. The PB1 domain allows p62 to interact with itself. The LIR or LC3 Interacting Region, allows it to bind to LC3. And the UBA domain allows it to interact with ubiquitin. The latter two regions allow p62 to bind ubiquitinated proteins and traffic them to autophagosomes and thus integrates cellular digestion pathways [89]. As mentioned above, oxidative damage is prevalent in PD. p62 helps manage oxidative stress by playing a role in the regulation of Nrf2/Keap1 interaction, an antioxidant signaling pathway. When p62 is bound to Keap1, Nrf2 ubiquitination is prevented and is allowed to translocate to the nucleus, thus enabling antioxidant genes to be expressed (**Figure 4**) [90].

A non-lysosomal mediated mechanism of protein turnover is the ubiquitin proteasome system (UPS). This system is an essential component of protein homeostasis but in PD animal models proteinaceous inclusions seem resistant to degradation by the proteasome and in culture aSyn proto-fibrils inhibit proteasome function [91] and in humans there is evidence that lysates from sporadic PD patients have reduced proteasome activity [92-94]. The UPS consists of the proteasome and a series of enzymes that tag proteins for degradation by addition of a poly-ubiquitin tail. First, an E1 ubiquitin activating enzyme is responsible for activating ubiquitin by ATP hydrolysis. It is then transferred to a second enzyme, an E2 ubiquitin conjugating enzyme. Lastly, the E3 ubiquitin ligase in concert with an E2 conjugating enzyme attaches ubiquitin with high specificity to target proteins. It has been found that the UPS and autophagy are linked in

aSyn metabolism, in so that if the UPS is inhibited, autophagy can compensate to a

certain extent, further suggesting the importance of autophagy [95].
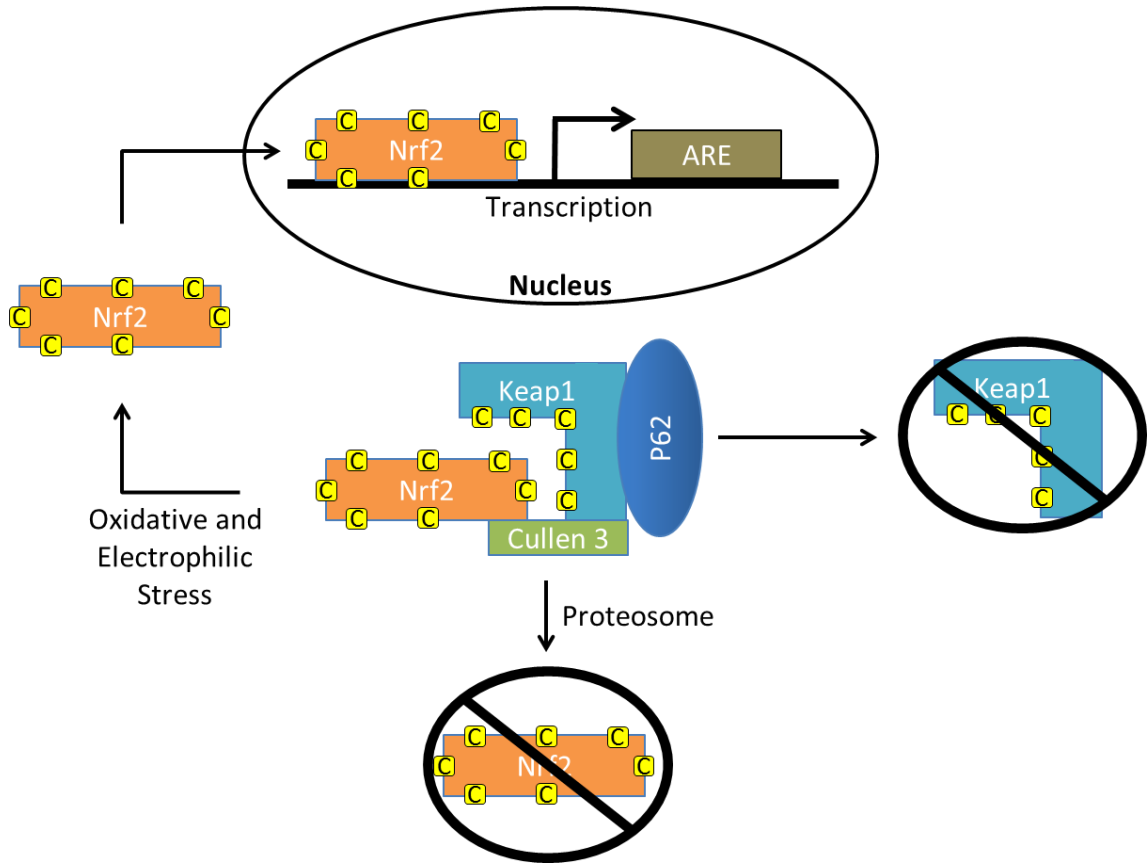
Figure 4: The role of p62 in oxidative stress. Under basal conditions Nrf2 is bound in the cytosol by interaction with Keap1. This interaction is modulated by modification of cysteine thiol groups on both proteins. Keap1 serves as an adapter, allowing Nrf2 to be ubiquitinated by Cullen 3. Once ubiquitinated, Nrf2 is sent to the proteasome for degradation. Keap1 can also interact with p62. This interaction can sequester Keap1 away from Nrf2, preventing its ubiquitination and degradation. When Nrf2 is not degraded, it can translocate to the nucleus and activate genes that contain antioxidant Response Elements (ARE)/electrophile-response element (EpRE).

Autophagy in neurons

Autophagy is especially important in neurons as they are mostly post-mitotic and are unable to dilute out toxic molecules through cell division. Indeed, in neurons, autophagy appears to be an indispensable cellular program as knockout of *Atg5* or *Atg7* in mice, genes crucial for proper phagophore formation, leads to behavioral abnormalities and reduced motor skills resultant from abnormal neuron function. These abnormalities progress and are co-morbid with animal death occurring several months after birth. Failure of autophagy was evidenced in several ways. First, neurons accumulated large quantities of un-cleared ubiquitinated proteins. Second, proteinaceous intracellular inclusions formed. Last, neurons exhibited altered morphology and accumulation of autophagosomes. Intriguingly, these observed phenotypes of autophagy failure bare resemblance to PD and other neurodegenerative diseases [96-98].

Because of the structure of the neurons, autophagy appears to be compartmentalized. Autophagosomes can arise either in the soma or in the neurite and be trafficked back through the axon. This trafficking is essential for autophagosomal degradation, as it is currently believed that autophagosome degradation by lysosomes only occurs in the soma [99, 100]. Moreover, how neurons respond to starvation signals and/or mTOR signaling may be different from cells in other tissues. For example, in the case of rapamycin treatment in cultured neurons, mTOR inhibition is insufficient to turn on autophagy in a 4 hour time frame [101]. Regardless of mTOR responsiveness, it is becoming clear that the primary role of autophagy in neurons is to maintain cellular protein pools and responding to stress. This is important in neurodegenerative diseases, where the failure of autophagy is repeatedly indicted in disease progression.

Autophagy modulating compounds

Pharmacologic modulators of autophagy have been instrumental in providing mechanistic insights and determining the impact of autophagy perturbation on neuronal function and survival. The target and function of these modulators are outlined in **Table 1** and a schematic is illustrated in **Figure 1**.

The autophagy inducer and mTOR inhibitor rapamycin was discovered in 1975 from soil samples obtained from the Pacific island Rapa Nui also known as Easter Island [102]. Rapamycin has been shown to activate autophagy and play a protective role in animal and cell culture models of diseases where aberrant protein aggregation is present [103, 104].

However, rapamycin has failed to leap into clinical use for PD. Furthermore, in neurons exposed to aSyn fibrils, it failed to clear aSyn aggregates and exacerbated aSyn fibril-induced cell death [105]. Other autophagy inducers have also been discovered. In 2007, 175 years after its original discovery in 1832, trehalose was found to induce autophagy in neuronal cell lines [106]. This disaccharide is composed of two glucose molecules and is native to yeast, flies, and certain plants. The exact mechanism of autophagy induction by trehalose is unknown, but it does appear to activate TFEB, a transcription factor that controls genes responsible for lysosome biogenesis [107].

Rapamycin and trehalose increase autophagosomes by increasing autophagy initiation. Initiation can be blocked and autophagosome formation halted pharmacologically. For example, 3-methyladenine (3MA) and wortmannin inhibit class III PI3Ks that are important for autophagy initiation. It has been reported that

Compound	Action	Target	Structure
3MA	Inhibitor	PI3K	
Bafilomycin	Inhibitor	V-ATPase (Lysosome)	
Chloroquine	Inhibitor	Lysosome	
E64	Inhibitor	Cysteine Proteases (Lysosome)	
Pepstatin A	Inhibitor	Aspartic Proteases (Lysosome)	
Rapamycin	Enhancer	mTOR	
Torin	Enhancer	mTOR	
Trehalose	Enhancer	Unknown (mTOR independent)	
Wortmannin	Inhibitor	PI3K	
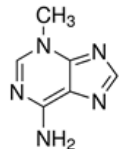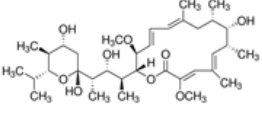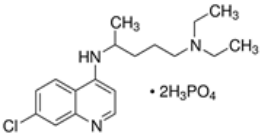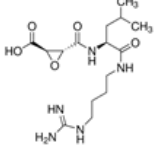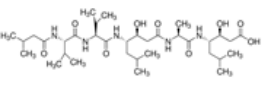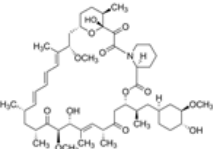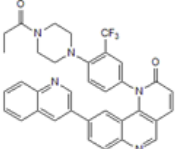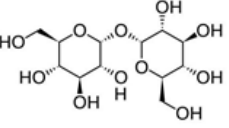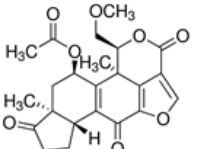
Table 1: Summary of commonly used autophagy modulators, the targets they act upon and the structures of the modulators.
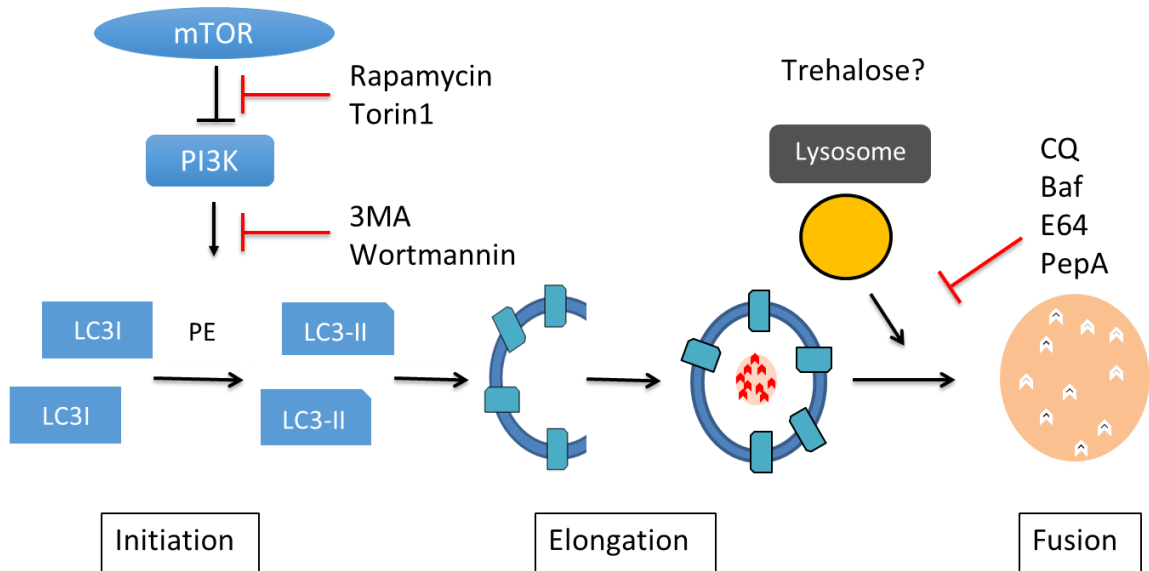
Figure 5: Illustration of the autophagy pathway and its modulators. Rapamycin and torin1 both inhibit mTOR, activating autophagy. Trehalose, activates autophagy but this mechanism is currently unknown. 3-methyladenine (3MA) and wortmannin are class III PI3K inhibitors and prevent autophagosome formation. Chloroquine (CQ), bafilomycin (baf), E64, and pepstatin A (PepA) work at the lysosome through either raising the pH or inhibiting specific enzymes.

wortmannin is a more selective inhibitor with effective concentrations in the nanomolar range whereas 3MA requires millimolar concentrations to be effective. Furthermore, 3MA's inhibitory effect on class III PI3K in MEFs is transient with inhibition only lasting between 6 and 9 hours [108]. And while 3MA and wortmannin are not used clinically, they are useful tools for probing autophagic flux in disease models where autophagic failure occurs.

Autophagy can also be inhibited by targeting specific classes of lysosomal proteases. For example, pepstatin A irreversibly inhibits aspartic proteases while E64 irreversibly inhibits cysteine proteases. One drawback to this method is that each inhibitor only prevents one class of hydrolases and may not completely block autophagy. Additionally, while E64 is water soluble and an analogue is being proposed for human

use in the context of Alzheimer's disease by reducing amyloid-β in mouse models [109], pepstatin A is only soluble in DMSO or ethanol at low concentrations. Thus achieving effective doses would necessitate adding high amounts of a water insoluble vehicle, consequently posing potential toxic side-effects limiting its therapeutic uses.

Another strategy is to raise the lysosomal pH, thus inhibiting the majority of hydrolases. This can be effectively accomplished by either chloroquine or bafilomycin. Chloroquine acts by passing into the cell and entering the lysosome. Once there, chloroquine becomes di-protonated and precipitates, trapping chloroquine in the lysosome. In contrast, bafilomycin works by inhibiting the lysosomal V-ATPase, the enzyme that acidifies the lysosome by increasing H^+ concentration (**Figure 6**). These two processes are able to substantially increase the pH of the lysosome and prevent proper hydrolase function, resulting in autophagy inhibition. Both compounds are useful as tools to measure autophagic flux and useful for studying the consequences of autophagy inhibition.

MITOCHONDRIAL MACHINERY AND MITOPHAGY

The mitochondrion is the sole means by which the cell can create the greatest amount of ATP for each glucose molecule, approximately 32 ATP created for each molecule of glucose. Mitochondria are a highly adapted organelle with specific machinery to make this energy conversion possible through oxidative phosphorylation. In addition, mitochondria are responsible for their own DNA replication, transcription and translation of mitochondrial proteins, import of nuclear-encoded proteins, calcium

storage, production and scavenging of oxidants, signaling, and sequestration of pro-

apoptotic proteins to sustain cell survival [110-112].
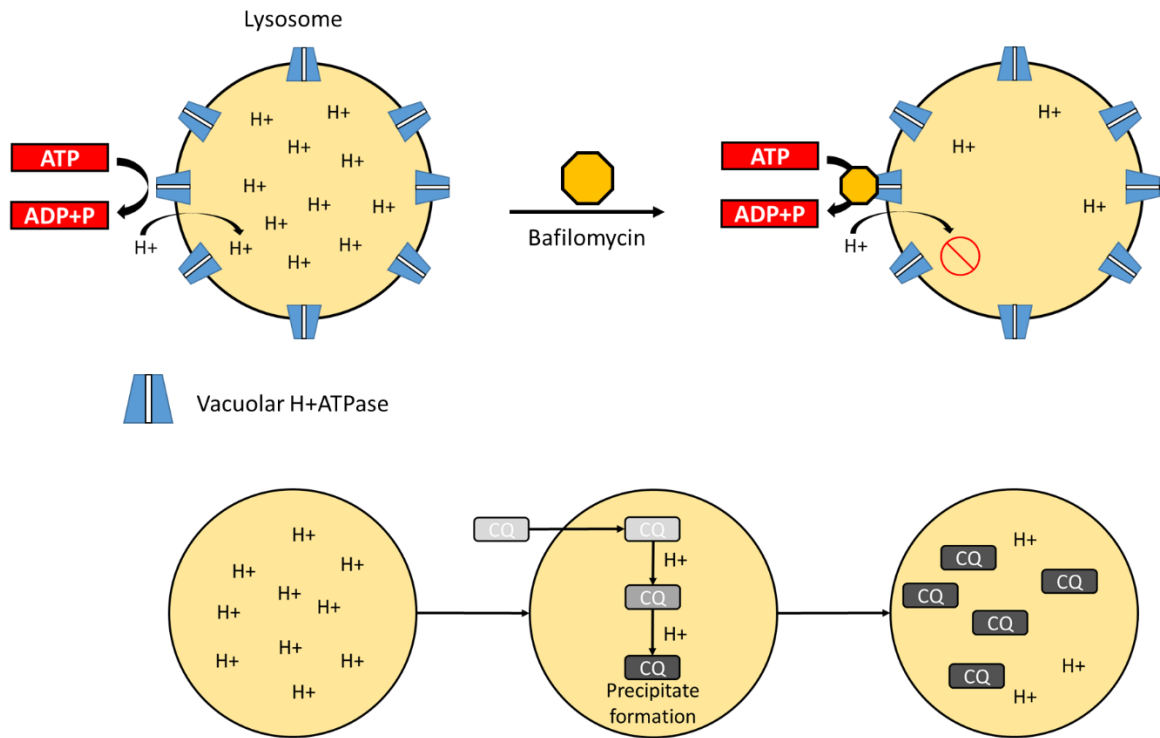
Figure 6: Schematic of lysosomal inhibition by either bafilomycin or chloroquine. Bafilomycin works by inhibiting the vacuolar H+ATPase and preventing the pumping of protons into the lysosome, raising the pH. Chloroquine (CQ) works by entering the lysosome and absorbing protons and raising the pH. The increased pH inactivates most lysosomal enzymes preventing them from degrading lysosomal contents.

Mitochondrial ETC and TCA components

The electron transport chain is composed of five key complexes (**Figure 7**).

Complex I, NADH dehydrogenase, pumps 4 H^+ into the intermembrane space while

donating 2 electrons to ubiquinone by oxidizing NADH from the TCA cycle. Complex II,

Succinate Dehydrogenase, accepts electrons from succinate, but does not pump any

protons into the intermembrane space. Complex III, cytochrome bc_1 complex, in the

process of pumping 4 H^+, takes electrons from the Q cycle and passes 2 electrons to

cytochrome C. Complex IV, Cytochrome C Oxidase, pumps 4 H^+ across the membrane

as electrons from all previous reactions are transferred to oxygen. Complex V, ATP-

synthase, is able to utilize the energy stored in the electrochemical gradient. Protons that

have been pumped by complexes I-IV move down their gradient through complex V

where the energy from 3 protons are used to create ATP from ADP and inorganic

phosphate. Of these 5 complexes, it is NADH dehydrogenase (complex I) that is often

observed to be inhibited in PD models [113]. This is particularly the case with rotenone.

However, aSyn has been shown to have a mitochondrial targeting sequence where it can

enter the mitochondria and inhibit complex I [65, 114].
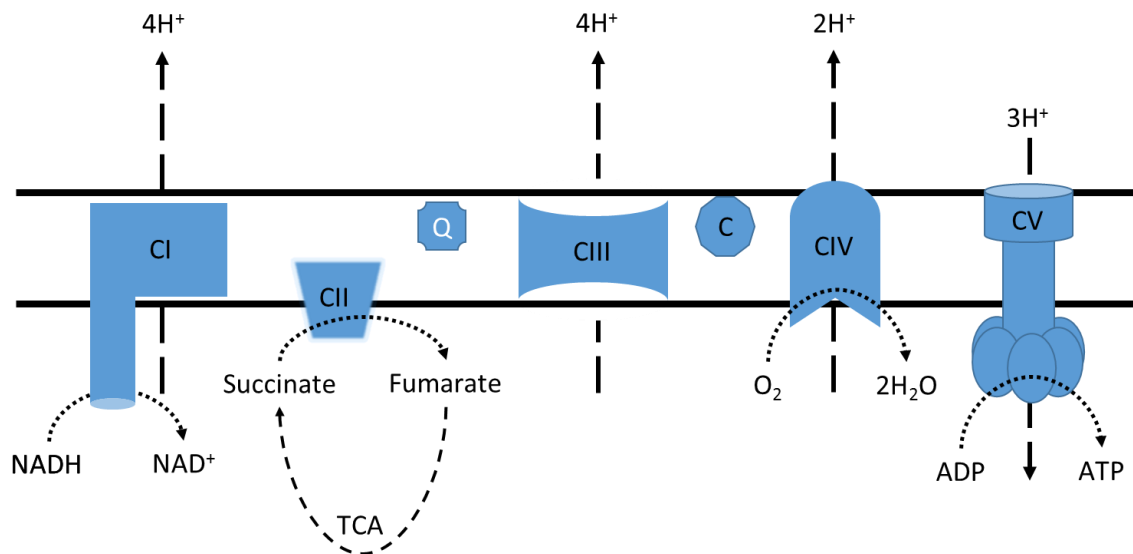
Figure 7: Schematic of the key components of the mitochondrial electron transport chain
(ETC). Briefly, protons are pumped from the mitochondrial matrix to the intermembrane
space and then move down the electrochemical gradient through Complex V (ATP-
Synthase) to convert ADP to ATP. Electrons that enter the ETC at Complex I and II are
ultimately donated to oxygen at Complex IV.

The tricarboxylic acid cycle (TCA), also known as the citric acid cycle or Krebs cycle, is a highly conserved metabolic program that is responsible for converting the energy in fats, carbohydrates, and protein into ATP and intermediates that can be utilized by the ETC. NADH and succinate created by this pathway can be utilized by complex I and II, respectively. This process consists of 10 steps and can feed into myriad cellular pathways. An important side pathway for neurons is glutaminolysis, which converts glutamine to glutamate, and then to alpha-ketoglutarate, a TCA intermediate. Key steps are outlined in **Table 2**. To date, there have been no comprehensive studies of the TCA cycle in PD-related cell culture or animal models. However, α-ketoglutarate dehydrogenase level was found decreased in post-mortem PD brains, specifically in neurons that showed degeneration [115]. Interestingly, exposing isolated mitochondria to MPP^+, the active metabolite of MPTP, has been shown to inhibit α-ketoglutarate dehydrogenase in addition to complex I [116]. And while in this dissertation we do not specifically study the TCA cycle in response to aSyn, we investigated changes of TCA metabolites in primary neurons in response to autophagy inhibition.

Table 2: Key steps of the tricarboxylic acid (TCA) cycle.

	Enzyme	**Substrates**	**Products**
0/10	Citrate Synthase	Oxaloacetate + Acetyl CoA	Citrate + CoASH
1	Aconitase	Citrate	cis-Aconitate
2	Aconitase	cis-aconitate	isocitrate
3	Isocitrate Dehydrogenase	Isocitrate + NAD+	Oxalosuccinate + NADH + H+
4	Isocitrate Dehydrogenase	Oxalosuccinate	α-Ketoglutarate
5	α-Ketoglutarate dehydrogenase	α-Ketoglutarate +NAD++CoASH	Succinyl-CoA + NADH + H+ + CO2

6	Succinyl-CoA synthetase	Succinyl-CoA + GDP	Succinate + CoASH + GTP
7	Succinate dehydrogenase	Succinate + ubiquinone	Fumarate + ubiquinol
8	Fumarase	Fumarate	L-Malate
9	Malate dehydrogenase	L-Malate	Oxaloacetate + NADH + H+
0/10	Citrate Synthase	Oxaloacetate + Acetyl CoA	Citrate + CoASH

Regulation of Mitophagy

Maintenance of a healthy mitochondrial population is essential for cellular function and survival, and is controlled by balancing biogenesis and turnover of mitochondria via autophagy (mitophagy) [117-119].

Mitochondrial dynamics are emerging as an important aspect of cellular physiology, and play an important role in regulating mitophagy [120]. In yeast, the Atg32/Atg11 complex recruits the fission machinery in response to nitrogen starvation through an interaction between Atg11 and Dnm1 (**Figure 8**). Mutations of the Atg11-interaction domain on Dnm1 protein decreased mitophagy [121]. In mammalian cells, mitophagy has been shown to occur in conjunction with fission events in hepatocytes [122]. Inhibition of mitochondrial fission by either *Fis1* siRNA or a dominant negative form of Drp-1 prevents mitophagy in INS-1 β-cells [123]. In mouse embryonic fibroblasts (MEFs), elimination of either glutamine or amino acids from the growth medium, but not elimination of glucose or serum, resulted in mitochondrial tubulation. MEFs with *Opa1* or *Mfn2* gene knockout exhibited increased mitophagy during starvation [124]. The mechanisms through which changes of fission or fusion due to Drp1, Opa1 or Mfn2 knockdown or knockout impact mitophagy may involve changes in mitochondrial morphology, mitochondrial membrane potential, and mitochondrial

bioenergetics [125-127]. Recent evidence also suggests that FIS1 may act downstream of

Drp-1 in response to calcium ionophores in *C. elegans*, or to Antimycin A or CCCP in

HCT116 cells, to initiate formation of nascent mitophagosomes by participation in the

mitochondrion-associated membrane (MAM) complex [128]. These studies demonstrate

that mitochondrial fission/fusion machinery plays a pivotal role in the regulation of

mitophagy.
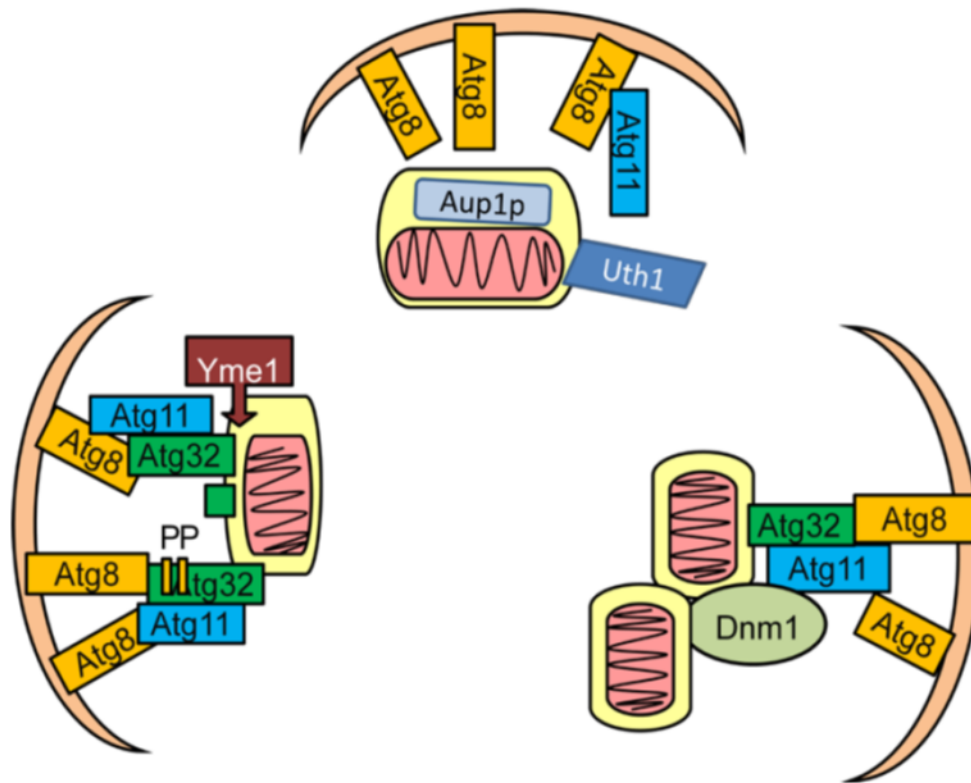
Figure 8: Adaptor proteins in mitophagy: In yeast, selective autophagy of mitochondria is mediated by mitochondrial targeted proteins such as Uth1, Aup1p, or Atg32.While the mechanisms of interaction between Aup1p and Uth1 and the autophagy machinery are still unclear, more is known regarding Atg32 function in mitophagy. Under starvation conditions, Atg32 localizes to the mitochondria and interacts with Atg8 and Atg11 to bring mitochondria to the autophagosome. Phosphorylation of Atg32 at Ser-114 and Ser-119, or cleavage of Atg32 by Yme1, facilitates its interaction with Atg11. Atg11 interaction with mitochondrial fission protein Dnm1 and recruitment of the fission complex to the mitochondria are also required for mitophagy in response to nitrogen starvation.

In addition to fission and fusion, mitochondrial membrane potential plays an important role in mitophagy. In rat hepatocytes, serum deprivation has been shown to induce mitochondrial depolarization and engulfment by autophagosomes [129]. How mitochondrial depolarization leads to mitophagy has been extensively studied in the context of understanding potential pathogenic mechanisms of PD, and it has been found that recessive genes identified in familial PD, *PARKIN*, *PINK1* and *DJ-1*, encode proteins involved in mitophagy. Studies using *Drosophila* models and established human cell lines have found that upon depolarization, PINK1 is imported into the mitochondria by the Translocase of the Outer Membrane (TOM) and Translocase of the Inner Membrane (TIM) complexes. PINK1 then anchors at the inner mitochondrial membrane (IMM) where it is processed by the rhomboid protease of the IMM, presenilin associated rhomboid-like protease (PARL) [130], and degraded by mitochondrial processing peptidases. However, when mitochondrial membrane potential is lost, PINK1 is not cleaved by PARL, and thus accumulates in the mitochondria [131].

Following accumulation of PINK1, the cytosolic E3 ubiquitin ligase Parkin is recruited to the mitochondria, where it ubiquitinates various mitochondrial proteins [132-134]. Endogenous PARKIN has been shown to ubiquitinate mitochondrial localized Mfn1 and Mfn2 in both *Drosophila* and human cells [135-139], while overexpressed PARKIN can also ubiquitinate VDAC (Voltage Dependent Anion Channel), components of the mitochondrial transport TOM complex, fission protein FIS1, pro-apoptotic protein BAK, mitochondrial movement Rho GTPases (MIRO) 1 and 2, and mitochondrial hexokinase [140-143]. These ubiquitinated mitochondrial proteins can either be degraded by the proteasome, thus coordinating mitochondrial shape, cell metabolism, and

mitochondrial movement with mitophagy, or be recognized by an LC3- and ubiquitin-binding autophagy adaptor protein p62/SQSTM1 thereby promoting mitophagy [132, 133, 139, 144]. Recent studies provided evidence that PARKIN interaction with AMBRA1, PINK1 interaction with BECN1, or sterile α and TIR motif containing 1 (SARM1) and tumor necrosis factor receptor-associated factor 6 (TRAF6), may also play a role in mitophagy [130, 145, 146]. These studies suggest an essential role of PINK1 and PARKIN in mediating mitophagy of depolarized mitochondria (**Figure 9**).

In parallel with the PINK1/Parkin pathway, DJ-1 is also involved in removal of damaged mitochondria [147]. DJ-1 levels increase at mitochondria following oxidative damage in both fibroblasts and neurons, with mitochondrial removal dependent on PARKIN and possibly PINK1 [148]. DJ-1 knockout neuroblastoma cells exhibit reduced mitochondrial membrane potential and increased mitochondrial fragmentation that is reversible upon treatment with glutathione [149]. These models demonstrate the importance of key mitophagy genes in maintaining proper mitochondrial health and function, as well as preventing damage associated with an increased production of free radical species.

It should be noted that PINK1 and PARKIN translocation to damaged mitochondria either by direct depolarization or exposure to other mitochondrial toxins is highly dependent on cell type, levels of PINK1 and PARKIN expression, and growth conditions [134, 150-153]. Additional factors, including AF-6 [154], and FBXO7 [155], have been identified as regulating mitophagy by direct interactions with PARKIN.

Several genome-wide screens have further identified other possible mitophagy regulators [156-158]. In a screen to detect genes required for virophagy, 96 were found
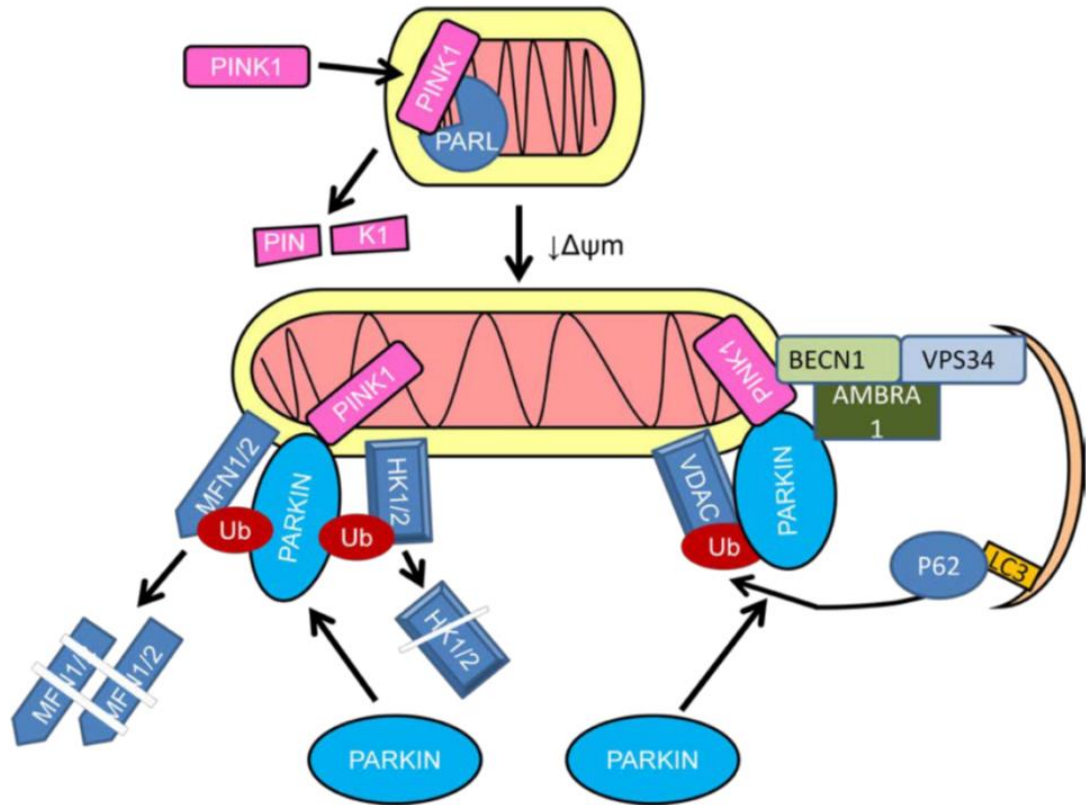
Figure 9: Mitophagy in response to loss of membrane potential. In healthy mitochondria PINK1 (PTEN-induced putative kinase 1) is targeted to the mitochondrial inner membrane where it is cleaved by the rhomboid protease of the IMM, presenilin associated rhomboid-like protease (PARL), and degraded. In stressed mitochondria with depleted membrane potential ($\downarrow\psi$ m), PARL is inactivated, and PINK1 accumulates in the mitochondria, recruiting the E3 ubiquitin ligase PARKIN. PARKIN can ubiquitinate Mitofusins 1 and 2 (MFN1 and 2), hexokinases, TOM complex components, FIS1, BAK, MIRO as well as VDAC. The ubiquitinated proteins are either degraded by the proteasome, or recognized by the ubiquitin and LC3-binding autophagy adaptor protein p62/SQSTM1 which recruits them to autophagosomes. PARKIN-AMBRA1 interaction, or PINK1-BECN1 interaction can also facilitate mitophagy.

to play a role in PARKIN-mediated mitophagy. From this screen, functions of one

particular protein, SMURF1 (SMAD specific E3 ubiquitin protein ligase 1 which encodes

a HECT-domain ubiquitin ligase), have been validated in mouse knockouts, as they

accumulate damaged mitochondria in the heart, brain and liver [156]. Another

independent screen has identified ATPIF1/IF1 (ATPase inhibitory factor 1) as promoting

collapse of ΔΨ and enabling of PARKIN recruitment to the mitochondria and mitophagy by blocking ATPase activity [159]. A third genome-wide siRNA screen further identified TOMM7, SIAH7, HSPA1L and BAG4, which can either enhance or decrease PARKIN accumulation at the mitochondria. Validation in additional cell lines confirmed that TOMM7 is not required for TOM-mediated general protein import, but plays an important role in anchoring PINK1 when ΔΨ is depleted, in both HCT116 cells and in human iPSC derived tyrosine hydroxylase positive neurons. SIAH3 knockdown in BE(2)-M17 neuroblastoma cells increased both PINK1 accumulation and PARKIN translocation to depolarized mitochondria. Independent of PINK1 protein accumulation, HSPA1L enhances, whereas BAG4 prevents PARKIN translocation to the mitochondria by direct interaction with PARKIN [158].

Downstream of PARKIN activation, it has been found that TBC1D15, a mitochondrial Rab GTPase-activating protein (Rab-GAP), inhibits excessive Rab7 activity, as well as associating with the mitochondria through binding FIS1 and with the isolation membrane through binding to LC3 family proteins. In addition to TBC1D15, TBC1D17 interacts with FIS1 and TBC1D15, and facilitates TBC1D15 function [160].

Recent studies have also identified additional mechanisms of mitophagy regulation in response to mtDNA damage, mitochondrial toxins, loss of iron, mitochondrial protein modification or viral infections. In bovine aortic endothelial cells, exposure to hemin led to mitochondrial dysfunction and activation of mitophagy [161]. In cybrid cells with a variety of pathogenic mtDNA mutations, loss of mitochondrial membrane potential alone could not trigger mitophagy. But when coupled with the inhibition of mTOR by rapamycin, mitophagy occurred [162]. In Akita$^{+/Ins2}$-derived β-

cells, mutations in the insulin 2 gene led to ER stress, mitochondrial damage, which was associated with increased Drp-1 and decreased Mfn1, p62 and PARKIN [163]. In primary human fibroblasts, iron chelation induced mitophagy, which was independent of PINK1 or PARKIN, but interestingly was dependent on glycolysis [164].

In cells undergoing high rates of oxidative phosphorylation, the GTPase Rheb can be recruited to the mitochondria, where it interacts with Nix and LC3 to promote mitophagy and maintain an active and healthy mitochondrial pool [165]. Starvation-induced PI3K/AKT activities block the translocation of DRAM to mitochondria by direct physical interactions between p-KT and DRAM, thereby attenuating mitophagy [166]. Additional factors, including HMGB1 and HSPB1 enable mitophagy, while the exact mechanisms of their actions are yet to be defined [167]. Interestingly, PINK1 can also engage mitophagy of energetically healthy mitochondria in response to expression of unfolded proteins in the mitochondrial matrix, or when LONP1, a mitochondrial protease, is knocked down [168]. In addition, autophagosome-independent, PARKIN and PINK1-dependent lysosome-mediated degradation of mitochondria has also been reported [169].

In primary cortical neurons and SH-SY5Y cells, rotenone, staurosporine, and 6-hydroxydopamine caused externalization of the mitochondrial lipid cardiolipin to the mitochondrial surface, which is then recognized by LC3 to signal removal by mitophagy. When cardiolipin synthesis or transport is blocked by siRNA-mediated knockdown of cardiolipin synthase or phospholipid scramblase-3, mitochondria are no longer engulfed by the autophagosome, indicating that cardiolipin externalization is necessary for mitophagy in response to these toxins [170].

In HepG2 cells, siRNA mediated knockdown of GCN5L1, an essential component of the mitochondrial acetyltransferase program, leads to an increase of mitochondrial associated LC3-II, p62 and protein ubiquitination, as well as an increase of LAMP-1 co-localization with the mitochondria, and decreased mitochondrial mass and protein levels. The GCN5L1 knockdown induced mitophagy is dependent on SIRT3, ATG5 and p62, but not PARKIN. The whole cell levels of p-S6K, p62 and LC3-II/LC3-I are unchanged in response to GCN5L1 knockdown, indicating a specific effect on mitophagy. Interestingly, the increased mitophagy in response to GCN5L1 depletion led to an increased resistance to mitochondrial stressors such as rotenone and paraquat [171].

Mitophagy in disease

Mitochondrial quality control is important in all disease as dysfunctional mitochondria may contribute to accumulation of reactive oxygen species (ROS) which can then damage nuclear and mtDNA [172]. However, in PD this especially important, rotenone has been show to induce mitophagy in SH-SY5Y cells and primary neurons, with externalization of cardiolipin acting as the signal to remove damaged mitochondria. Once externalized cardiolipin is recognized and bound by LC3 to recruit mitochondria to the autophagosome [170]. MPP$^+$, a metabolite of MPTP which induces parkinsonism in humans as mentioned above, has been shown to induce mitophagy in neuroblastoma SH-SY5Y cells in a MAPK, ATG5, ATG7, and ATG8 dependent, but BECN1 independent manner [173].

SUMMARY

PD is a complex disease influenced by both genetic background and environmental exposure. Even though the exact causes of idiopathic PD are unknown, as discussed in this Chapter, there is strong evidence that an interplay between aggregated aSyn, autophagic failure and mitochondrial dysfunction is present and that they contribute to disease pathogenesis. However, the exact role of how autophagy affects mitochondrial quality and protein homeostasis remains unclear. Research accomplished in this thesis will specifically address two key points: the impact of autophagy on mitochondrial metabolism and on neuronal survival upon exposure to exogenous aSyn fibrils.

Chapter 2 will summarize the necessary materials and methods used in our studies including neuronal culture, protein analysis via western blot and immunocytochemistry, cell death assays, and mitochondrial bioenergetics, structural fragmentation, damage, and targeted metabolomics.

Mitochondria are important for cell metabolism and ATP generation via oxidative phosphorylation through the electron transport chain, fatty acid oxidation, and the TCA cycle. Targeted removal of dysfunctional or damaged mitochondria via mitophagy is presumed to be essential in maintaining mitochondrial quality, cell viability and homeostasis. To our knowledge, there have been no prior studies that have specifically examined mitochondrial bioenergetics and TCA cycle metabolism in response to pharmacological inhibition of autophagy in primary neurons. Chapter 3 will present data that specifically addresses this issue by using lysosomal inhibitors and investigating

mitochondrial damage, bioenergetics, and TCA metabolism in rat primary cortical neurons.

Furthermore, as aSyn is an important protein associated with PD pathology and it can spread from neuron to neuron and propagate disease progression. Chapter 4 will present studies on how neuronal accumulation of endogenous aSyn on exposure to exogenous aSyn fibrils is affected by autophagy activation and whether neuronal survival can be enhanced by autophagy activation.

In Parkinson's disease, current therapies seek to only mitigate symptoms whereas autophagy provides a potential therapeutic pathway to target in order to clear protein aggregates and restore neuron health through restoration of mitochondrial quality by mitophagy and clearance of aberrant protein aggregation through autophagy.

Through the studies presented in this thesis, we found that active autophagy is essential for mitochondrial maintenance in primary cortical rat neurons and when autophagy is inhibited mtDNA damage accumulates, mitochondrial respiration decreases, and TCA metabolites are altered. These data highlight the importance of mitophagy in maintaining cellular health. In primary cortical mouse neurons exposed to aSyn pre-formed fibrils we found that aSyn accumulates in neurons and became phosphorylated. Interestingly, even though trehalose was able to increase autophagosome levels and increase basal cell viability on its own, these mechanisms were insufficient to remove aggregates or prevent aSyn fibril-induced cell death.

Taken as a whole, these studies suggest that autophagy is needed to maintain neuronal health, but under PFF exposure and likely in PD as well, aSyn fibrils may

escape autophagic clearance and still induce cytotoxicity. Chapter 5 will discuss these points further and examine remaining unanswered questions and future directions.

A COMPREHENSIVE APPROACH TO ASSESS MITOCHONDRIAL QUALITY
CONTROL MECHANISMS AND CELLULAR CONSEQUENCES

by

MATTHEW REDMANN, GLORIA BENAVIDES, WILLAYAT WANI, TAYLOR
BERRYHILL, XIAOSEN OUYANG, MICHELLE JOHNSON, SARANYA RAVI,
STEPHEN BARNES, VICTOR DARLEY-USMAR, AND JIANHUA ZHANG

In preparation

Adapted for dissertation

32

CHAPTER 2

METHODS

INTRODUCTION

Mitochondria are complex cellular organelles responsible for maintaining cellular

energy status and homeostasis through near constant production of ATP and ion buffering

[174]. Mitochondria produce energy by establishing an electrochemical gradient through

the pumping of hydrogen ions from the mitochondrial matrix across the inner membrane

into the intermembrane space. These ions flow back through ATP synthase converting

ADP to ATP. The electron transport chain serves to facilitate the movement of hydrogen

ions and the removal of electrons via oxygen. These organelles are highly dynamic and in

a constant state of structural flux through fission and fusion processes and have important

roles in cellular signaling cascades [175].

Mitochondrial quality is maintained by autophagy, which is an indispensable

cellular process responsible for the clearance of cellular debris, organelles, and damaged

proteins [73, 85, 176]. This complex process has been outlined above but briefly, the

process of macroautophagy consists of three main stages [177]. First is an initiation step

that results in autophagosome nucleation and while many regulatory proteins work on

concert to fine tune the on/off state of autophagy initiation, mTOR (mammalian target of

rapamycin) acts as a master regulator of canonical autophagy initiation [178]; while other

mechanisms also exist, such as those initiated by the disaccharide trehalose [106]. The

subsequent elongation step ends with a fully developed double membrane

autophagosome that has sequestered cellular cargo. The cycle is completed in the final

stage where the autophagosome combines with the lysosome and its contents are

degraded by lysosomal hydrolases. This process is essential for cellular health [179, 180].

Specific recycling of mitochondrial by autophagy, termed mitophagy, is important for

maintaining proper mitochondrial function [127, 181, 182]. Over time mitochondria

acquire damage to both DNA and protein [183-185]. If this damage continues to accrue

and is not cleared through mitophagy, the network as a whole is unable to provide

adequate energy through ATP and other metabolites [186].

Mitochondrial dysfunction is a hallmark of pathologies in tissues that are highly

energetic, in particular the heart and brain. In the heart when mitochondria lose their

energetic capacity, cardiomyocyte dysfunction occurs, ultimately leading to cardiac

disease [187]. In the brain, mitochondrial dysfunction has been frequently implicated in a

range of neurodegenerative diseases, including Parkinson's disease (PD). The exact cause

of PD is unknown, but there appears to be a cytotoxic interplay between protein

aggregation and mitochondrial dysfunction, ultimately both playing a role in significant

loss of dopaminergic neurons [188]. Notable examples of the importance of mitochondria

at the center of this disease are evidenced by toxin-induced models of PD via

administrations of rotenone, paraquat, and MPTP [64]. These compounds have been

reported to act through either complex I inhibition or through redox cycling [189-191].

In order to provide substrates for ATP production through oxidative

phosphorylation, mitochondria are also tasked with taking key breakdown products from

glycolysis and converting them to usable intermediates. This is accomplished through the

TCA cycle. This pathway is highly integrated with cellular metabolism, but is comprised

of 9 key enzymes that are responsible for supplying the electron transport chain (ETC) with its energy carrying intermediates. Many other pathways feed into the TCA cycle, one such pathway important for neurons is glutaminolysis, which is the serial conversion of glutamine to glutamate and finally to alpha-ketoglutarate that can be utilized as a TCA intermediate.

Protocol Concept

Given the importance of mitochondria in health and disease, here we have outlined a workflow using a comprehensive approach of existing technology to investigate different facets of mitochondrial health in a given disease paradigm (**Figure 1**). We have grouped similar modalities together allowing labs to pick and choose the methods available to them. Noting the importance of mitochondria in neurodegenerative disease and for the purposes of this dissertation, we have included methods for assaying aSyn levels as well. The workflow is organized by specific questions. Techniques include western blot analyses, confocal imaging analyses, quantitative PCR, bioenergetic assessment using Seahorse extracellular flux analyses, and metabolomics using mass spectrometry.

Materials

Tables of needed chemicals, PCR primers, antibodies, consumables and equipment needed are listed in **Tables 1 through 4.**
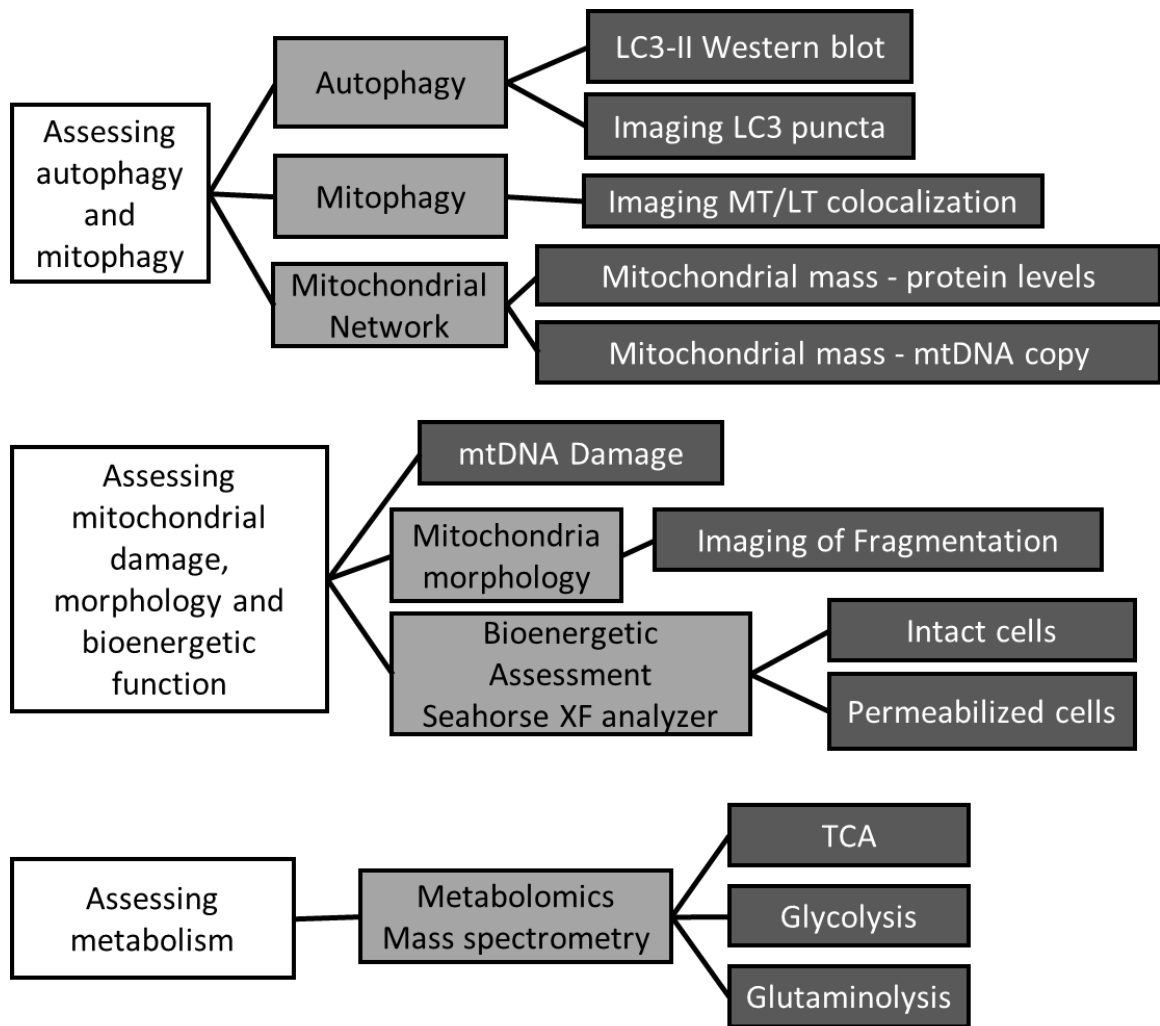
Figure 1: Workflow of comprehensive mitochondrial assessment. Using primary neurons, a comprehensive assessment of mitochondrial function can be obtained by employing diverse techniques. Shown here is a comprehensive list of experiments used to examine autophagy, mitophagy, mitochondrial damage, mitochondrial morphology, bioenergetic function, and metabolic activities that involve the mitochondrion.

Table 1: Minimum required equipment and consumables	
Equipment	**Consumables**
Seahorse Biosciences XF-96 extracellular flux analyzer	1.5mL tubes
37°C 5% CO2 incubator	15mL tubes
37°C non-CO2 incubator	50mL tubes
-80 freezer	p20-1000 tips
37°C water bath	XF96 Seahorse Plates
Pipetboy	12, 24, and 48 well plates
Multi-channel pipets for plating	Nunc® Lab-Tek® II chambered coverglass
pH meter	60x15mm petri dishes
Centrifuge capable of spinning 1.5mL, 15mL and 50mL conical tubes.	100x20mm petri dishes
Hemocytometer	Glass culture tubes and caps
Dissection tools	Cuvettes
Dissecting scope	PCR plates/Strips
PCR Cycler	PVDF
Real-time PCR cycler	
UV spectrophotometer	
HPLC system	
Mass spectrometer	
SDS-PAGE boxes	

Table 2: Required reagents				
Compound	**Manufacturer**	**Catalog #**	**Function**	**Conc.**
Chloroquine	Sigma	C6628	Lysosome Inhibitor	40µM
3MA	Sigma	M9281	PI3K CIII Inhibitor	10mM
E64	Sigma	E3132	Cysteine Protease Inhibitor	10-100µM
Pepstatin A	Sigma	P5318	Aspartic Protease Inhibitor	100 µM
Neurobasal medium	Gibco	21103-049	Cell Growth Medium	1x
Neurobasal A Medium	Gibco	10888-022	Cell Growth Medium	1x
B27 neuronal supplement	Gibco	17504044-044	Medium Supplement	1x
Penicillin/streptomycin	Gibco	15140-122	Antimicrobial Agent	1%
L-glutamine	Gibco	25030-081	Medium Supplement	0.5mM

Glutamax	Gibco	35-050-061	Medium Supplement	0.25X
Trypan Blue	ThermoFisher	15250061	Cell Counting	0.04%
Papain	Worthington	LS003118	Tissue digestion	1mg/mL
Oligomycin	Sigma	75351	ATP synthase inhibitor	1 µg/mL
FCCP	Sigma	C2920	Uncoupling agent	1 µM
Rotenone	Sigma	R8875	Complex I Inhibitor	1 µM
Antimycin-A	Sigma	A8674	Complex III Inhibitor	10 µM
Pyruvate	Sigma	P5280	TCA Intermediate	10mM
Malate	Sigma	M6413	TCA Intermediate / Standard	1mM
ADP	Sigma	A2754	CIV substrate	1mM
Succinate	Sigma	S2378	TCA Intermediate / CII substrate / Standard	10mM
PMP	Seahorse	102504-100	Permeabilizer	1nM
Sodium Azide	Sigma	S2002	Complex IV/V Inhibitor	20mM
TMPD	Sigma	T7394	Electron Donor	0.5mM
Ascorbate	Sigma	A7631	Reducing agent for TMPD	2mM
Oxaloacetate	Sigma	O4126	Citrate Synthase Activity	20mM
Acetyl-CoA	Sigma	A2056	Citrate Synthase Activity	10mM
DTNB	Sigma	D8130	Citrate Synthase Activity	20mM
Sodium Pyruvate	Sigma	P2256	TCA Intermediate / Standard	0.05-10 mg/ml
Lactate	Sigma	71720	TCA Intermediate / Standard	0.05-10 mg/ml
Citrate	Sigma	251275	TCA Intermediate / Standard	0.05-10 mg/ml
cis-Aconitate	Sigma	A3412	TCA Intermediate / Standard	0.05-10 mg/ml
Isocitrate	Sigma	I1252	TCA Intermediate / Standard	0.05-10 mg/ml
Alpha-Ketoglutarate	Sigma	K2010	TCA Intermediate / Standard	0.05-10 mg/ml
Succinate	Sigma	S3674	TCA Intermediate / Standard	0.05-10 mg/ml
Fumarate	Sigma	47910	TCA Intermediate	0.05-10

			/ Standard	mg/ml
Malate	Sigma	240176	TCA Intermediate / Standard	0.05-10 mg/ml
Oxaloacetate	Sigma	O4126	TCA Intermediate / Standard	0.05-10 mg/ml
Glutamate	Sigma	G1251	TCA Intermediate / Standard	0.05-10 mg/ml
Glutamine	Sigma	G3126	TCA Intermediate / Standard	0.05-10 mg/ml

Table 3: Western blot and imaging antibodies and dyes			
Antibody	Manufacturer	catalog #	Concentration (WB/ICC)
Aconitase	n/a	n/a	1:1000
Actin	Sigma	A5441	1:2500
Alpha-Synuclein	Santa Cruz	SC-7011-R	1:2500
Alpha-Synuclein S129	Bioreagents	PA1-4686	N/A / 1:2000
Alpha-Synuclein S129	Covance	MMS-5091	N/A / 1:5000
Citrate Synthase	Abcam	AB96600	1:1000
Complex I	Abcam	AB110413	1:1000
Complex II	Abcam	AB110413	1:1000
Complex III	Abcam	AB110413	1:1000
Complex IV	Abcam	AB110413	1:1000
Complex V	Abcam	AB110413	1:1000
GFAP	Dako	Z0334	N/A / 1:500
LC3	Sigma	L8918	1:2000 / 1:500
LysoTracker Green	Molecular Probes	L7526	110nM
MAP2	Sigma	M4403	N/A / 1:1000
MitoTracker CMXRos	Molecular Probes	M7512	30-50nM
MitoTracker Green	Molecular Probes	M7514	30-50nM
p62	Abnova	H00008878-M01	1:2000
PGC-1a	Santa Cruz	SC-13067	1:1000

Table 4: Mitochondrial DNA assay primers				
Assay	Species	Target	Direction	Sequence
Copy Number	Mouse	18s Ribosome	Forward	AAACGGCTAC CACATCCAAG
Copy Number	Mouse	18s Ribosome	Reverse	CAATTACAG GGCCTCGAAAG
Copy Number	Mouse	MSMT	Forward	CCCCAGCCATA ACACAGTATCAAAC

Copy Number	Mouse	MSMT	Reverse	GCCCAAAGAAT CAGAACAGATGC
Copy Number	Rat	18s Ribosome	Forward	CGAAAGCAT TTGCCAAGAAT
Copy Number	Rat	18s Ribosome	Reverse	AGTCGGCATC GTTTATGGTC
Copy Number	Rat	RMT	Forward	CCAAGGAATT CCCCTACACA
Copy Number	Rat	RMT	Reverse	GAAATTGCGA GAATGGTGGT
DNA Damage	Mouse	M13281	Forward (short)	GCAAATCCATA TTCATCCTTCTCAAC
DNA Damage	Mouse	M13597	Forward (long)	CCCAGCTACTACC ATCATTCAAGTAG
DNA Damage	Mouse	M13361	Reverse	GAGAGATTTTAT GGGTGTAATGCGGTG
DNA Damage	Rat	RMT	Forward (long)	GGACAAATATCA TTCTGAGGAGCT
DNA Damage	Rat	RMT	Reverse (long)	GGATTAGTCAGC CGTAGTTTACGT
DNA Damage	Rat	RMT	Forward (short)	CCAAGGAATTCC CCTACACA
DNA Damage	Rat	RMT	Reverse (short)	GAAATTGCGAGA ATGGTGGT

PROTOCOL: STEPS AND PROCEDURES

Neuron Preparation

Primary neurons isolated from either rat or mice provide an excellent platform in which to test aspects of neuropathologies, especially before, during, or after either neurotoxin or neuroprotective treatments administered through genetic and/or pharmacological means. And while there are certainly some alterations of metabolism due to being cultured, primary neurons provide more relevant read-outs than immortalized cells. This is especially true when measuring parameters of mitochondrial metabolism and function.

The neuron isolation workflow is diagrammed in **Figure 2**. The day before isolation, coat 24 well tissue plates for ≥1 hour at room temperature in a poly-L-lysine coating solution (25 mL water, 12.5 mL 200 mM Boric Acid, 10 mL 50 mM Borax, 2.5 mL of 2 mg/mL filtered Poly-L-lysine). After coating, wash plates twice with ddH_2O and allow to dry before storing at 4°C until use. Brain tissue can then be isolated from E18 pups excised from Sprague-Dawley rats. Once cortices are removed from the brain, they are to be dissected in ice cold HBSS media and placed in a short-term storage solution (2 mL per brain) until further processing (500 mL HBSS supplemented with 250 µL 20% Glucose, 5 mL 1M HEPES pH 7.3, 5 mL 100x Pyruvate). Long exposures of the tissue to open air should be avoided if possible during isolation.

Next, decant storage media from cortex tissue and replace with 1 mL per brain of papain solution (activate papain for ~15 min at 37°C prior to addition) and incubate for 20 min at 37°C with gentle agitation every few minutes. After 20 min, add 2 mL of neurobasal media (NBM) supplemented with B27, pen/strep, and L-glutamine per brain to dilute digestion solution. Then wash brain tissue once with 1 mL per brain of NBM. Mechanically separate tissue by trituration in 4 mL per brain of NBM. After allowing a few minutes to settle, remove debris and add 10 µL per brain of 40 µg/mL DNase I. To remove cells from DNase solution, pellet the cells by centrifugation for 5 min at ~250 x g. Decant the supernatant, and resuspend the cells in 2 mL of NBA per brain and count by hemocytometer. Neurons can then be plated at desired densities for analysis by western blot, seahorse, imaging or metabolomics approaches.
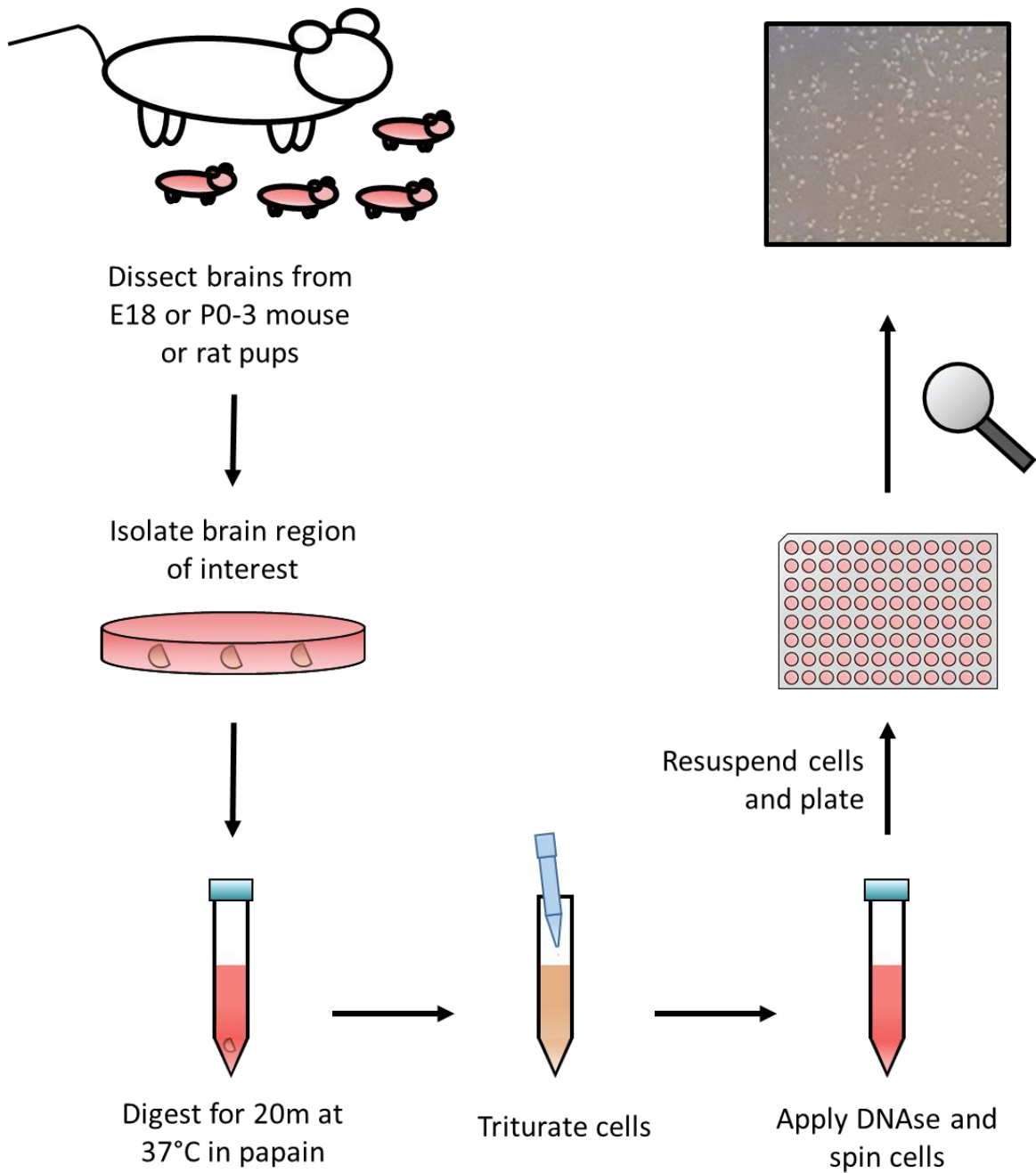
Figure 2: Primary neuronal culture. Briefly, pups can be obtained from mice or rats ranging from E18 to p0-3 in age. Desired brain region can then be micro-dissected from the brain. Tissue is then digested using a papain solution for 20 min at 37°C with gentle agitation every ~3 min. Cells are then triturated using 1 mL pipet tip with smooth edges. Remaining debris should be removed and DNase added. Cells are then centrifuged at ~250 x g for 5 mins. Cells are then to be resuspended, counted, and plated.

Exposing cells to biological or pharmacological reagents

Primary neurons can be maintained for several weeks during their culture and as they age and mature, they extend their cellular processes and integrate into ever more reticulated networks. We have traditionally performed experiments between 7 and 21 days *in vitro* (DIV). For exposing neurons to reagents or treatments, half of the media is to be removed and then replaced with NBM containing only pen/strep and L-glutamine for short studies. For long treatment times B27 should be included. B27 is a potent cocktail of signaling molecules, antioxidants, and supplements, and depending on the study can be excluded if it interferes experimentally.

Assessing effects of lysosome inhibitors on autophagy proteins

Given the importance of autophagy in maintaining healthy mitochondrial populations, an initial assessment of two key autophagy components can be utilized to determine if aberrations in autophagy may alter mitochondrial quality. For western blot analyses, we routinely plate neurons in 24 well plates at 480K cells per well. After treatments, protein can be collected by first washing the cells with ice cold PBS. Cells can then be lysed with RIPA buffer (50 mM Tris pH 7.8, 150 mM NaCl, 2 mM EDTA, 1% Triton X-100, and 0.1% SDS) in the presence of protease and phosphatase inhibitors. After 20 min on ice, cells can then be scraped from the wells and placed in 1.5 mL Eppendorf tubes for centrifugation at 16,800 x g for 20 min at 4°C. Protein content can then be determined by DC protein assay. Equal amounts of protein can be loaded and separated by SDS-PAGE using 12% or 15% gels.

In **Figure 3** we have measured the scaffold, ubiquitin binding and autophagy substrate protein p62 as well as both cytosolic LC3-I and autophagosome incorporated LC3-II in response to various autophagy modulators by western blot analyses. In response to 3-methyladenine, an autophagy initiation inhibitor, LC3-II levels remained unchanged, but significant increases in p62 are indicative of decreased clearance through autophagy inhibition. However, in the case of lysosomal inhibitors E64 and Pepstatin A, no changes were observed in p62 but significant increases in LC3-II were noted. Furthermore, the LC3-II / LC3-I ratio can be calculated to measure the conversion of LC3-I to LC3-II (**Figure 3 A-E**). Similar to other lysosome inhibitors, chloroquine (CQ) induces accumulation of LC3-II as well as increasing the LC3-II/LC3-I ratio (**Figure 3 F-J**). CQ has the benefit of being water soluble and inhibits lysosome enzyme function through increased pH, opposed to inhibition of specific lysosomal proteases as E64 and pepstatin A.

Using chloroquine, autophagic flux can be determined. This is the rate in which autophagosomes are being cleared by the lysosome. Chloroquine, by increasing lysosomal pH inhibits autophagosome clearance, causing a buildup. This buildup can be inferred to be the amount of autophagy induction. This concept is further explained in **Figure 4**.

Additional measurements of the autophagy protein LC3 can be made by immunocytochemistry. **Figure 5** shows primary neurons probed for LC3 after 24 h CQ exposure. This experiment was performed by plating neurons at 240,000 cells per well on autoclaved glass coverslips in 24 well plates. After treatment, cells were fixed using a mixture of 4% paraformaldehyde and 4% sucrose for 20 minutes followed by washes
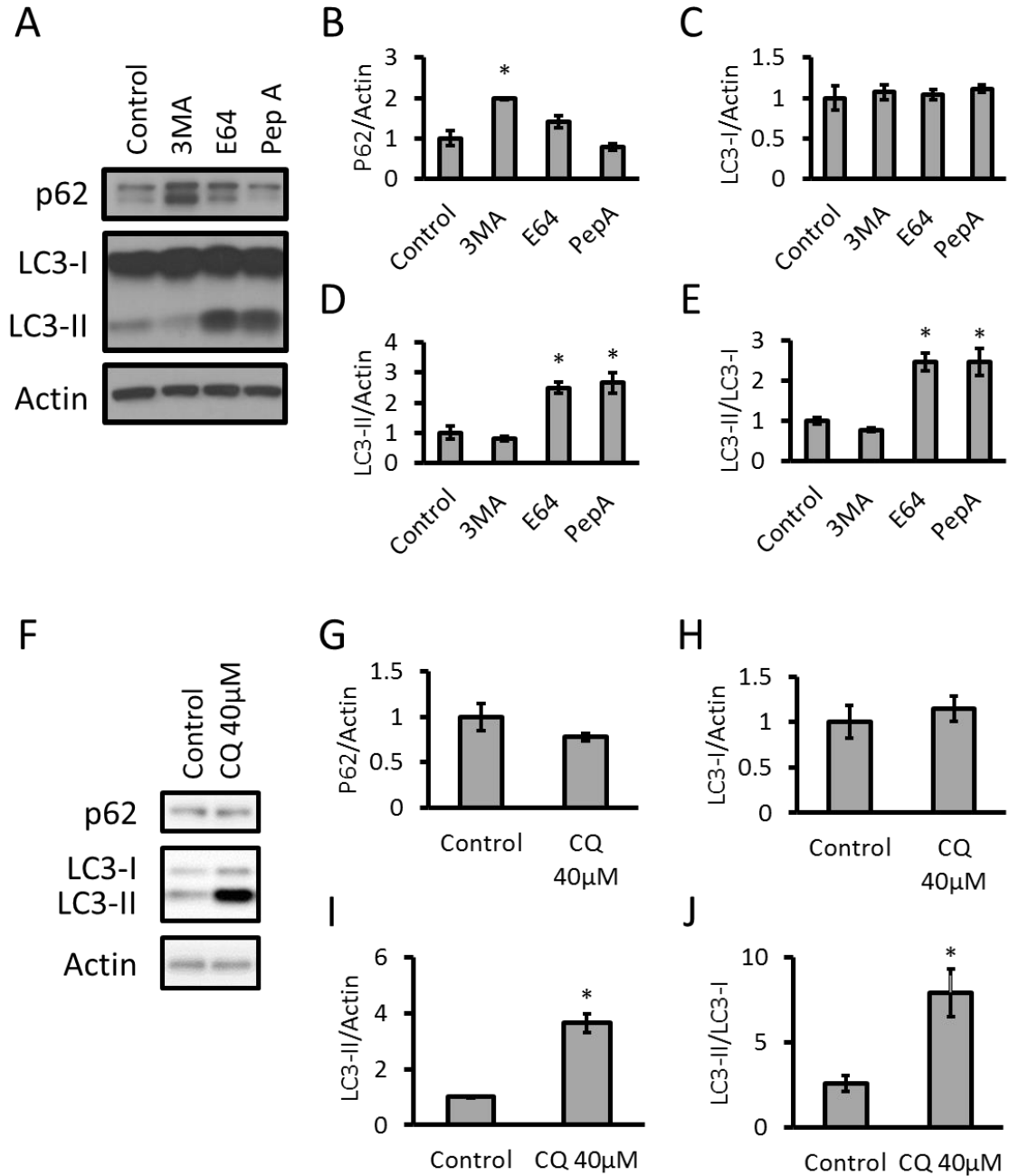
Figure 3: Assessing autophagosomal LC3-II and autophagy adaptor/substrate p62 levels. (**A-E**) Primary cortical rat neurons were exposed to 3MA (10mM), E64 (100µM), or pepstatin A (100 µM) for 24 h. Levels of p62, LC3-I and LC3-II were measured by western blot analysis. A p62 isoform can occasionally be observed as a doublet if the gel is run long enough, as seen in A. (**F-J**) Primary cortical rat neurons exposed to 40 µM chloroquine (CQ) for 4 h and then analyzed by western blot for p62, LC3-I and LC3-II. *$p < 0.05$ compared to control, n=3 experimental repeats.
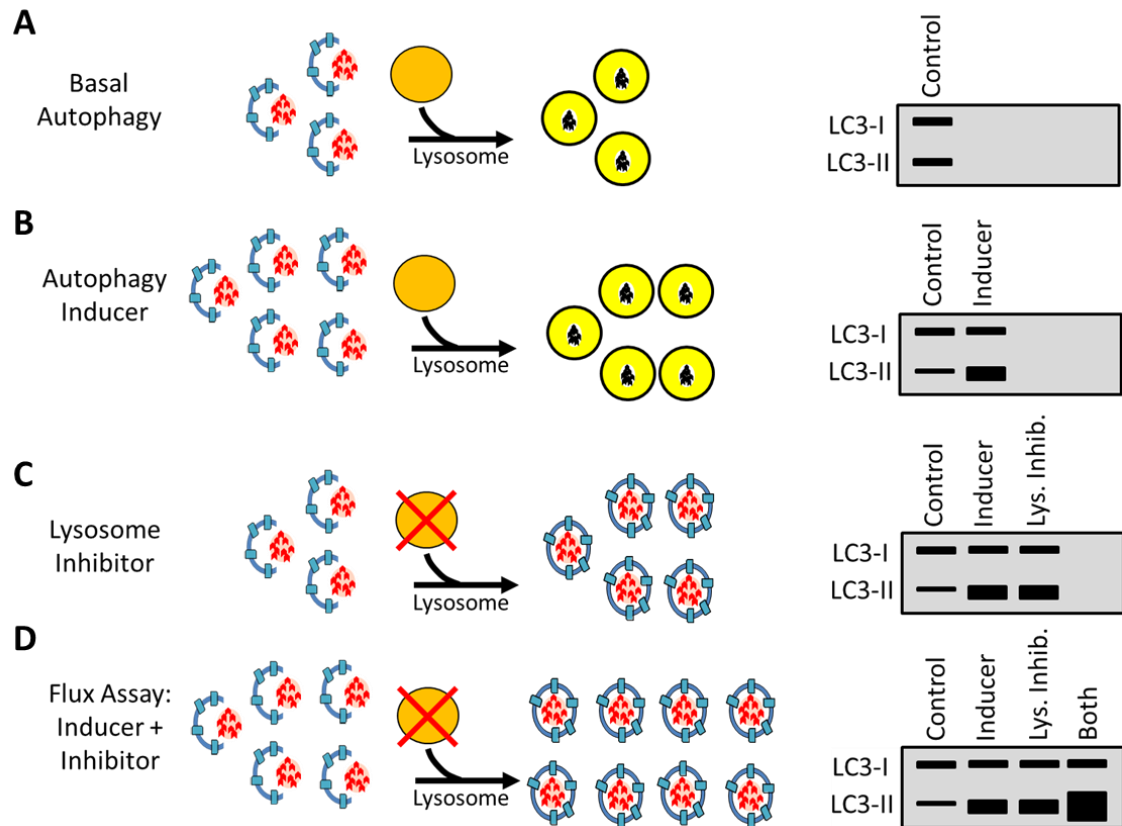
Figure 4: Schematic of assessing autophagic flux using lysosomal inhibitors. (**A**) Idealized western blot of LC3 under basal autophagy conditions. (**B**) Addition of autophagy inducer causes levels of LC3-II to increase. (**C**) Addition of lysosome inhibitor induces LC3-II increase similar to that of autophagy inducer alone. Note that autophagy induction and inhibition lead to similar outputs. (**D**) Co-treatment of an inducer and inhibitor lead to a greater increase than either treatment alone and thus autophagic flux can be inferred.

with PBS. After fixation, cells were blocked with 5% BSA and 10% horse serum and then probed for LC3 (1:500). Alexa Fluor 488 (1:2000) and Hoechst (1:2000) were added before slides were mounted with Fluoromount G and visualized with a Leica TCS SP5 V confocal laser scanning microscope. Quantification can be done by counting puncta per cell or cells with puncta. This same protocol can be utilized with other antibodies for MAP2 (1:1000) and GFAP (1:1000).
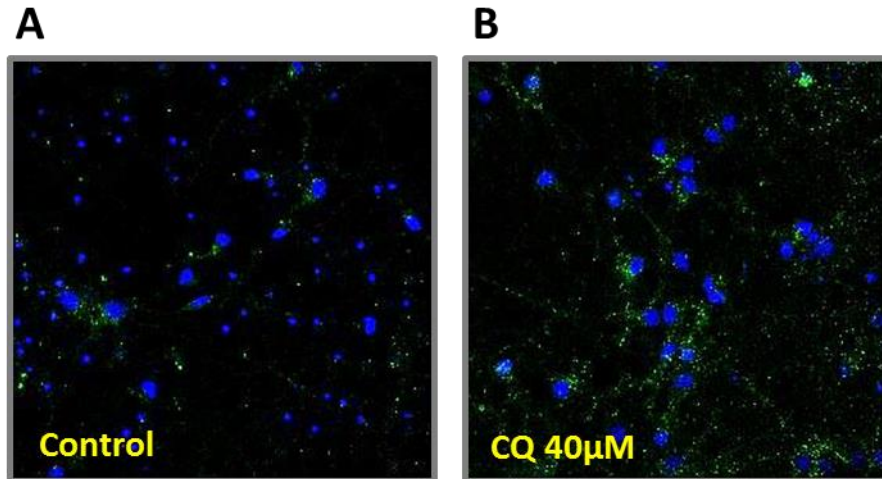
Figure 5: Assessment of LC3-II puncta. (**A**) Representative immunocytochemistry images of primary neurons plated at 250,000 per well and probed for LC3 puncta (green) and counterstained with nuclear dye Hoechst (blue). (**B**) Neurons as before, but treated with 40 µM chloroquine for 4 hours where increased autophagosome puncta staining is evident. Typically, ~200 neurons can be used for each experiment for quantification with n=3 experimental repeats.

Assessing changes in aSyn after PFF exposure.

For assessment of aSyn by western blot, cells can be seeded on 24- well plates at 480,000 or at 240,000 on 48-well plates. For treatment of cells with aSyn pre-formed fibrils, PFFs can be generated by expressing in *E. coli* a human wildtype *SNCA* gene cloned into pRK172, as reported previously [192]. Bacteria can then be grown under antibiotic selection, harvested, homogenized and dialyzed before being purified through size exclusion and ionic exchange columns. Five mg/mL of protein are then to be incubated at 37ºC for 1 week to produce fibrils. Before applying to cells, fibrils should be sonicated 60 times over 40 seconds [193]. After treatment, cells can be analyzed by western blot or immunocytochemistry. For western blot, cells can be lysed, prepared, and separated by SDS-PAGE as above. For assessment of aSyn by immunocytochemistry, cells can be seeded on autoclaved glass coverslips as above. Insoluble fractions of aSyn

can be determined by the addition of 1% Triton X-100 to the 4% PFA/Sucrose fixative

mixture before fixation of the neurons. After fixation, cells can be permeabilized with

0.1% Triton TX-100 and blocked with 3% BSA in PBS for 20 minutes. Determination of

the amount of S129 phosphorylated aSyn can be determined by specific antibodies. In

this dissertation we have employed two: Affinity Bioreagents (PA1-4686 1:2000) and

Covance-81A (MMS-5091 1:5000).

Assessing changes in mitochondrial protein

Once the state of autophagy has been investigated, the levels of all five

mitochondrial complexes can be assayed by measuring representative subunits from each

complex. This can be done individually by purchasing separate antibodies and probing

each complex individually. However, one efficient alternative approach is to use

commercially available antibody cocktails that probe for all five complexes at once

(**Figure 6 A, B**). At this stage, further investigation of mitochondrial proteins involved in

the TCA cycle can be performed. In **Figure 6 C** we have performed western blot analyses

for aconitase and citrate synthase as representative TCA enzymes.

Assessing changes in mitochondrial DNA

It is also important to measure mitochondrial DNA copy number as an additional

indicator of mitochondrial mass. For DNA analyses, we routinely plate neurons in 24

well plates. This can be done by real-time PCR using mtDNA directed primers and

normalizing to nuclear DNA primers targeted to the 18S ribosome [194, 195] (**Table 4**).

We and others have used a mitochondrial DNA damage assay that calculates the amount

of lesions per mitochondrial genome, providing an assessment of mitochondrial health

[196, 197]. Lesion frequency was calculated as follows [196]:

$$\text{Lesion frequency per 16kb of each sample} = -Ln \left[\frac{\text{long PCR product / short PCR product}}{\text{mean of (long PCR product / short PCR product) from control group}} \right]$$
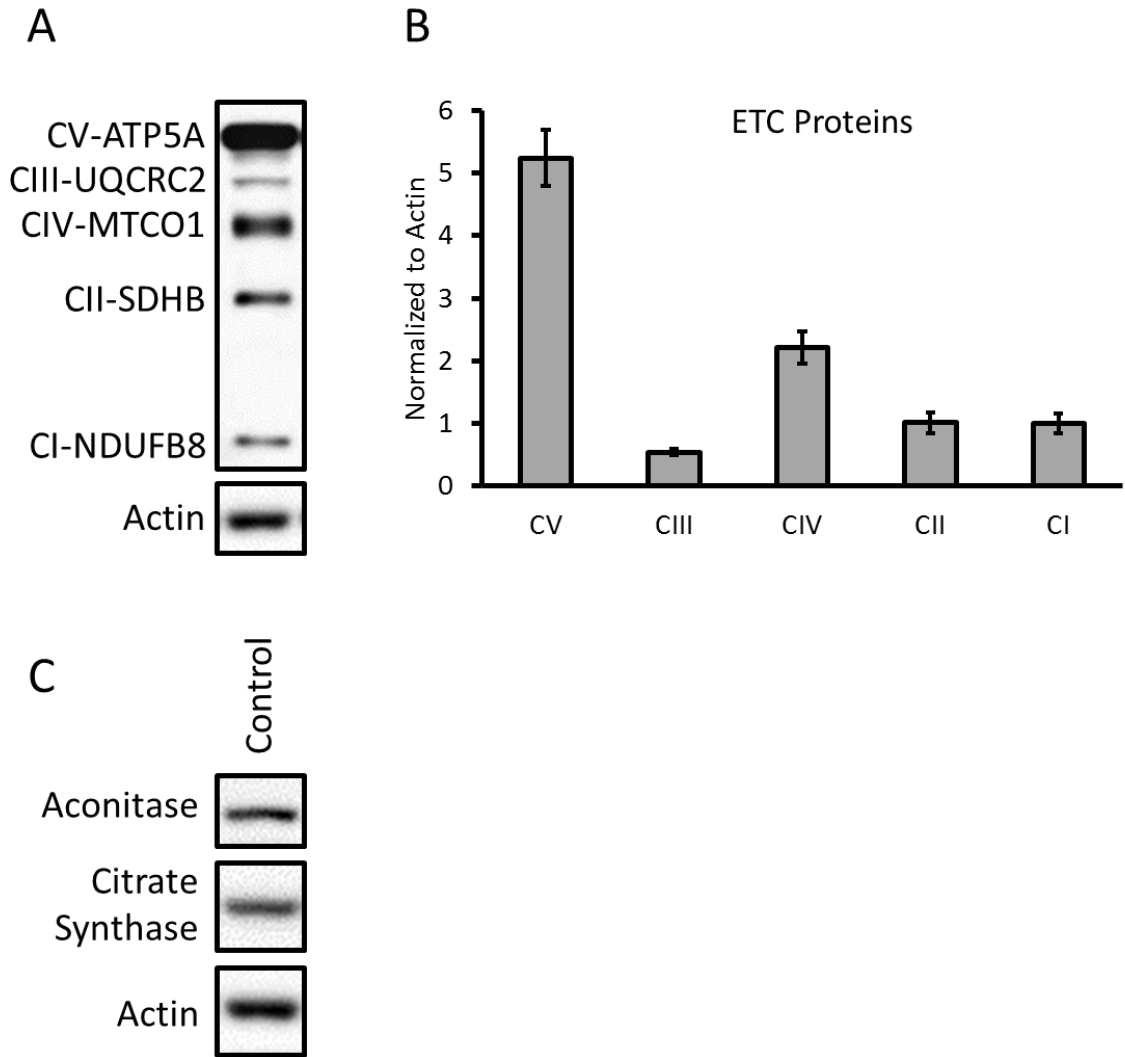
Figure 6: Assessment of mitochondrial ETC and TCA proteins. (**A, B**) Levels of mitochondrial electron transport chain complex proteins were analyzed by western blot of extracts from primary cortical neurons by using Abcam's total OXPHOS rodent antibody cocktail, n=3 experimental repeats, normalized to CI, no statistical analysis performed. (**C**) Levels of mitochondrial TCA enzymes aconitase and citrate synthase were measured by western blot.

Assessment of mitochondrial function utilizing Seahorse extracellular flux

The development of Seahorse extracellular flux technology has been instrumental to research that measures mitochondrial function. The last several years have also seen the development of several innovative techniques to measure novel parameters of mitochondrial function [198]. The principles and approaches of these methods have been outlined elsewhere, including how to optimize for plating densities and titrations for the optimal amount of oligomycin, FCCP, and antimycin A. Here we show how they can be employed as part of an integrated approach to assess mitochondrial quality control. For this analysis, we routinely plate neurons in XF96 plates with 5-10 technical repeats and then repeat experiments a minimum of 3 times using additional plates. In **Figure 7**, an idealized mitochondrial stress test consisting of sequential injection of oligomycin, FCCP, and antimycin A is presented to showcase the measurement of basal (OCR before oligomycin minus OCR after antimycin), ATP-linked (OCR before oligomycin minus OCR after oligomycin), proton leak (OCR after oligomycin minus OCR after antimycin), maximal (OCR after FCCP minus OCR after antimycin), reserve capacity (OCR after FCCP minus OCR before oligomycin), and non-mitochondrial (OCR after antimycin) parameters of mitochondrial oxygen consumption. **Table 2** lists all seahorse assay compounds and their optimized concentrations. After the assay, protein can be determined in individual wells and OCR can be normalized to total protein, thus correcting for any changes in cell density from well to well. An example set of data from a mitochondrial stress test is presented in **Figure 8** and relevant ETC modulators and their targets are illustrated in **Figure 9**.
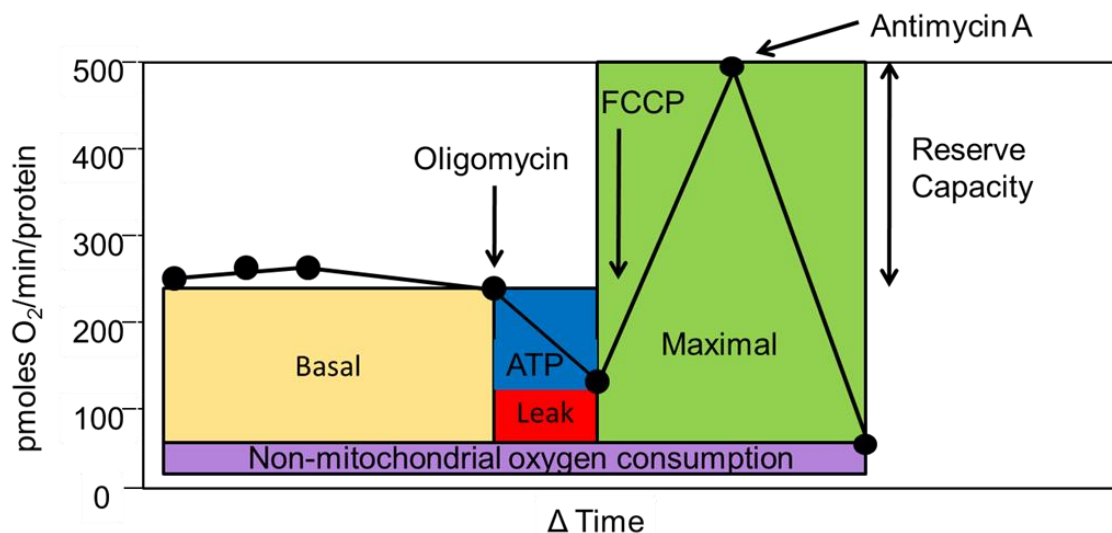
Figure 7: Schematic of mitochondrial stress test. Idealized OCR profile from mitochondria exposed to sequential injection of oligomycin, FCCP and antimycin A. From this trace, basal, ATP-linked, proton leak, maximal, reserve capacity and non-mitochondrial oxygen consumption can be calculated. The reserve capacity rate is determined from the difference between maximal and basal OCRs.

The intact-cell mitochondrial stress test used above is ideal for assessing the mitochondria's ability to provide energy in a cellular milieu. However, it may be necessary to assay for the function of individual mitochondrial complexes. This can be achieved by permeabilizing the cells and providing specific substrates for each complex [198]. In **Figure 10 A, B**, complex I and II substrate linked activities were measured by permeabilization with PMP and concurrent injection of pyruvate and malate that provides complex I substrates by generation of NADH through the TCA cycle. ADP is also added as a substrate for complex V. The serial injection of rotenone followed by succinate and additional ADP, serves to inhibit complex I linked oxygen consumption and while providing substrates for complex II. Under these conditions both complex I and II substrate linked oxygen consumption can be calculated under conditions in which ATP synthesis through complex V is rate limiting. Due to permeabilization and loss of cellular protein, normalizing to cellular protein is problematic and raw data is typically presented.

51
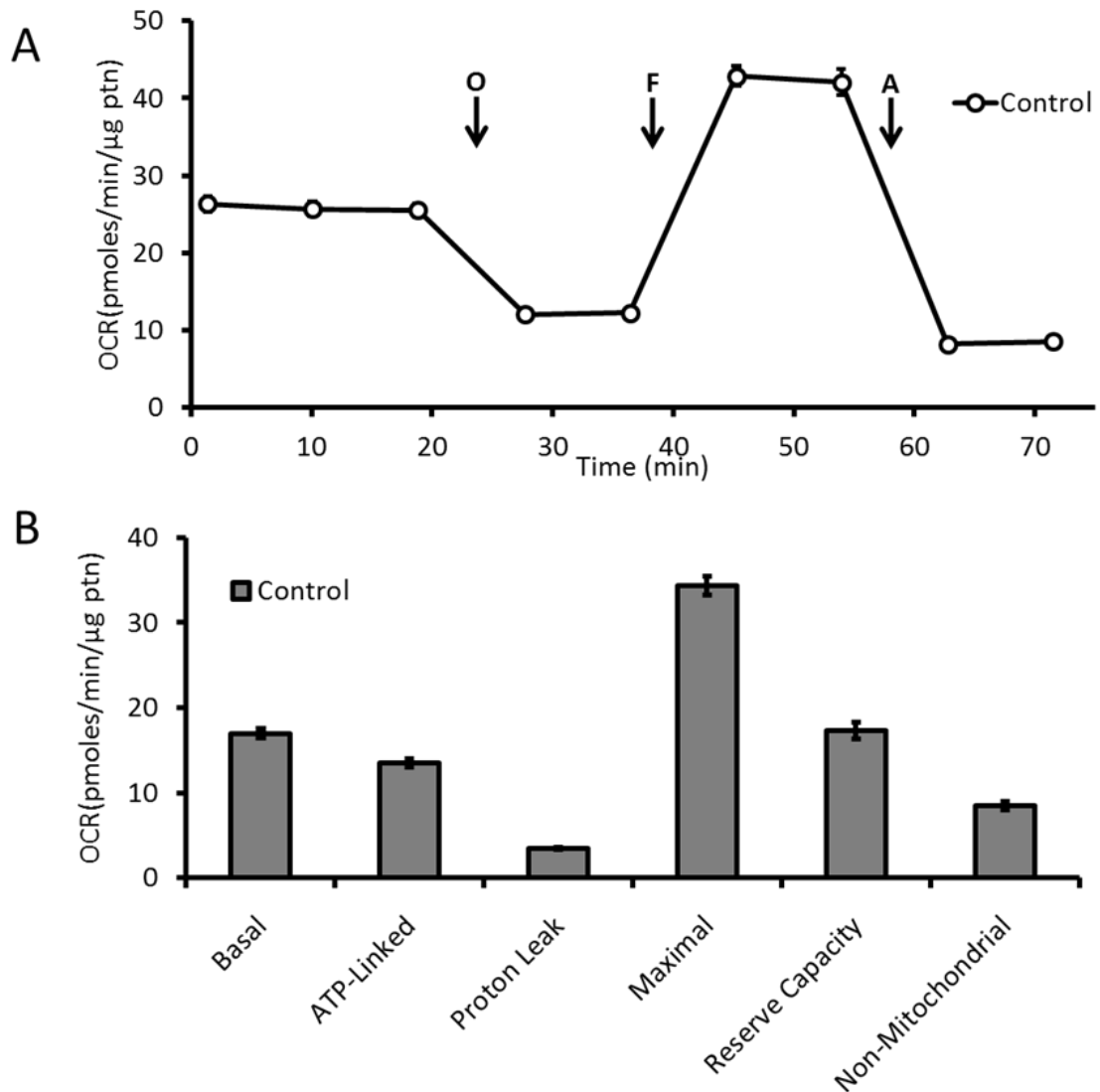
Figure 8: Measurement of bioenergetic profile of intact cells. (**A**) Seahorse extracellular flux analysis of primary cortical rat neurons exposed to sequential injection of oligomycin (O), FCCP (F), and antimycin A (A). (**B**) From panel A, basal, ATP-linked, proton leak, maximal, reserve capacity, and non-mitochondrial linked oxygen consumption rates were calculated. Shown is a representative experiment with data=mean±SEM, n≥3 independent experiments, $p < 0.05$.
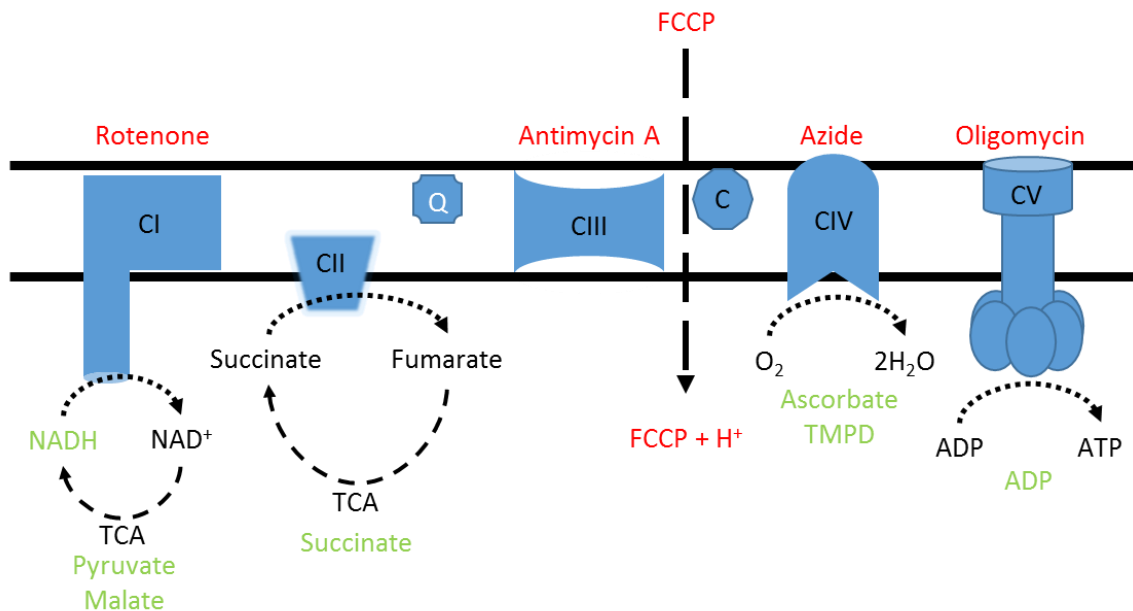
Figure 9: Electron transport chain components and relevant inhibitors and substrates. Mitochondrial ETC complexes and additional electron carriers are represented in blue. ETC substrates utilized in bioenergetic assays are labeled in green. Inhibitors are in red next to their mitochondrial targets.

In similar fashion to the mitochondrial stress test employed in **Figure 8** where FCCP was employed to determine the maximal OCR, the same can be performed in permeabilized cells. In **Figure 11 A**, sequential injection of substrates and inhibitors was added as before, however, this time the injection of FCCP in the place of ADP allows for the maximal rate to be determined as ATP synthesis through complex V has been uncoupled (**Figure 11 B**).

Complex IV substrate linked activities can be determined in similar fashion by using ascorbate and TMPD allowing the flow of electrons through complex IV. Rotenone is used to mitigate the possible effect of reverse electron flow through complex I. Lastly, the addition of azide is used to terminate the experiment (**Figure 12**)

To determine whether any pharmacological reagent directly impacts mitochondrial bioenergetics, the compound can be directly injected into the assay wells.

OCR can be observed as long as desired, then cells can be subjected to a traditional stress test at the end of the exposure, as in **Figure 8** or any other relevant experimental design (**Figure 13**).
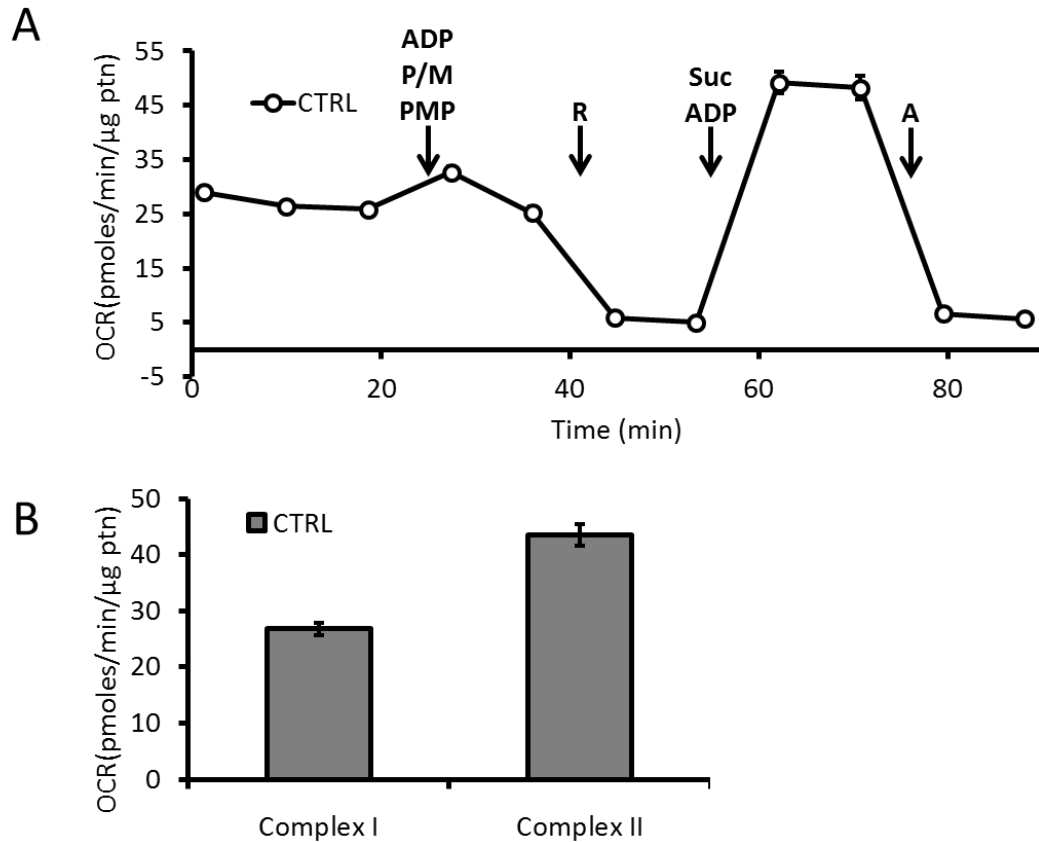
Figure 10: Measurement of complex I and II substrate linked activities in permeabilized cells. (**A**) Seahorse extracellular flux analysis in PMP permeabilized primary cortical rat neurons after 7 days in culture. (**B**) Complex I substrate linked activities were measured by the addition of pyruvate (P) and malate (M) (calculated as OCR after these substrates minus OCR after rotenone (R). Complex II substrate linked activities were measured by the addition of succinate (suc) (calculated as OCR after substrates minus OCR after antimycin A (A)). Rotenone (R) was added to inhibit complex I before complex II measurements. Antimycin A (A) was added to inhibit respiration through ETC. ADP was added in the assay to determine OCR under ATP synthase limiting conditions. Shown is a representative experiment with data=mean±SEM n≥3 independent experiments, p<0.05.
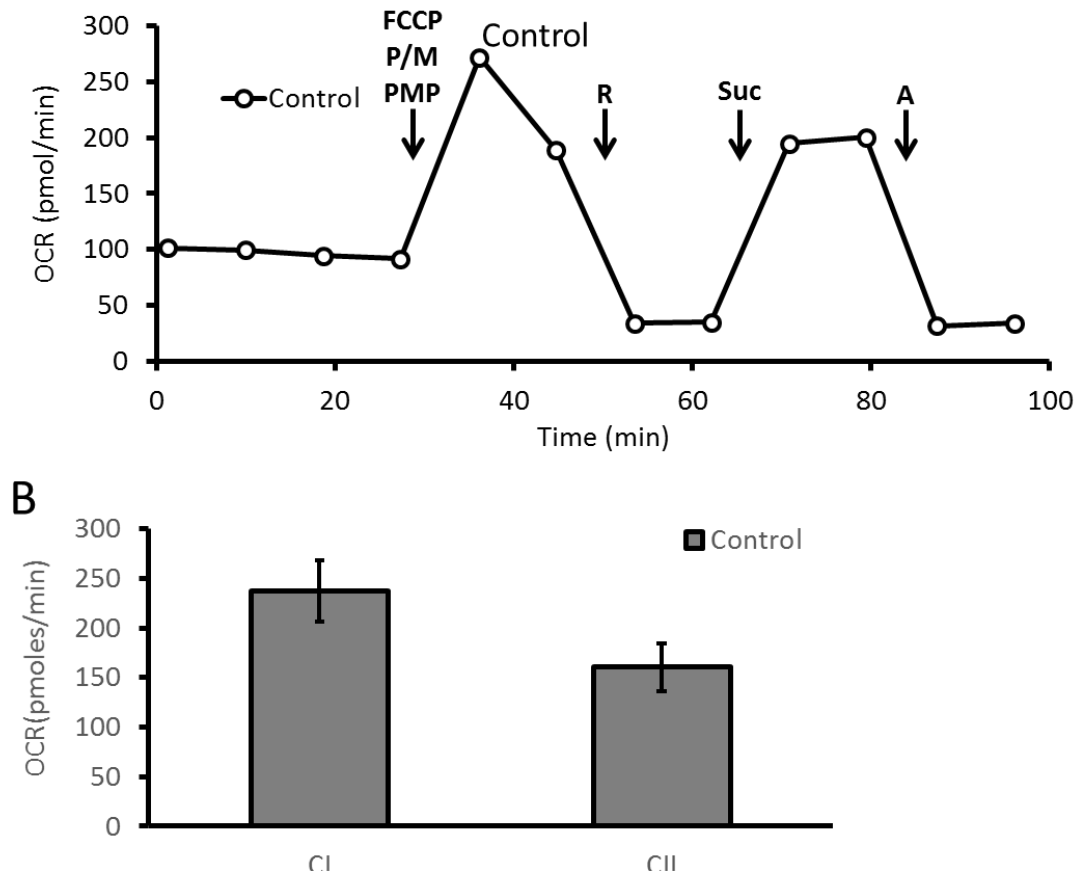
Figure 11: Measurement of maximal complex I and II substrate linked activities. (**A**) Seahorse extracellular flux analysis of PMP permeabilized primary cortical rat neurons after 7 days in culture. (**B**) As before, complex I and II linked activities were determined by the sequential injection of pyruvate (P), malate (M), rotenone (R), succinate (suc) and antimycin A (A). However, addition of FCCP during permeabilization allows for the maximum rate of respiration in the presence of substrates for each respective complex to be calculated. Shown is a representative experiment with data=mean±SEM n≥3 independent experiments, p<0.05.
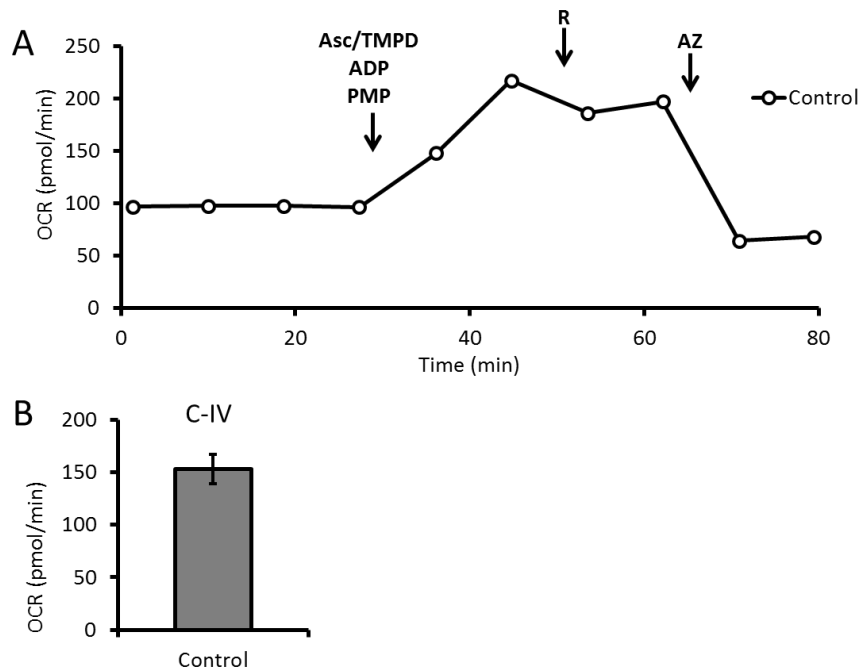
Figure 12: Determining complex IV substrate linked activities. (**A**) Seahorse extracellular flux analysis of PMP permeabilized primary cortical rat neurons 7 days in culture. (**B**) Complex IV substrate linked activities were calculated as OCR after substrates ascorbate (asc), TMPD, and rotenone (R), minus OCR after azide (AZ). Shown is a representative experiment with data=mean±SEM n≥3 independent experiments, $p<0.05$.
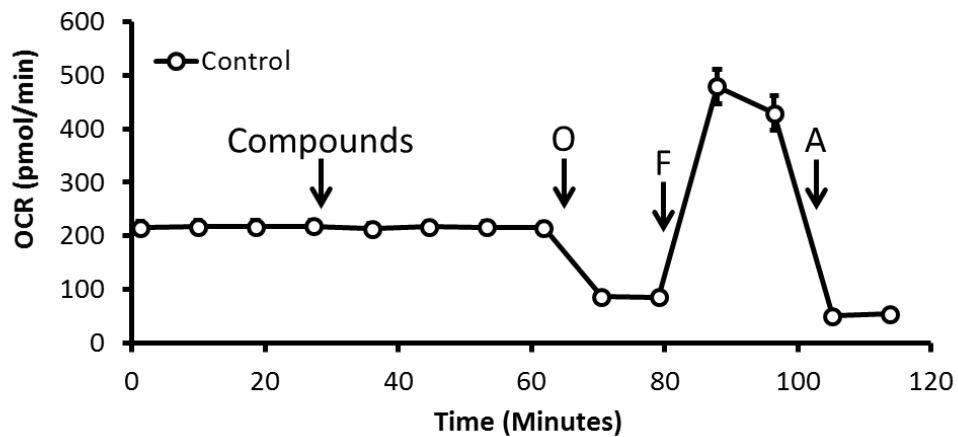
Figure 13: Assessment of immediate mitochondrial inhibition. Seahorse extracellular flux assessment of intact primary cortical rat neurons exposed directly during assessment to Control injection. Four basal measurements were taken then Control was directly injected to the wells where four more basal readings were measured. This was followed by a mitochondrial stress consisting of serial injection of oligomycin (O), FCCP (F), and antimycin A (A). Shown is a representative experiment with data=mean±SEM n≥3 independent experiments, $p<0.05$.

Targeted metabolomics of TCA cycle metabolites

To assess mitochondrial function in controlling TCA metabolites, we performed targeted metabolomics studies assessing pyruvate, lactate, TCA cycle metabolites, and those involved in glutaminolysis (**Figure 14 A-L**). When observing changes induced by experimental groups, suspect enzymes can be analyzed for their level of activity. For an example, we have measured the activity of citrate synthase (**Figure 14 M**).

Assessment of the mitochondrial network and mitophagy

Beyond measurements of metabolism, confocal imaging can be used to measure both the morphology of the mitochondrial network, which is highly dynamic in response to stress and can change shape either through fission or fusion, and mitophagy. The level of fission/fragmentation in response to stress can be measured by quantification of the length of a cell's mitochondrial population. We have measured mitochondrial fragmentation in response to 4-hyrdoxynonenal (HNE), as HNE has been described to alter cellular bioenergetics [199] and autophagy [200]. Neurons were plated on 8 well Nunc™ Lab-Tek™ Chambered coverglass plates at a density of 100,000 per well. After a 4 h exposure to 4-HNE, 25 nM MitoTracker Green FM was added to the cells for approximately 20 min before being washed three times with pre-warmed and equilibrated media. Images were taken with a Zeiss700 laser-scanning microscope. Mitochondrial length was measured using proprietary ZEN Blue software. Approximately 300-500 total mitochondria were counted from 3 images for each treatment group on each experimental replicate. Only in focus mitochondria with defined borders were used for measurements. We found that 15 µM HNE for 4 h induced mitochondrial fragmentation (**Figure 15**).
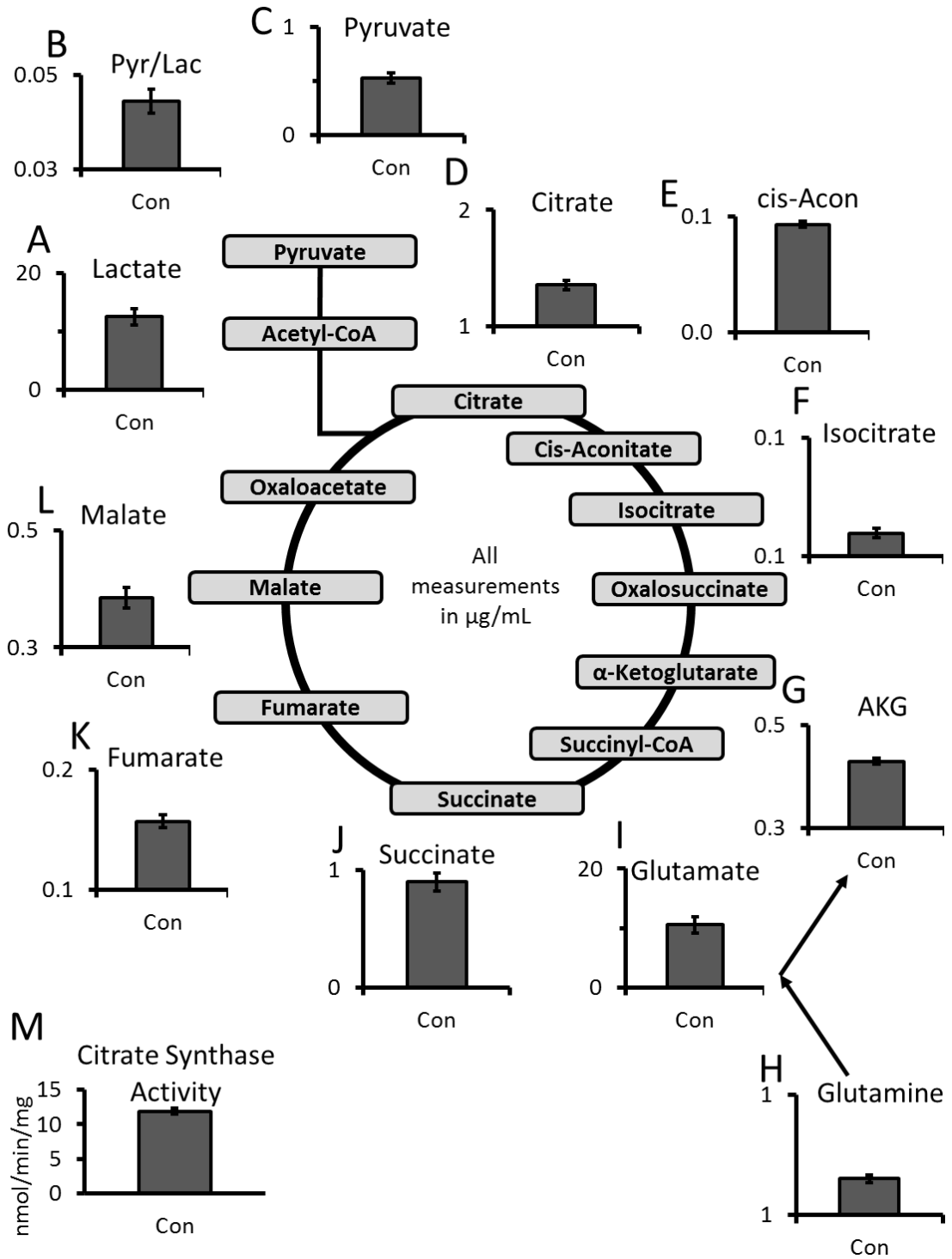
Figure 14: Targeted TCA metabolomics. (**A-L**) Targeted metabolomics of primary cortical rat neurons after 8 days in culture. Key TCA metabolites, including those important for glutaminolysis were measured by LC-multiple reaction ion monitoring-mass spectrometry. Metabolite levels are shown in μg/mL. *p<0.05 compared to control. (**M**) Activity levels of citrate synthase or other enzymes can be calculated.
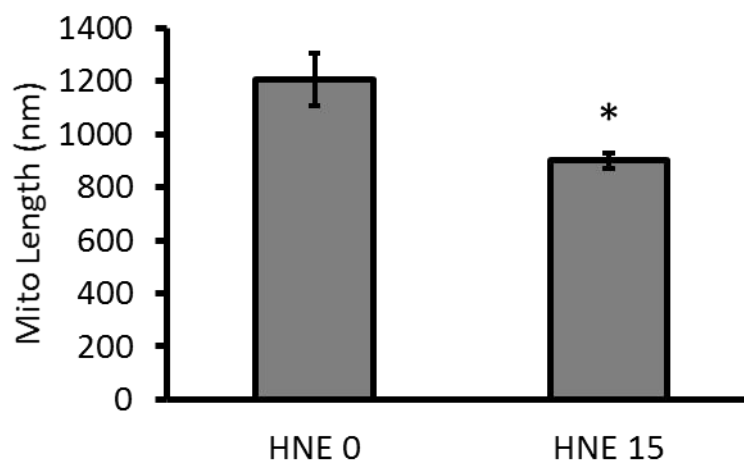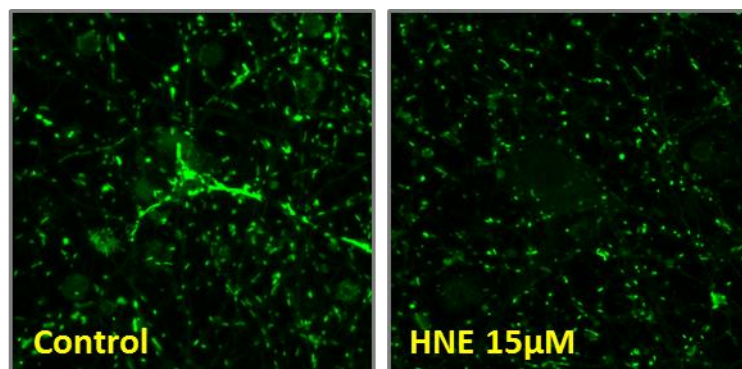
Figure 15: Quantification of mitochondrial fragmentation. Neurons were exposed to 4-HNE and then incubated with 25 nM MitoTracker Green for 15 min and imaged using laser scanning confocal microscopy. Bar graph shows the quantification of the combined average mitochondrial length following treatment. Data = mean ± SEM, typically ≥200 mitochondria are counted per group per experiment, n≥3 independent experiments.

In addition to morphology, recycling of mitochondria by autophagy can be

measured. Mitophagy can be assayed by measuring the co-localization between

MitoTracker red and LysoTracker green. The overlap of these two dyes can be used to

infer mitophagy. 100k cells per well were plated on 8 well Lab-Tek chambered cover-

glass slides pre-coated coated with poly-L-lysine. After 4 hour CQ exposure, cells were

washed with phenol free media and incubated with 25 nM MitoTracker Red and 100 nM

LysoTracker Green. After 30 min, cells were imaged using a Zeiss LSM 710 Confocal

Microscope. The percentage of red pixels overlapping with green pixels was quantified

using ImageJ (NIH Bethesda, MD USA). One limitation of this technique is that an

increase of co-localization between MitoTracker and LysoTracker does not distinguish

between increases in mitophagy or a blockade in degradation of mitochondria by the

lysosome (**Figure 16**).
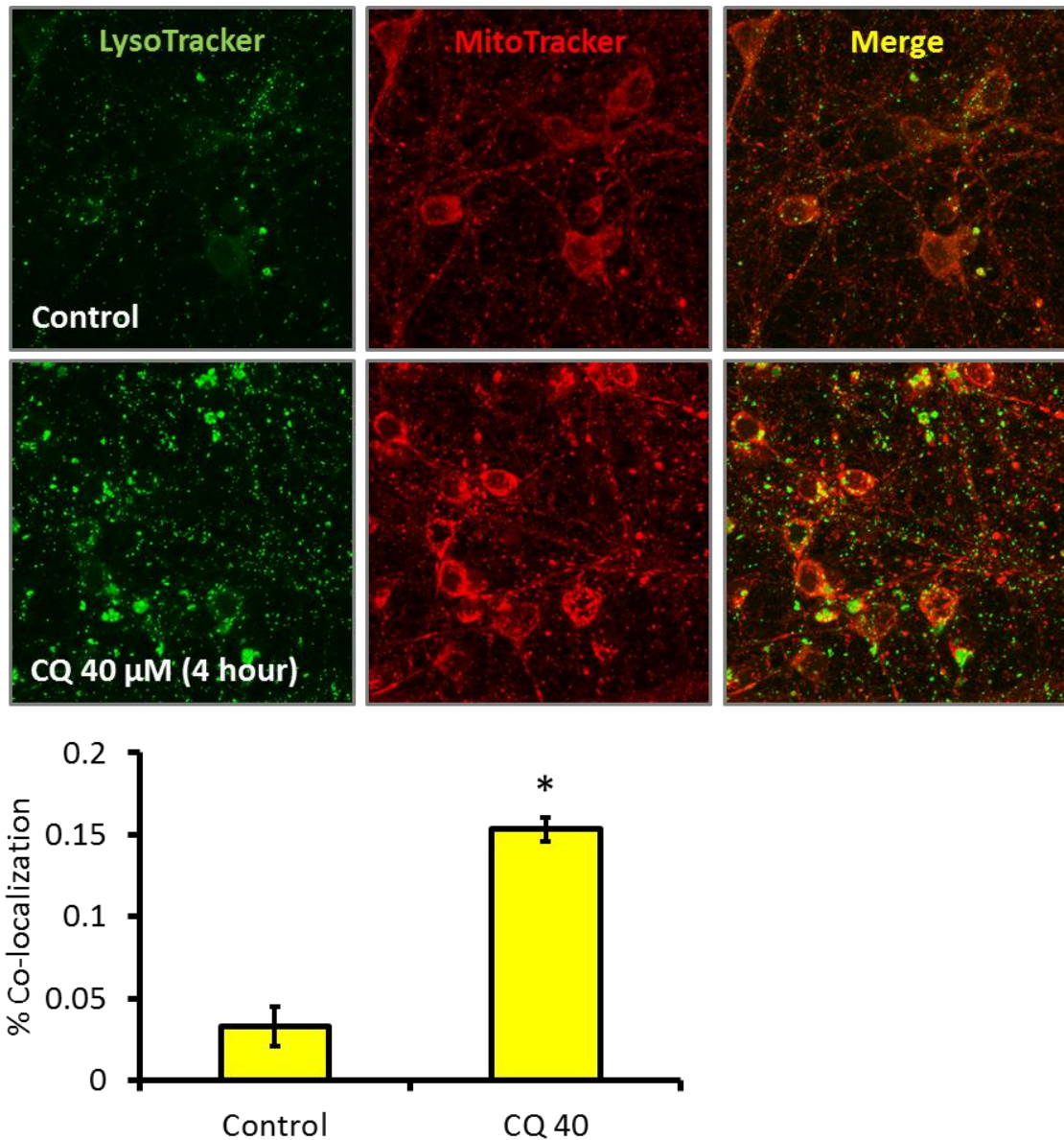
Figure 16: Quantification of MitoTracker and LysoTracker co-localization. Cells were exposed to vehicle versus 40 µM CQ for 4 h and probed with LysoTracker (green) and MitoTracker (red) then live cell imaged at 63x. The co-localization was quantified as the percentage of red signal co-localized with the green signal per field. Data = mean ± SEM, typically 20+ neurons are counted per experiment, n=3 independent experiments.

Assessment of cell viability

The viability of neuronal cells can be measured in several ways. We have employed two of the available methods. The first using vital dyes. Cells can be trypsinized from culture plates, then trypan blue can be added to cell suspensions, cells excluding the dye can be counted as viable. Issues with this method include variable efficiency in removing all the cells from the plate and given the reticulated nature of neurons, cell damage can be incurred during the removal process.

The second method that can be employed is the MTT cell death/proliferation assay. This method involves the addition of a tetrazolium salt and media mixture to the cells. Cells are incubated for several hours where MTT is reduced to formazan crystals. These crystals can then be suspended in DMSO and can be read colorimetrically at 550nM via a plate reader. This method is inexpensive and avoids the pitfalls of the trypan blue method, but since MTT reduction relies on cell metabolism, the health of mitochondria may play a role.

GENERAL CONSIDERTATIONS AND CONCLUDING REMARKS

Using mouse or rat primary neurons provides an excellent approach to investigate mitochondrial function, mitochondrial quality, mitochondrial quality control through autophagy, and protein aggregation. Caveats and concerns include: the existence of a minor population of non-neuronal cell types in cultures and the requirement of measuring OCR in unbuffered media that precludes prolonged continuous measurement of mitochondrial OCR over time. Taken together, we show here a workflow that allows researchers to thoroughly investigate mitochondrial function and quality control that is

61

adaptable to any cell based system and should assist in helping researchers in addressing key questions of how mitochondria function and autophagy are intertwined in disease.

INHIBITION OF AUTOPHAGY WITH BAFILOMYCIN AND CHLOROQUINE
DECREASES MITOCHONDRIAL QUALITY AND BIOENERGETIC FUNCTION IN
PRIMARY NEURONS

by

MATTHEW REDMANN, GLORIA BENAVIDES, TAYLOR BERRYHILL,
WILLAYAT WANI, XIAOSEN OUYANG, MICHELLE JOHNSON, SARANYA
RAVI, STEPHEN BARNES, VICTOR DARLEY-USMAR, AND JIANHUA ZHANG

CHAPTER 3

INHIBITION OF AUTOPHAGY WITH BAFILOMYCIN AND CHLOROQUINE
DECREASES MITOCHONDRIAL QUALITY AND BIOENERGETIC FUNCTION IN
PRIMARY NEURONS

INTRODUCTION

The autophagy-lysosomal pathway plays an important role in protein and

organelle homeostasis [76, 117, 200, 201]. This pathway involves the engulfment of

proteins or organelles by autophagosomes and subsequent degradation by lysosomes.

This is a multi-step, dynamic process involving greater than 32 autophagy related

proteins and lysosomal components [76, 85, 117, 118, 200, 201]. Pharmacological

inhibitors of autophagy either at initiation or completion have been used widely in both

normal and pathologic states in a variety of cells and tissues to provide insights into the

protective or deleterious roles of autophagy. Their use has been indispensable in

measuring autophagy and lysosomal activities and in some instances these inhibitors have

been used in the clinic as well [109, 202-207]. However, whether these compounds have

off target effects on cellular bioenergetics is not clear. Interestingly, targeting the

autophagy-lysosomal pathway would be expected to inhibit mitophagy and result in

decreased mitochondrial quality. This view is supported by data in mitochondria isolated

from ATG7 knockout mouse skeletal muscle that shows decreased mitochondrial

respiration. Furthermore, MEFs isolated from these mice also show decreased basal and

maximal oxygen consumption rates [208]. In this study we hypothesized that two

structurally diverse and commonly used pharmacological agents, which both inhibit autophagy at the level of the lysosome through distinct mechanisms, should exhibit convergent effects on mitochondrial quality and cellular bioenergetics. This was tested using bafilomycin and chloroquine by assessing their effects on LC3-II accumulation, bioenergetics, and metabolism in primary neurons.

The macrolide antibiotic bafilomycin A1 was among the first of this class isolated from *Streptomyces gresius*, and has been shown to be a potent inhibitor of the Vacuolar H^+ATPase which controls pH in the lysosome (V-ATPase) [209-211]. Through this mechanism bafilomycin inhibits autophagic flux by preventing the acidification of endosomes and lysosomes [212, 213]. The mechanisms of action of bafilomycin are complex. In one study, it was shown that it does not affect the *E. coli* F_1,F_o-ATPase or the *N. crassa* mitochondrial F_1,F_o-ATPase *in vitro* over a wide range of concentrations [209]. On the other hand, bafilomycin at low nM concentrations was reported to act as a potassium ionophore and at 30-100 nM decreases mitochondrial membrane potential and O_2 consumption, and at ~300 nM induces swelling in isolated mitochondria from rat liver [214]. In differentiated PC12 cells, SH-SY5Y cells and cerebellar granule neurons, bafilomycin (at 50-250 nM after 45 min) partially uncouples mitochondria due to a decrease in the proportion of polarized mitochondria, i.e. stochastic flickering. Furthermore, it was shown to decrease the mitochondrial pH, Ca^{2+} and $\Delta\Psi m$. This was associated with an elevation of mitochondrial respiration as assayed by MitoXpress and PtCPTE-CFR9 fluorescent probes both dose and time dependently [215]. These data suggest that bafilomycin has a number of off-target effects on mitochondria directly, making it difficult to determine which are a consequence of inhibiting autophagy. This is

potentially important as the translational capability of bafilomycin is being explored in a wide range of models. For example, there is evidence that bafilomycin inhibits viral replication of Influenza A and B in canine kidney cells [216, 217]. In cancer, bafilomycin alone or as a co-treatment appears to be effective in enhancing the efficacy of other therapies [218-220]. Given the complex interactions between metabolism and autophagy, we reasoned additional insight could be gained by comparing the impact of bafilomycin on cellular bioenergetics. This is an integrated measure of mitochondrial metabolism, with the cell providing its own substrates compared to measurements of individual components of the respiratory chain under conditions where substrates are not limiting. This can then be compared with parameters of mitochondrial quality to determine mechanism.

Similar to bafilomycin, the former malaria drug chloroquine (CQ) is now widely used as an inhibitor of autophagy in both cell culture and *in vivo* [207]. Chloroquine has a long history of human use and is currently being tested as a sensitizing agent for certain cancers, making understanding its mechanisms of action both topical and important [202-204]. Chloroquine is a lysosomotropic weak base, which in the monoprotonated form diffuses into the lysosome, where it becomes diprotonated and becomes trapped. Protonated chloroquine then changes the lysosomal pH, thereby inhibiting autophagic degradation in the lysosomes [221]. And while the direct effects of chloroquine on mitochondria have not been, to our knowledge, extensively studied, there is evidence to suggest that in already compromised mitochondria, as is the case in cardiac pressure overload, chloroquine exacerbates the decrease in mitochondrial quality and function [222].

Autophagy plays a critical role in maintaining healthy mitochondrial populations through mitochondrial specific recycling termed mitophagy. Mitochondria are key components in the cell responsible for not only energy production but for varied and diverse signaling pathways [111, 223]. Failure to maintain a population of healthy mitochondria can lead to decreased energy production, increased reactive oxygen species production and eventually to cytotoxicity. These outcomes are especially evident in chronic diseases including neurodegenerative and heart diseases [111, 117, 118, 200, 224, 225]. Since pharmacological inhibitors of autophagy are frequently used and combined with measurements of mitochondrial function, it is important to determine their effects in a defined cellular system. In addition to oxidative phosphorylation, mitochondria metabolism is also essential for multiple cellular functions beyond energetics [226-228].

In the present study, we have used primary cortical rat neurons to evaluate how the autophagy inhibitors chloroquine and bafilomycin affect mitochondrial bioenergetics and metabolism. We used the Seahorse extracellular flux analyzer and a targeted metabolomics approach to determine parameters of mitochondrial bioenergetics and metabolism in intact neurons providing a cellular context for understanding the autophagy pathway and its inhibitors. We have found that both chloroquine and bafilomycin decrease mitochondrial quality to a similar extent when levels are titrated to achieve a comparable level of autophagy inhibition.

MATERIALS AND METHODS

Chemicals

Bafilomycin A1 (B1793), chloroquine (C6628), oligomycin (75351), FCCP (C2920), rotenone (R8875), antimycin-A (A8674), pyruvate (P5280), malate (M6413), ADP (A2754), succinate (S2378) were all obtained from Sigma. Neurobasal medium (21103-049), B-27 supplement (17504044-044), L-glutamine (25030-081) and penicillin-streptomycin (15140-122) were obtained from Life Technologies. PMP (102504) was obtained from Seahorse Bioscience.

Cell culture

Primary cortical rat neurons were isolated at embryonic day E18. Dissections were performed in HBSS media and plated on poly-L-Lysine coated plates using Neurobasal media supplemented with L-glutamine, B27, and Penicillin/Streptomycin. Experiments were performed on DIV7, when half of the media was replaced with each compound diluted in Neurobasal supplemented with L-glutamine and Penicillin/Streptomycin only.

Cell viability

Cells were plated at 80k on XF96 plates and exposed for 24 h to bafilomycin or chloroquine. Cell viability was measured 24 hours after the exposure by the Trypan Blue exclusion method.

Western blot analysis

Neurons were plated on 24-well plates seeded at 480k cells per well. After exposures to the pharmacological compounds, medium was aspirated. Cells were then washed once with ice cold PBS, and 40 µL of RIPA lysis buffer (50 mM Tris pH 7.8, 150 mM NaCl, 2 mM EDTA, 1% Triton X-100, and 0.1% SDS) with 1x Roche protease inhibitors (4693132001) was added to each well and cells were scraped. Two wells were then combined and centrifuged at 16,800 x g for 15 min at 4°C. The supernatant was collected and protein was measured using the BCA protein assay. 5x loading buffer was added to samples and then separated by SDS-PAGE using 12% or 15% polyacrylamide gels. Membranes were then immunoblotted for LC3 (Sigma L8918 1:2000), Citrate synthase (AB96600 1:1000), PGC1-α (SC-13067 1:1000), p62 (Abnova H00008878-M01 1:2000), aconitase (affinity purified as previously described [229], was a generous gift from Scott Ballinger at UAB) and actin (Sigma A5441 1:2500). Subunits of mitochondrial oxidative phosphorylation complexes I-V were blotted for by using Abcam's total OXPHOS rodent antibody cocktail (AB110413). Images were collected using an Amersham™ Imager600. Images were then analyzed using ImageJ [230].

Mitochondrial DNA copy number and DNA damage assays

Cells were plated at 480k cells per well on 24 well plates and were treated for 24 h. After treatment, DNA was extracted. Quantitative real-time PCR was performed using SYBR green in an ABI 7500 machine. Mitochondrial DNA copy number was determined by normalizing results from primers targeted to mtDNA (Forward: 5'-CCAAGGAATTCCCCTACA CA-3' and Reverse: 5'-

GAAATTGCGAGAATGGTGGT-3') against results from primers targeted to nuclear

18S DNA (Forward: 5'-CG AAAGCATTTGCCAAGAAT-3' and Reverse: 5'-

AGTCGGCATC GTTTATGGTC-3') [194, 195]. Mitochondrial DNA damage was

determined by PCR as previously described [231]. Briefly, mtDNA long segments

(Forward: 5'-GGACAAATATCATTCTGAGGAGCT-3' Reverse: (5'-

GGATTAGTCAGCCGTAGTTTACGT-3') and short segments (Forward: 5'-

CCAAGGAATTCCCCTACACA-3' Reverse: 5'-GAAATTGCGAGAATGGTGGT-3')

were amplified using an AccuPrimeTM Taq DNA Polymerase High Fidelity kit (Life

Tech Corp). The products were separated on agarose gels, visualized by ethidium

bromide, and analyzed by ImageJ. mtDNA Long PCR conditions were: 94°C for 11 s, 25

cycles of denaturation at 94°C for 15 s, annealing and extension at 67°C for 12 min, and

final extension at 72°C for 10 min. mtDNA Short PCR conditions were: 94°C for 6 s, 18

cycles of denaturation at 94°C for 20 s, annealing and extension at 65°C for 1 min, and

final extension at 72°C for 10 min. Lesion frequency was calculated as follows [196]:

$$\text{Lesion frequency per 16kb of each} = -Ln\left[\frac{\text{long PCR product / short PCR product}}{\text{mean of (long PCR product / short PCR product) from control}}\right]$$

Bioenergetic Analysis

Bioenergetic profiles were determined using the Seahorse Bioscience

Extracellular Flux Analyzer (XF96) [199]. Cells were isolated as above and plated at 80k

cells per well on XF96 plates. For mitochondrial stress test in intact neurons, after

exposure to autophagy inhibitors, cells were switched to XF media 30 min prior to

measurement of oxygen consumption rate (OCR), followed by sequential injection of

oligomycin (1 µg/mL), FCCP (1 µM), and rotenone (1 µM) + antimycin A (10 µM), with 2 OCR measurements after each injection [199]. Total protein per well was measured by Lowry DC protein assay and OCR normalized to protein. Basal OCR was calculated as OCR before oligomycin minus OCR after Antimycin. Maximal OCR was calculated as OCR after FCCP minus OCR after Antimycin. Reserve Capacity was calculated as OCR after FCCP minus OCR before oligomycin. ATP-linked OCR was calculated as OCR before oligomycin minus OCR after oligomycin. Proton leak OCR was calculated as OCR after oligomycin minus OCR after Antimycin. Non-mitochondrial OCR is the OCR after antimycin injection.

For mitochondrial activity assay in permeabilized cells, 5 min prior to assay, cells were switched to MAS buffer (70 mM sucrose, 220 mM mannitol, 10 mM KH_2PO4, 5 mM $MgCl_2$, 2 mM HEPES, 1 mM EGTA, adjusted pH to 7.2) [198]. OCR was measured after injection 1 nM PMP (Seahorse Plasma Membrane Permeabilizer) plus complex I modulators (10 mM pyruvate, 1 mM malate and 1 mM ADP or 1 µM FCCP) for complex I activity assays, then injected with 1 µM rotenone to inhibit complex I activity, followed by injection of complex II modulators (10 mM succinate) to assay for complex II activity, then injected with 10 µM Antimycin. Complex IV activity was measured in PMP permeabilized neurons in MAS buffer by injection of PMP (1 nM) plus TMPD 0.5 mM, ascorbate 2 mM, and 1 mM ADP; after 2 measurements the inhibitor azide 20 mM was injected. Complex I activity was calculated as the difference between before and after rotenone injection. Complex II activity was calculated as the difference between before and after antimycin injection. Complex IV activity was calculated as the difference after ascorbate injection and after azide injection. The experiments were repeated with >3

independent cultures. Because of significant protein loss during assays utilizing MAS

buffer, accurate measure of total protein was unobtainable, thus raw data is represented.

Metabolomics

Cells were plated on 24 well plates at 480k per well and treated with autophagy

modulators for 24 hrs. Upon completion of treatment the cells were washed with 1 mL of

ice cold PBS. The cells were then lysed and scraped in 500 µL of HPLC grade ice cold

methanol and incubated at -80°C for 2 hrs. Plates were scraped again and cell lysates

were transferred to glass tubes where they were centrifuged at ~1000 x g for 20 min at

4°C. Supernatants were transferred to new glass tubes and stored at -80°C until further

processing [232].

Standards were generated as a master mix of all compounds at 100 µg/mL in H_2O

and serial diluted to 10x of the final concentrations (0.05-10 µg/ml, 9 standards).

Standards were further diluted to 1x in methanol to a total volume of 1 mL, and dried by

a gentle stream of N_2. For cell extracts, 1 mL of each were transferred to a glass tube and

dried under a gentle stream of N_2. Standards and samples were resuspended in 50 µl of

5% acetic acid and vortexed for 15 seconds. Amplifex™ Keto Reagent (SCIEX,

Concord, Ontario, Canada) (50 µL) was added to each sample and allowed to react for 1

h at room temperature. Standards and samples were then dried under a gentle stream of

N_2 and resuspended in 1 mL and 200 µL of 0.1% formic acid, respectively.

Samples were analyzed by LC-multiple reaction ion monitoring-mass

spectrometry. Liquid chromatography was performed by LC20AC HPLC system

(Shimadzu, Columbia, MD) with a Synergi Hydro-RP 4 µm 80A 250 x 2 mm ID column

(Phenomenex, Torrance, CA). Mobile phases were: A) 0.1% formic acid and B) methanol/0.1% formic acid. Compounds were eluted using a 5-40% linear gradient of B from 1 to 7 min, followed by a column wash of 40-100% B from 7 to 10 min, and re-equilibrated at 5% B from 10.5 - 15 min. Column eluant was passed into an electrospray ionization interface of an API 4000 triple-quadrupole mass spectrometer (SCIEX). The following mass transitions were monitored in the positive ion mode: m/z 261/118 for α-ketoglutarate, m/z 247/144 for oxaloacetate and m/z 204/144, 204/118 and 204/60 for pyruvate. In the negative mode, the following transitions are monitored: m/z 115/71 for fumarate, m/z 89/43 for lactate, m/z 117/73 for succinate, m/z 133/115 for malate, m/z 173/85 for cis-aconitate, m/z 191/87 for citrate, m/z 191/73 for isocitrate, m/z 147/129 for 2-hydroxyglutarate, m/z 146/102 for glutamate, m/z 145/42 for glutamine and m/z 132/88 for aspartate. The 16 transitions were each monitored for 35 ms, with a total cycle time of 560 ms. MS parameters were CAD 4, CUR 15, GS1 60, GS2 30, TEM 600, IS -3500 volts for negative polarity mode and IS 4500 for positive polarity mode. Peak areas of metabolites in the sample extracts are compared in MultiQuant software (SCIEX) to those of the known standards to calculate metabolite concentrations.

Citrate activity assay

Neurons were plated at 480k/well on 24 well plates. Cells were scraped into RIPA lysis buffer as before and frozen until assayed. Activity was measured using a Beckman Coulter DU800 spectrophotometer. 945 µL of 100 mM Tris (pH 8.0 at 37°C) with 0.1% Triton X-100 was added to cuvette followed by 25 µL of sample, 10 µL of 10 mM acetyl-CoA, 10 µL 5,5′-dithiobis(2,4-nitrobenzoic acid), and 10 µL 20 mM oxaloacetate.

Activity was measured for 4 min. The rate was calculated from the linear range and was normalized to total protein.

Normalized activity calculations

Citrate synthase activity (nmol/min/mg protein) was expressed as the ratio of enzyme activity to relative levels of citrate synthase protein as determined by western blotting. Complex I, II and IV-linked OCR were expressed as the ratio of their respective OCR normalized to relative levels of specific subunits within each complex as determined using western blotting.

Statistics

All results were expressed as mean±SEM. Statistical analysis of data were performed by using one-way ANOVA followed by Tukey's post hoc test. Values of $p<0.05$ were considered statistically significant.

RESULTS

Effects of autophagy inhibitors on LC3-II accumulation and viability

During the autophagy process, LC3-I is converted to LC3-II by lipidation, resulting in LC3-II migrating differently on SDS/PAGE. LC3-II is used as a quantitative marker of autophagy since it is required for the formation of the autophagosome and its level is proportional to the amount of autophagosomes in the cell [207, 233, 234]. To determine concentrations of bafilomycin and chloroquine which result in an approximately equivalent level of autophagy inhibition, cultured primary cortical rat

neurons at 7 d *in vitro* (DIV7) were exposed to a range of concentrations for both

compounds for 24 h. Significant increases in LC3-II were observed at 10 and 100 nM but

not at 1 nM bafilomycin exposure (**Figure 1 A, B**). Significant increases in LC3-II were

observed at 10, 20, and 40 µM concentrations of CQ (**Figure 1 C, D**). No significant

changes in LC3-I were observed. There were no significant changes in the cell viability

after exposure to chloroquine for 24 h. However, exposure to 100 nM but not 10 nM

bafilomycin, decreased cell viability by approximately 35% (**Figure 1 E**). In a direct

comparison of these two autophagy modulators, we observed no significant changes in

LC3-I, but statistically similar increases in LC3-II for both bafilomycin and chloroquine

exposures. The LC3-II/I ratio reflects the conversion of the protein from the cytosolic

form to the autophagosome associated form upon autophagy activation and was also

calculated and showed significant increases for both bafilomycin and chloroquine

treatments, although chloroquine was statistically further increased, albeit modestly, from

bafilomycin. The autophagy substrate p62 was also measured and showed increased

levels for bafilomycin (**Figure 1 F-J**). Given the toxicity of 100 nM bafilomycin and the

similar accumulation of LC3-II with 10nM bafilomycin and 40 µM chloroquine

treatments, all subsequent 24 h time point experiments were performed with these

concentrations.
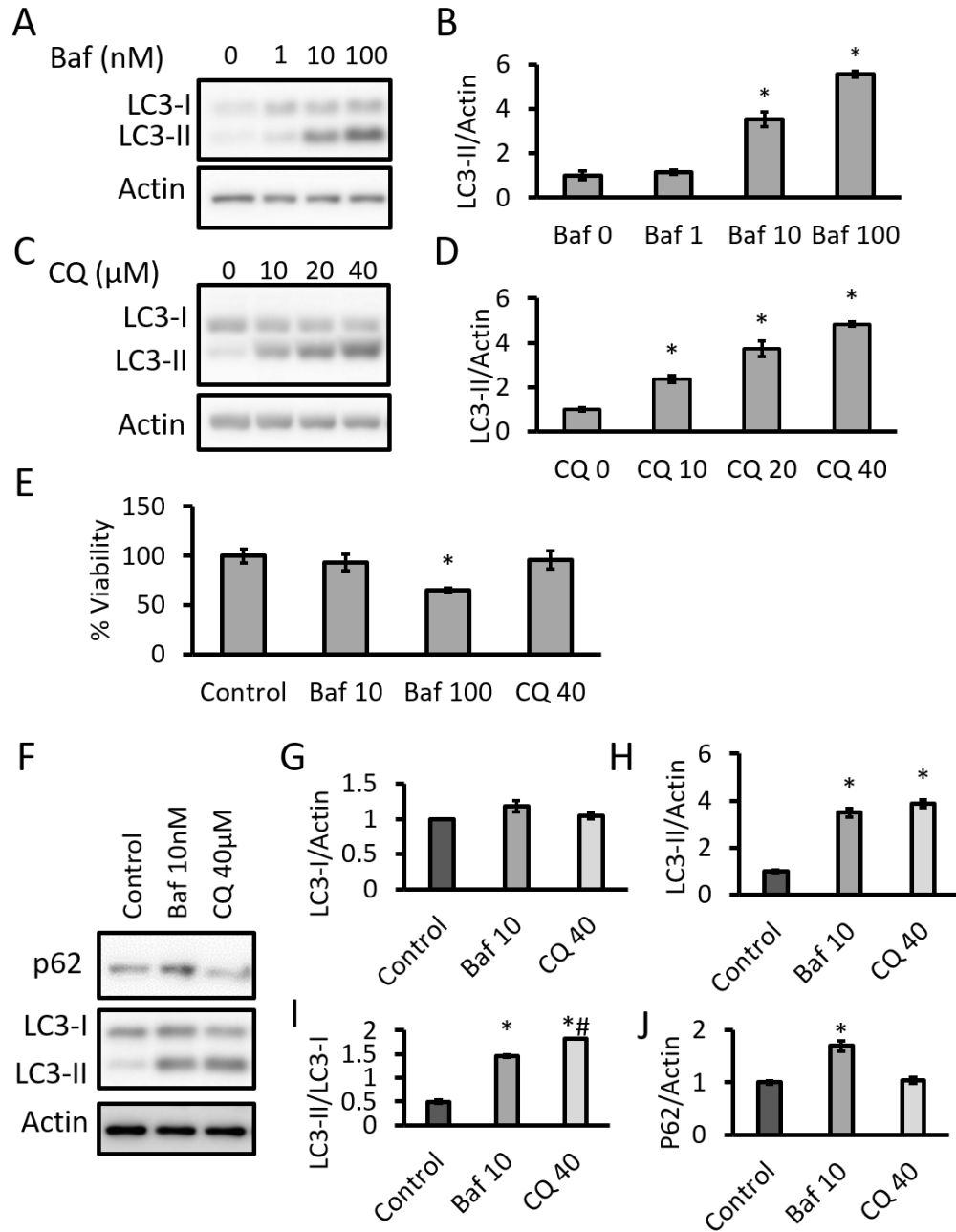
Figure 1: Effects of bafilomycin and chloroquine on autophagy and cell survival. Primary rat cortical neurons at DIV7 were used for experiments. (**A-D**) Western blot analyses of LC3-I and LC3-II in lysates in neurons exposed to increasing concentrations of bafilomycin (baf) or chloroquine (CQ) for 24 h. (**E**) Trypan blue exclusion assay of cell viability after 24 h exposure to baf or CQ at indicated concentrations. (**F-J**) Western blot analyses of p62, LC3-I and LC3-II in lysates in neurons exposed to 10 nM baf and 40 μM CQ. *p<0.05 compared to control, #p<0.05 between baf and CQ, n=3 independent experiments.

Effects of bafilomycin and chloroquine on cellular bioenergetics in intact neurons

Primary cortical rat neurons were exposed to autophagy modulators for 24 h as before and medium was replaced by XF media free of autophagy modulators, followed by a mitochondrial stress test in intact cells using XF media. These cells exhibited the typical profile for the mitochondrial stress test we have previously reported for primary neurons [195, 235]. As expected, after establishing a stable baseline measurement of oxygen consumption rate (OCR) the injection of oligomycin resulted in a decrease in OCR due to the inhibition of ATP synthase. Next, FCCP, a mitochondrial uncoupler was found to stimulate OCR by depleting the proton gradient. Finally, antimycin was injected to inhibit consumption of oxygen by the mitochondrial electron transport chain [199, 225]. Basal, ATP-linked, maximal, reserve capacity, proton leak, and non-mitochondrial OCR were determined from this trace (**Figure 2 A**). Both bafilomycin exposure at 10 nM and chloroquine exposure at 40 µM resulted in similar decreases in overall OCR for basal, ATP-linked, maximal, reserve capacity and non-mitochondrial related parameters of oxygen consumption. No significant changes in proton leak were noted (**Figure 2 B-G**). Extracellular acidification rate (ECAR), a measurement of proton production from glycolysis and the TCA cycle, was also recorded using the same injection protocol as above. Statistically significant decreases in ECAR were observed for both bafilomycin and chloroquine and in the plot of OCR vs ECAR the cells a show a similar and a less energetic status (**Figure 3 A-C**).

Since bafilomycin has been reported to inhibit the mitochondrial ATP synthase and chloroquine can modulate organellar pH, either compound could acutely inhibit mitochondrial function. To test this, we measured basal OCR for 4 consecutive readings
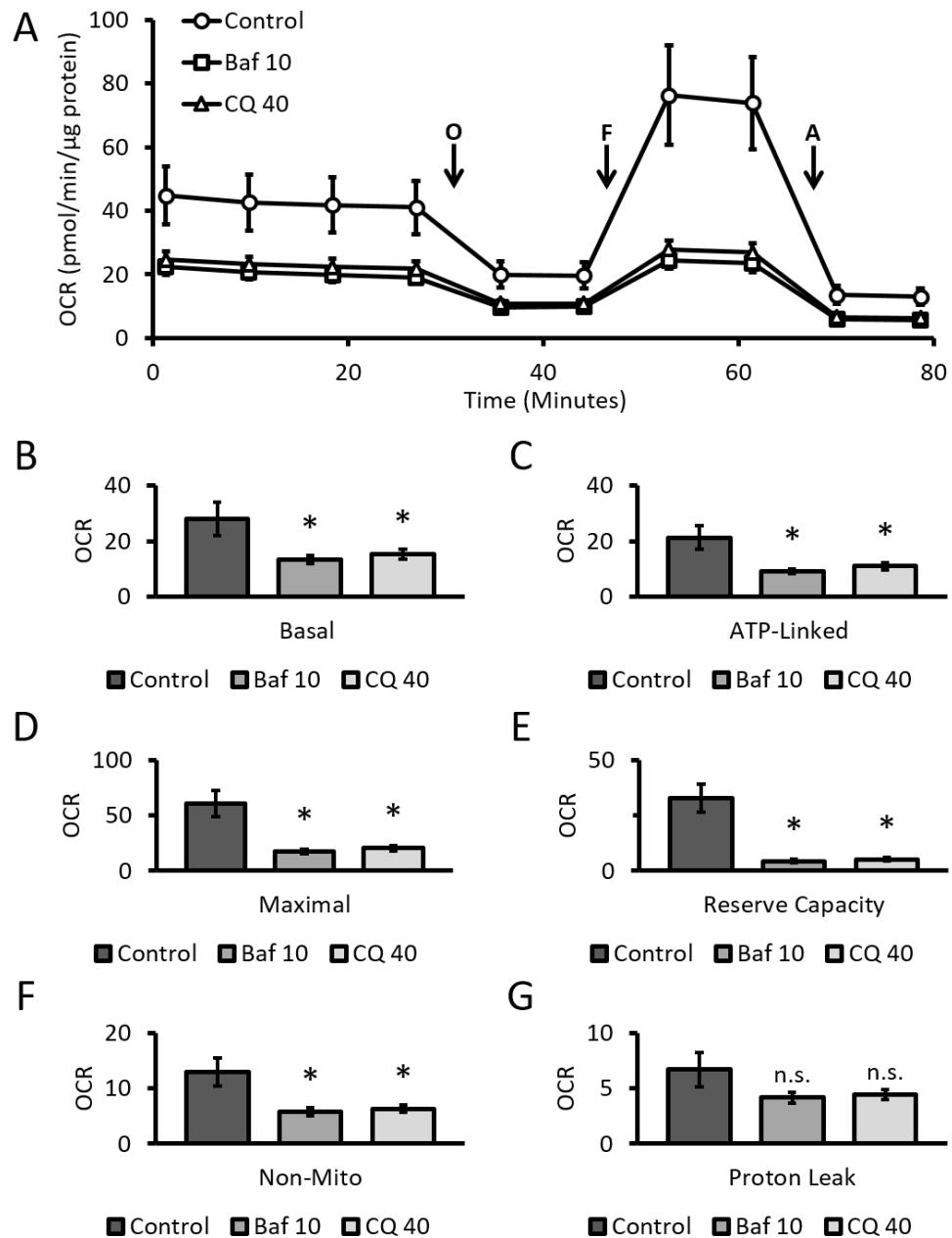
Figure 2: Effects of bafilomycin and chloroquine on parameters of bioenergetics in intact neurons. (**A**) Oxygen consumption rate (OCR) from primary cortical neurons exposed to bafilomycin (10 nM) and chloroquine (40 µM) for 24 h was determined by the mitochondrial stress test. OCR was measured before and after sequential injection of Oligomycin (O, 1 µg/mL), FCCP (F, 1 µM), and Antimycin A (A, 10 µM). (**B-G**) Basal, maximal, reserve capacity, ATP linked, proton leak, and non-mitochondrial OCR were calculated from (A) as described in the Methods. *p<0.05 compared to control, from 3 independent experiments. Shown is a representative experiment with data=mean±SEM n≥3 replicates, n.s.: not significant.
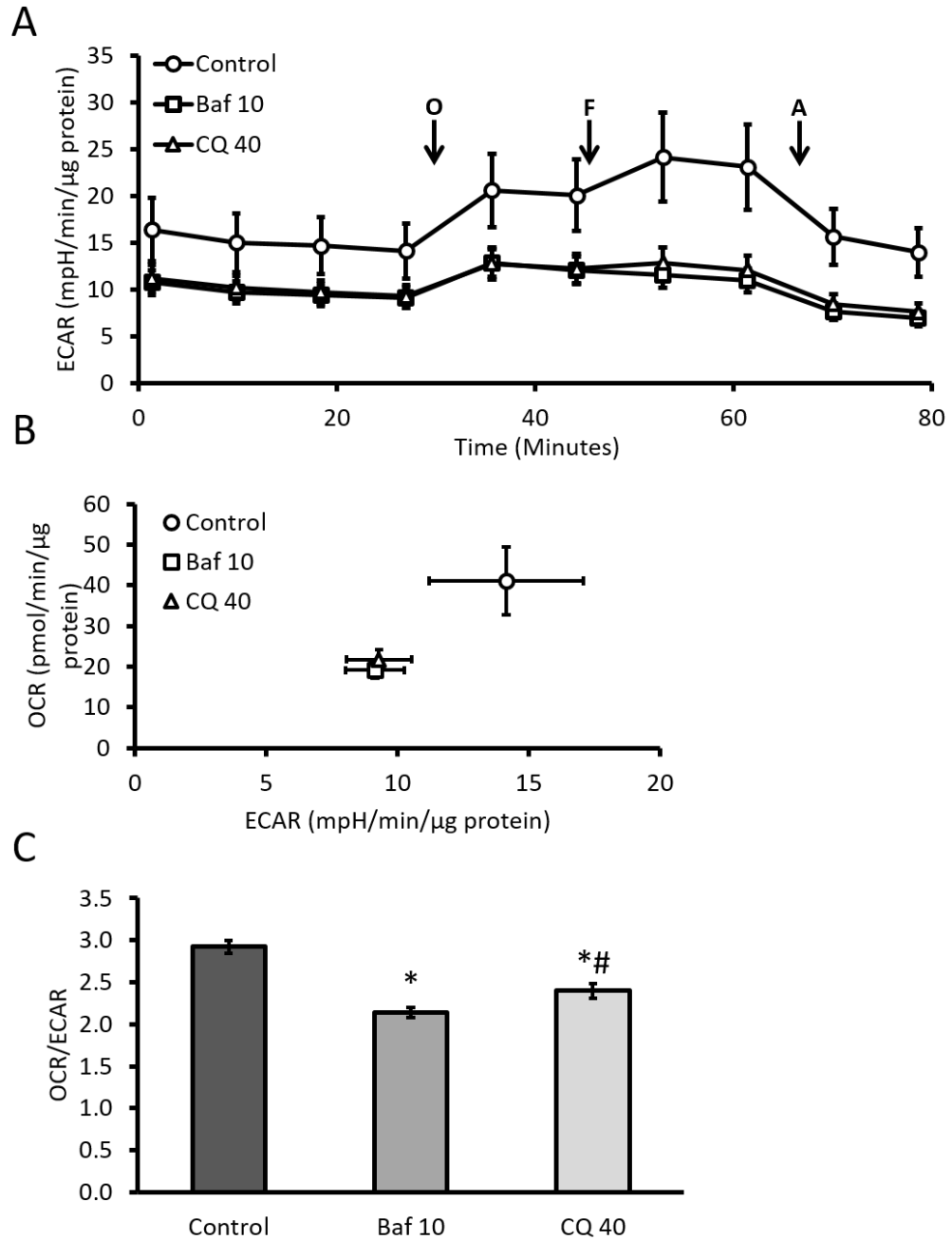
Figure 3: Extracellular acidification rate is decreased after autophagy modulator treatment. (**A**) Extracellular acidification rate (ECAR) was determined from primary cortical neurons exposed to bafilomycin (10 nM) and chloroquine (40 µM) for 24 h and were then subjected to a mitochondrial stress test consisting of the sequential injection of Oligomycin (O, 1 µg/mL), FCCP (F, 1 µM), and Antimycin A (A, 10 µM). (**B**) ECAR from (A) versus OCR from Figure 2A were plotted. (**C**) The OCR and ECAR ratios were also determined in these conditions. *p<0.05 compared to control, from 3 independent experiments. Shown is a representative experiment with data=mean±SEM n≥3 replicates.

and then directly injected the compounds, recorded 4 more basal readings and then

proceeded with a mitochondrial stress test. No discernable decreases of OCR were

observed during the 30 min immediately after direct injection of the compounds or during

the stress test (**Figure 4 A**). No significant alterations in p62, LC3-I, or LC3-II protein

levels nor any changes in viability were observed (**Figure 4 B-F**).

*Effects of bafilomycin and chloroquine on mitochondrial complex I, II and IV substrate–
linked respiration.*

To assess the effect of the autophagy inhibitors on mitochondrial complexes, cells

were exposed to 10 nM bafilomycin or 40 µM chloroquine (24 h) under the conditions

described in Figure 2 and then switched to MAS buffer before permeabilization with

PMP and OCR measurements with complex I, II or IV-linked substrates. Complex I

linked respiration was diminished by approximately 65% and 55% for bafilomycin and

chloroquine treatment in the presence of ADP, respectively. In the presence of FCCP,

decreases in OCR between 70% and 80% were observed after autophagy inhibitor

treatment (**Figure 5 A**). Complex II linked activities were diminished by 50% in the

presence of ADP and by 60% in the presence of FCCP after either bafilomycin or

chloroquine exposure (**Figure 5 B**). Complex IV substrate-linked OCR in the presence of

ADP was decreased by ~47% with bafilomycin and by ~30% with chloroquine (**Figure 5
C**).
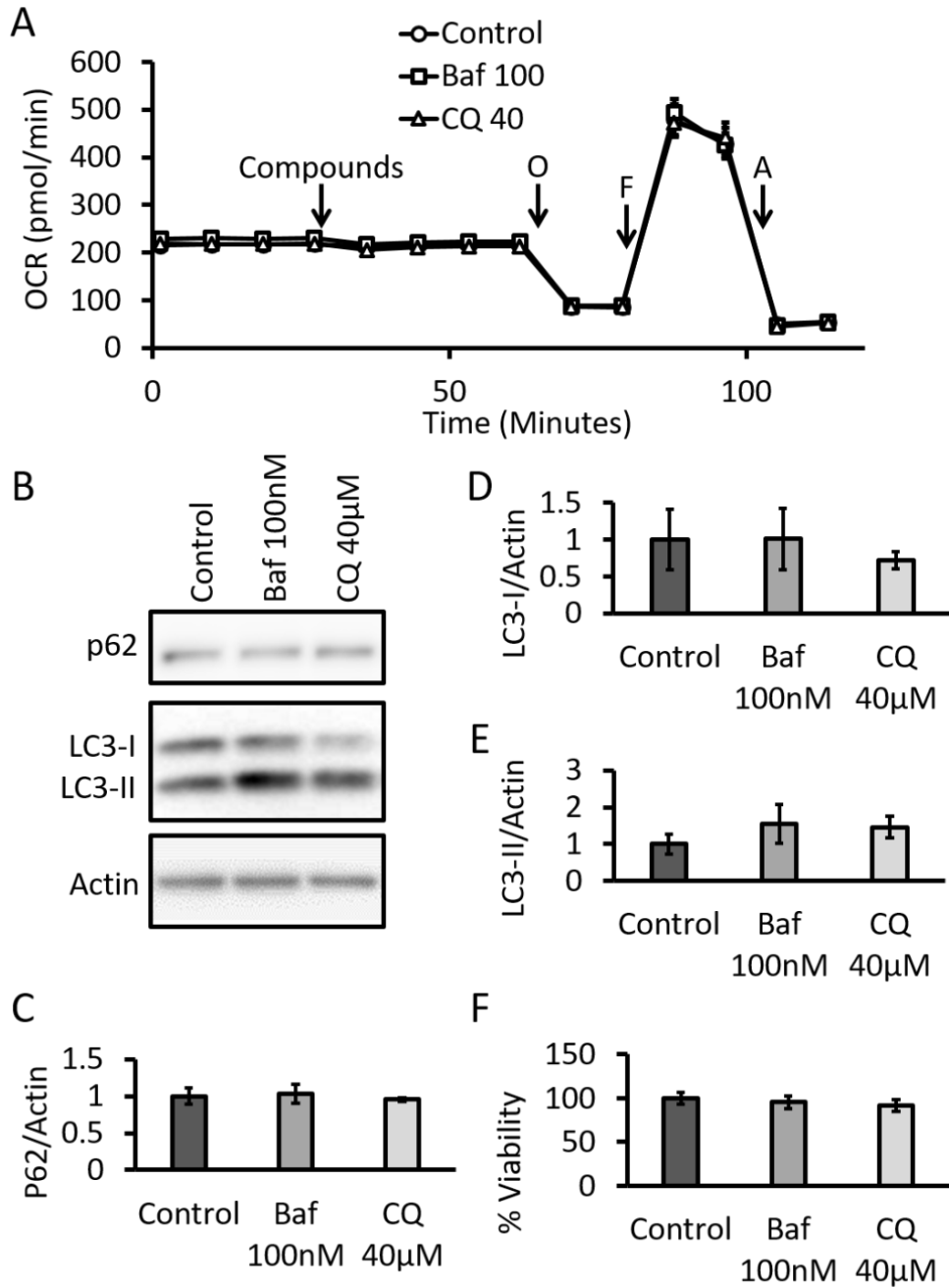
Figure 4: No change in parameters of bioenergetics in intact neurons after short-term exposure to bafilomycin (Baf) and chloroquine (CQ). (**A**) Mitochondrial oxygen consumption rate (OCR) was measured for 4 consecutive readings and then 100 nM baf and 40 µM CQ were injected. OCR was measured for an additional 4 readings. A mitochondrial stress test consisting of sequential injection of oligomycin (O), FCCP (F), and Antimycin A (A) was performed. No significant differences in OCR were observed, from 3 independent experiments. Shown is a representative experiment with data=mean±SEM n≥3 replicates. (**B**) Western blot analysis of primary neurons exposed to baf and CQ 32 min after direct injection. (**C-E**)
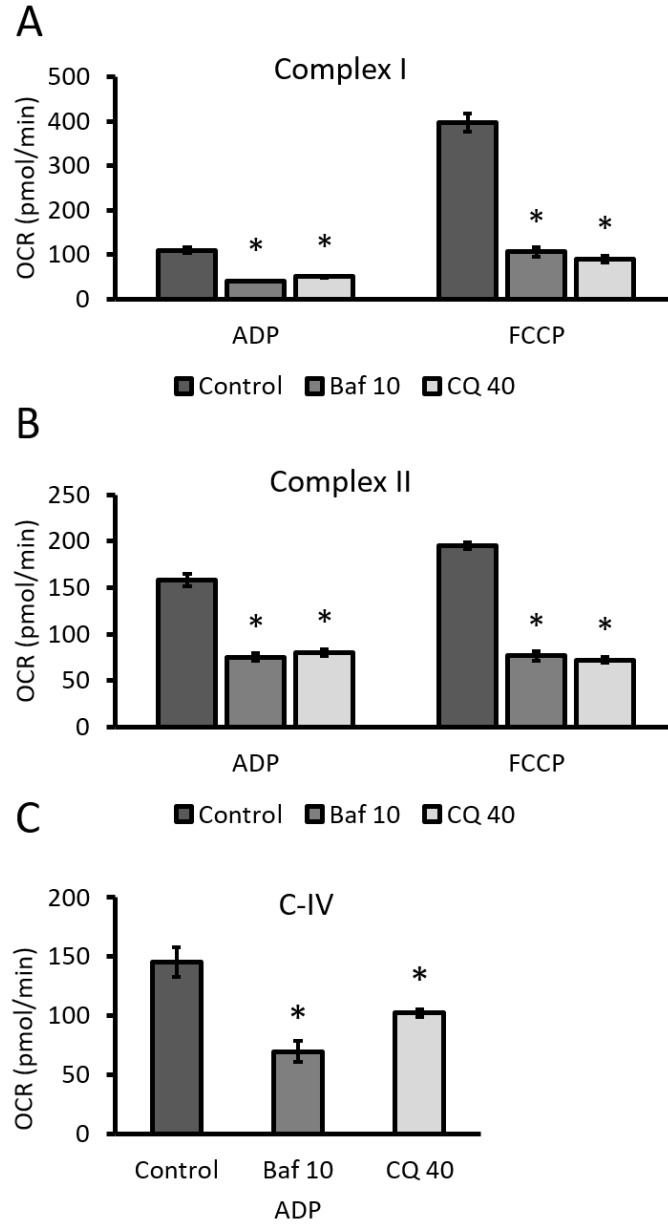
Figure 5: Effects of bafilomycin and chloroquine on complexes I, II and IV substrate-linked OCR in permeabilized neurons. Neurons were exposed to 10 nM bafilomycin (baf) or 40 μM chloroquine (CQ) for 24 h. (**A**) The activities of complex I were determined in neurons permeabilized with PMP in the presence of complex I substrates (pyruvate and malate) utilizing either ADP or FCCP. (**B**) Complex II linked activities were determined in similar fashion utilizing complex II substrate succinate in the presence of either ADP or FCCP. (**C**) Complex IV linked activities were again measured using ascorbate and TMPD as substrates with ADP in permeabilized cells. *p<0.05 compared to control, from 3 independent experiments. Shown is a representative experiment with data=mean±SEM n≥3 replicates.

Effects of autophagy inhibitors on levels of mitochondrial proteins and DNA

Given the significant decrease in all mitochondrial respiratory complexes after 24 h exposure we reasoned this could be due to either a decrease in mitochondrial quality or mitochondrial number. This was tested using a number of approaches. First, we determined if levels of selected mitochondrial electron transport chain complexes and Krebs cycle enzymes were altered by autophagy inhibitors after a 24 h exposure (**Figure 6 A**). No significant changes in representative subunits of mitochondrial complexes I-V were observed (**Figure 6 B-F**). Using these data and the respiratory chain complex activities (**Figure 5**), a normalized activity was calculated for each complex. **Figure 7** shows the complex I, II and IV activities normalized to protein and demonstrates that they are suppressed by bafilomycin or chloroquine by ~40-80% for all the respiratory chain complexes. It does not appear mitochondrial biogenesis is activated since we did not observe any changes on PGC-1α, (**Figure 6 G**). The levels of Krebs cycle enzyme aconitase did not change, while citrate synthase showed a modest increase in protein levels (**Figure 6 H, I**). Importantly, no significant changes in mtDNA copy number were observed; however, a significant increase in the amount of mitochondrial DNA damage occurred after bafilomycin or chloroquine exposure for 24 h, consistent with a decrease in mitochondrial quality (**Figure 6 J, K**).
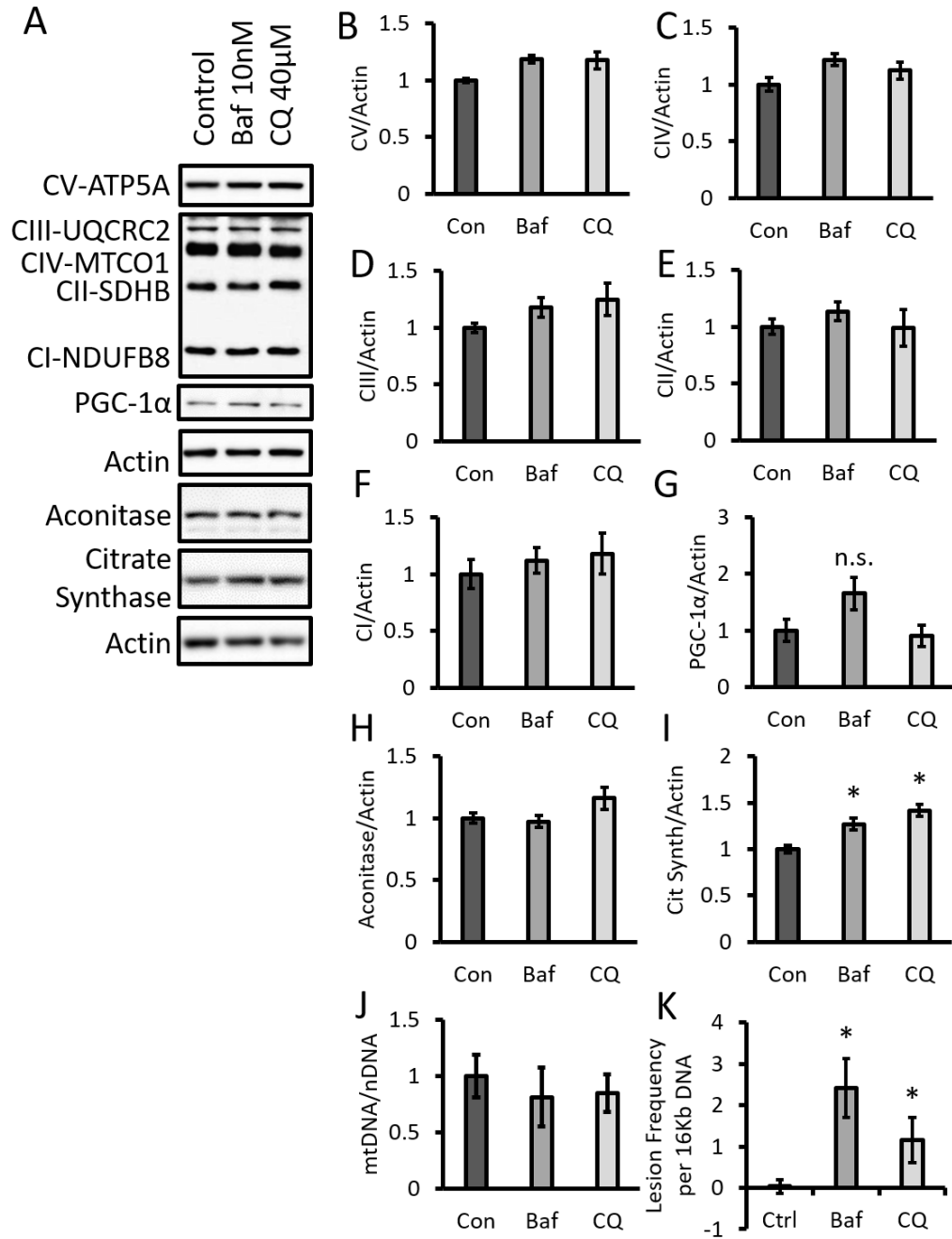
Figure 6: Increased mitochondrial DNA damage without significant changes of PGC-1α, key electron transport chain proteins or mitochondrial DNA copy number in response to bafilomycin or chloroquine. (**A**) Western blot analysis of subunits of complex I-V, PGC-1α, aconitase, and citrate synthase, in lysates from cells exposed to 10 nM bafilomycin or 40 μM chloroquine for 24 h. (**B-I**) Relative quantification of western blots (A). (**J**) Analysis of mitochondrial DNA copy number normalized to nuclear DNA. (**K**) Analysis of mitochondrial DNA damage. *p<0.05 compared to control, n≥3 independent cultures.
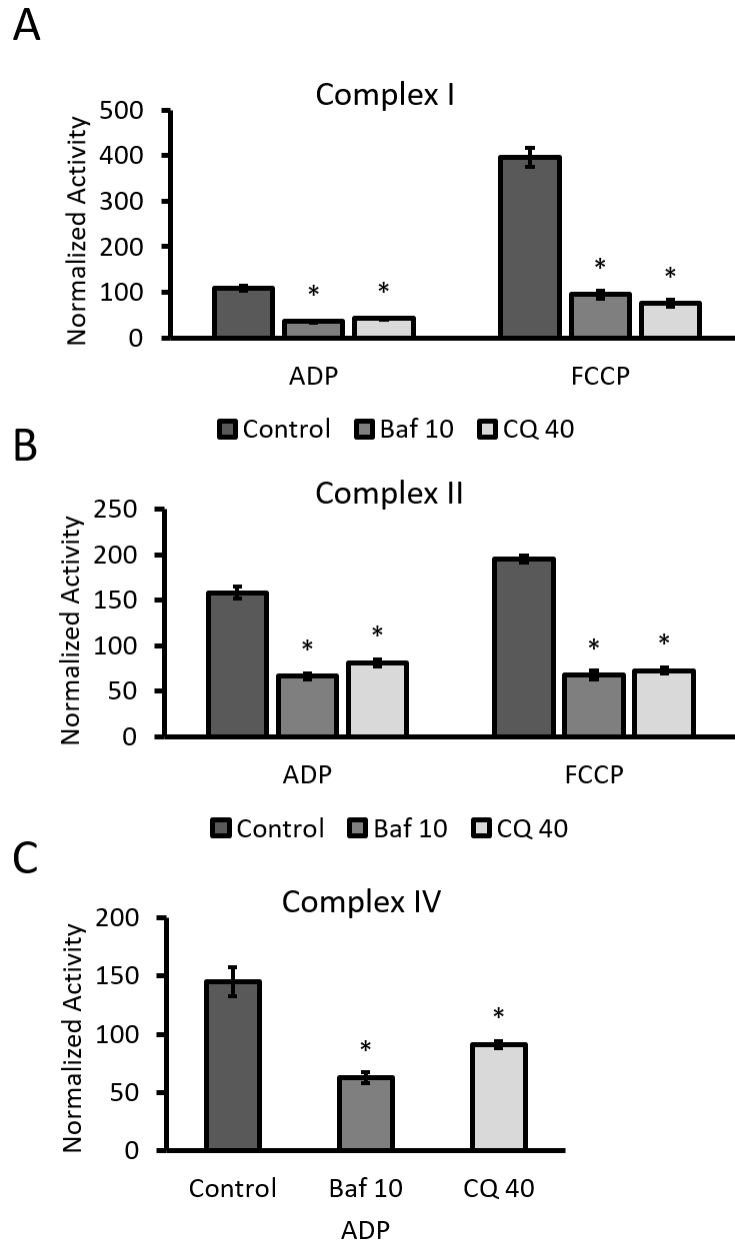
Figure 7: Normalized activities of mitochondrial complexes are decreased after exposure to bafilomycin (Baf) and chloroquine (CQ). (**A, B**) Mitochondrial complex normalized activity was calculated by normalizing complex I and complex II substrate-linked OCRs in the presence of either ADP or FCCP (Figure 3) to subunits of mitochondrial complex protein levels determined in Figure 4. (**C**) Normalized activity of Complex IV was determined in the presence of ADP (Figure 3) and normalized to protein levels as in Figure 4. *$p<0.05$ compared to control, OCR data were from 3 independent experiments. Shown is a representative experiment with data=mean±SEM n≥3 replicates. Western blot analyses were from n≥3 independent cultures.

Effects of autophagy inhibitors on Krebs cycle intermediates

We next determined the level of Krebs cycle metabolites and lactate using a targeted metabolomics approach (**Figure 8**). We detected no significant changes in lactate levels but observed a trend towards decreased pyruvate levels after bafilomycin and chloroquine exposure. The pyruvate to lactate ratio was then calculated and significant decreases of similar levels were observed after both bafilomycin and chloroquine exposure (**Figure 8 A-C**). Citrate, cis-aconitate and isocitrate levels were also measured, with significant decreases of both citrate and isocitrate in response to both bafilomycin and chloroquine. Interestingly, cis-aconitate was decreased by bafilomycin but increased by chloroquine (**Figure 8 D-F**). Key components of glutaminolysis, including α-ketoglutarate, glutamate, and glutamine, were significantly decreased by both bafilomycin and chloroquine while succinate levels remained unchanged (**Figure 8 G-J**). Fumarate and malate were also decreased but achieved significance with chloroquine only (**Figure 8 K, L**). To determine the potential mechanism behind the decrease of Krebs cycle intermediates in response to bafilomycin or chloroquine, we measured citrate synthase activities and found that it significantly decreased by ~20% after either bafilomycin or chloroquine exposure (**Figure 8 M**). Furthermore, we normalized its activity to levels of citrate synthase protein present in the cells, and found an even further decrease of ~40%, consistent with a substantially lower level of active protein (**Figure 8 N**).
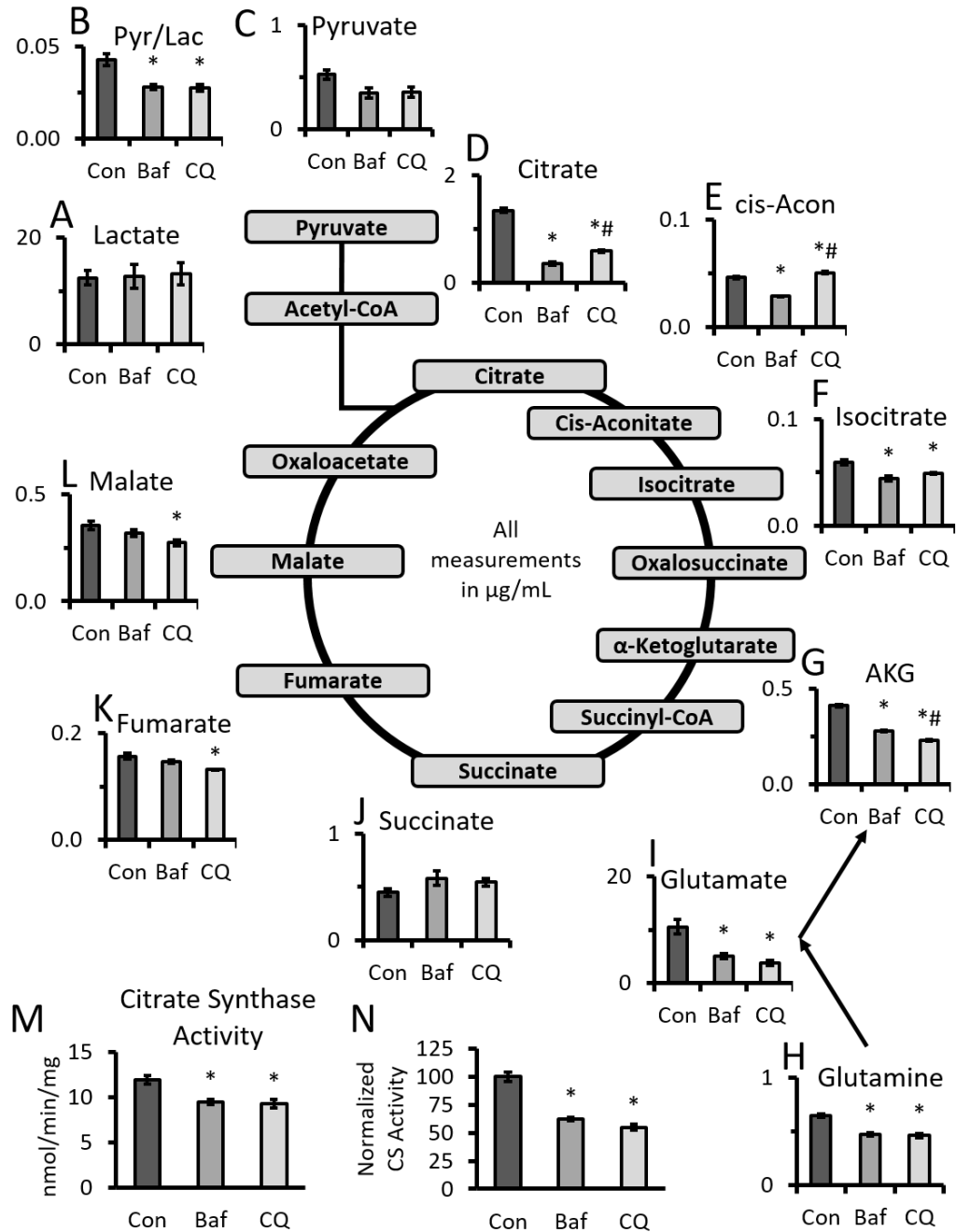
Figure 8: Effects of bafilomycin and chloroquine on Krebs cycle metabolites. (**A-L**) Targeted metabolomics of primary cortical neurons exposed to 10 nM bafilomycin or 40 μM chloroquine for 24 h. Levels of metabolites were shown in μg/mL. *$p<0.05$ compared to control, #$p<0.05$ compared between bafilomycin and chloroquine, n=5 samples. (**M**) Measurement of citrate synthase activity after 24 hr exposure to bafilomycin or chloroquine. Activities were normalized to total protein. (**N**) Citrate synthase activities were normalized to relative citrate synthase protein levels shown in Figure 4A, 4I, and expressed as a percentage of untreated controls. *$p<0.05$ compared to control, n=3-5 independent cultures.

DISCUSSION

Autophagy gene *Atg7* knockout in skeletal muscle, mouse embryonic fibroblasts and pancreatic β cells has been previously found to exhibit decreased state IV, State III, or basal, ATP-linked, and maximal activities. *Atg7* knockout mouse embryonic fibroblasts also exhibited increased DCFDA fluorescence suggesting increased production of reactive oxygen species, and *Atg7* knockout pancreatic β cells exhibited accumulation of swollen dysmorphic mitochondria [208]. This suggests that autophagy failure leads to a decrease in mitochondrial quality. In this study we have provided the first direct comparison on the effects of two widely used autophagy inhibitors, bafilomycin and chloroquine, on bioenergetics.

Attenuated autophagy has been reported to accompany cellular bioenergetic dysfunction in various genetic and oxidative stress models [112, 236-238]. Previous studies suggested that bafilomycin has a direct effect on mitochondrial function [214, 215]. It has also been reported that bafilomycin appears to slow down axonal transport of autophagosomes, but does not appear to slow down axonal trafficking or motility of mitochondria after a short 4 h treatment [101]. In our study, neither bafilomycin nor chloroquine for 32 min changed OCR in intact cells (**Figure 4 A**). These data indicate that the observed deficits in mitochondria function are not due to off target effects of the compounds on mitochondria but rather through autophagy failure resulting in accumulation of damaged mitochondria. Our studies demonstrate that in neurons, a 24 h exposure to autophagy inhibitors also inhibits parameters of mitochondrial function (**Figure 2**), even in the absence of p62 accumulation, as the case in chloroquine exposure. Furthermore, decreases were observed for complex I, II, and IV substrate-linked

respiration in permeabilized cells, indicating widespread deficiencies in mitochondrial electron transport chain function (**Figure 5**). These deficiencies occurred without any changes in PGC-1α, mitochondrial electron transport chain proteins, or matrix proteins except for an increase in citrate synthase and a trend toward increased aconitase protein which did not reach significance (**Figure 6 A-I**). However, while citrate synthase protein levels were modestly increased, its activity was diminished and its normalized activity, was diminished even further (**Figure 6 M, N**). Mitochondrial DNA damage was also increased (**Figure 6 J, K**). Taken together, these observations are all consistent with a decrease in mitochondrial quality.

Cellular metabolic programs play important roles in health and disease [232, 239-241]. How metabolic pathways respond to autophagy inhibition have not been fully investigated. In the metabolomics analysis we observed that pyruvate or lactate levels themselves showed no significant change, the more sensitive measure of the relative activity of glycolysis to mitochondrial function, the pyruvate/lactate ratio, was decreased after bafilomycin or chloroquine exposure, consistent with a relative increase in glycolysis (**Figure 8 A-C and Figure 3**). Furthermore, Krebs cycle intermediates, including citrate, cis-aconitate, and isocitrate are diminished. This is likely resulting from the inhibition of citrate synthase and its inability to provide substrates for downstream processing which was confirmed by direct measurement of citrate synthase activity (**Figure 8 D-F, M**). The differences in cis-aconitate levels in response to bafilomycin and chloroquine also suggest a possible decrease in aconitase activity. Additionally, key components of glutaminolysis, α-ketoglutarate, glutamate, and glutamine, were decreased while succinate, fumarate and malate have approximately been restored (**Figure 8 G-L**).

This observation would be consistent with an increase in glutaminolysis in an attempt to restore downstream intermediates.

In summary, at a concentration and duration of exposure that led to a similar level of accumulation of LC3-II, we found that both bafilomycin and chloroquine also decreased parameters of mitochondrial function in intact neurons. The levels of representative mitochondrial electron transport chain and mitochondrial matrix proteins were essentially unchanged by bafilomycin or chloroquine, but all showed a decrease in normalized activity suggesting multiple deficits in mitochondrial enzymes in oxidative phosphorylation and the TCA cycle.   Furthermore, mtDNA levels were unchanged but damage was increased. These findings are consistent with a secondary effect on bioenergetics by bafilomycin and chloroquine due to autophagy inhibition and a resulting decrease in mitochondrial quality.

TREHALOSE DOES NOT IMPROVE NEURONAL SURVIVAL IN EXPOSURE TO
ALPHA-SYNUCLEIN PRE-FORMED FIBRILS

by

MATTHEW REDMANN, WILLAYAT WANI, LAURA VOLPICELLI-DALEY,
VICTOR DARLEY-USMAR, AND JIANHUA ZHANG

CHAPTER 4

TREHALOSE DOES NOT IMPROVE NEURONAL SURVIVAL IN EXPOSURE TO
ALPHA-SYNUCLEIN PRE-FORMED FIBRILS

INTRODUCTION

Parkinson's disease (PD) is a neurodegenerative condition that clinically

manifests with abnormalities in movement, olfactory senses, gastrointestinal function and

an overall decline in cognitive abilities as the disease progresses. These symptoms are

associated with the progressive loss of dopaminergic neurons in the substantia nigra

[242]. Sharing with other neuropathologies, including dementia with Lewy bodies and

multiple systems atrophy, the majority of PD patient postmortem brains exhibit

accumulation of α-synuclein (aSyn) protein in highly phosphorylated, ubiquitinated and

insoluble aggregates observed as Lewy bodies and Lewy neurites [18, 243, 244]. Recent

studies indicate that aSyn may be released from neurons and seed aggregations in

adjacent neurons thus propagating disease progression [245].

Recently studies have started to investigate how aSyn intracellular inclusion

formation impacts recipient neuronal survival using a model in which aSyn pre-formed

fibrils (PFFs) can enter the cell and recruit endogenous aSyn in the neuron to form

insoluble, ubiquitinated and phosphorylated high molecular weight aSyn, characteristic of

those in human Lewy bodies and Lewy neurites [193, 245, 246]. Since one of the

strategies to help maintain intracellular protein homeostasis is through macroautophagy

[247], determining the impact of macroautophagy regulators on accumulation of aSyn

aggregates and neuronal survival in response to PFF exposure is thus essential to understanding PD.

Autophagy can be activated by the inhibition of the mammalian target of rapamycin (mTOR) by rapamycin. Many *in vitro* and *in vivo* studies have reported positive results using rapamycin to mitigate the effects of aSyn toxicity [248]. However, clinical use of rapamycin carries with it disadvantages that make its prolonged use in humans undesirable [249]. In addition, previous studies have demonstrated that autophagy induction by starvation or rapamycin post PFF transduction did not decrease PFF-induced intracellular aSyn aggregations and further exacerbated cell death [193]. Given that targeting of mTOR has limited therapeutic applications in humans in the realm of neurodegenerative treatments, compounds that activate autophagy independently of mTOR have been tested. One compound that has been found to be effective in activating autophagy in cell lines is the disaccharide trehalose [250], which appears to mediate its effects through both initiation of autophagy and activation of TFEB, turning on genes for increased lysosomal biogenesis [107, 251, 252]. Important for our study, neurons lack the enzyme trehalase that breaks down trehalose, thus the level of trehalose should be persistent over long periods of time in culture [253]. In humans, a single bolus of 50 g or less has been deemed safe, and in 2000 the US FDA gave notice that trehalose is generally regarded as safe for human consumption [254]. Although its administration has not been studied in the context of humans and PD, trehalose decreases aSyn in PC12 cells [250], decreases Tau accumulation in mice [255], and reduces neurodegeneration in amyotrophic lateral sclerosis [256], Huntington's [257], and Alzheimer's [258] disease models. In this study we specifically test the effects of trehalose on decreasing aSyn

aggregation and cell death upon exposure to PFFs, thus helping to evaluate the

therapeutic potential of trehalose in PD.

MATERIALS AND METHODS

Cell Culture

Primary wildtype (C57BL/6 strain bred in house from mice ordered from Charles

River and WT mice bred from a cathepsin D knockout colony) [259-261], or aSyn

knockout (The Jackson Labs C57BL/6N-Snca^{tm1Mjff}/J) [25] cortical mouse neurons were

derived from p0 pups. All mouse experiments were done in compliance with the

University of Alabama at Birmingham Institutional Animal Care and Use Committee

guidelines (IACUC09019 and IACUC20354). Briefly, cells were seeded on plates coated

with Poly-L-Lysine solution containing 0.1 mg/mL Poly-L-Lysine, 50 mM Boric acid,

and 10 mM Borax for a minimum of 1 hour. Cells were grown and maintained in

Neurobasal A medium supplemented with Glutamax, Penn/Strep, and B27 neuronal

supplement. Treatments were performed by removing half the media and adding back

the same volume of media with the treatment media. Tissue culture medium and reagents

were obtained from Life Technologies. Trehalose (T0167-25G), chloroquine (C6628-

25G) sucrose (S-5016) and AraC (C1768-500MG) were obtained from Sigma.

Generation of aSyn PFFs

A human wildtype aSyn gene was cloned into pRK172 and expressed in *E. coli* as

previously reported [192]. Bacteria grown under antibiotic selection were harvested,

homogenized and dialyzed before purification through size exclusion and ionic exchange

columns. Five mg/ml of protein was incubated at 37ºC for 1 week to produce fibrils.

Before applying to the cells, fibrils were sonicated 60 times over 40 seconds [193].

Using the Pierce LAL chromogenic endotoxin quantification kit, we have determined that

≤ 0.004 ng/mL of endotoxin was present in the PFF samples.

Cell Viability

Cell viability was measured in two ways. First, viability was measured utilizing

the trypan blue exclusion method. Cells were trypsinized and then trypan blue was added

to the cells. Cells excluding the dye were counted. Second, viability was measured using

the MTT cell death/proliferation assay. Briefly, a media and tetrazolium salt mixture was

added to the cells where it is reduced to insoluble formazan crystals. These crystals were

dissolved in DMSO and measured at 550 nm using a plate reader. Cells were plated on

96-well plates at 80,000 cells per well for both assays.

Immunocytochemistry

Cells were seeded at 240,000 cells per well on autoclaved glass coverslips that

were placed in 24-well plates. After treatment, cells were fixed with a mixture of 4%

paraformaldehyde and 4% sucrose. The addition of 1% Triton X-100 to the fixative was

used to determine the soluble from insoluble protein in the cell. After fixing, cells were

permeabilized with 0.1% Triton X-100 and then blocked with 3% BSA in PBS. Cells

were probed with antibodies for p-Ser-129 using either Affinity Bioreagents (PA1-4686

1:2000) for Figure 1 G or Covance-81A (MMS-5091 1:5000) for the remaining figures.

For non-aSyn staining, cells were plated and fixed as above but were blocked with 10%

horse serum and 5% FBS in PBS. Cells were probed with either LC3 (L8918 Sigma

1:500), MAP2 (Sigma M4403 1:1000), or GFAP (Dako Z0334 1:500). Alexa Fluor 488 (Invitrogen A11001, A11008 1:500) or 568 (Invitrogen A11004 1:500) secondary antibodies were subsequently added to the wells. Cells were then counter stained with nuclear dye Hoechst 33342 (Sigma 861405) and mounted with Fluoromount-G (Southern Biotechnology). All images were acquired using a Leica TCS SP5 V confocal laser scanning microscope.

Western blot analysis

For immunoblot analysis, cells were plated at 240,000 cells per well on 48 well plates or 480,000 per well on 24 well plates and then washed with ice cold PBS and then lysed with RIPA buffer (50 mM Tris pH 7.8, 150 mM NaCl, 2 mM EDTA, 1% Triton X-100, and 0.1% SDS) in the presence of protease (Roche) and phosphatase inhibitors (Sigma) after treatments. After 20 min on ice, cells were scraped from the wells and placed in 1.5 mL Eppendorf tubes for centrifugation at 16,800 x g for 20 min at 4°C. Protein content in supernatant was determined by DC Protein assay (Bio-Rad). Equal amounts of protein for each sample were loaded and separated by SDS-PAGE using 12% or 15% gels. Protein was wet-box transferred to PVDF membranes and probed with the following antibodies: LC3 (Sigma L8918 1:2000), p62 (Abnova H00008878-M01 1:2000), α-synuclein (Santa Cruz sc-7011-R 1:2500), and β-actin (Sigma A5441 1:2500). Blots were visualized by film or Amersham™ Imager 600 (GE Healthcare Biosciences; Pittsburg PA).

Statistical analysis

All data are reported as the mean ± SEM, p values of less than 0.05 were deemed statistically significant after being analyzed by Student's t-test or ANOVA.

RESULTS

aSyn pre-formed fibrils (PFFs) induce intracellular aSyn protein aggregation

To measure the dose-dependent effects of extracellular exposure to aSyn pre-formed fibrils, we cultured primary cortical neurons from mouse pups, and at DIV7 exposed them to human wildtype aSyn PFFs for 14 days at concentrations 0.1 to 2.5 µg/mL for western blot analysis of total aSyn and immunocytochemistry for insoluble S129 p-aSyn. Western blot analysis revealed a small but significant increase in the monomeric aSyn at 2.5 µg/mL of PFFs. An approximately 2-fold increase of total aSyn (monomeric and high molecular weight aSyn) was found in response to PFF at concentrations of 1.0 and 2.5 µg/mL (**Figure 1 A-C**). Whether accumulation of aSyn is more severe in response to PFF, compared to un-aggregated monomeric aSyn, was determined by exposing cells to similar concentrations of monomeric aSyn. In the latter case, we observed no changes in the aSyn monomer, whereas a modest increase of total aSyn was observed with 1 µg/mL and 2-fold increase with exposure to 2.5 µg/mL monomeric aSyn (**Figure 1 D-F**).

To determine if these aSyn aggregates shared common features with both classical Lewy bodies and previously characterized PFF-induced aggregates [193, 245, 246], we performed immunocytochemistry analyses after exposing fixed cells to 1% Triton X-100 [193]. As shown in **Figure 1 G**, S129 phosphorylated aSyn that is
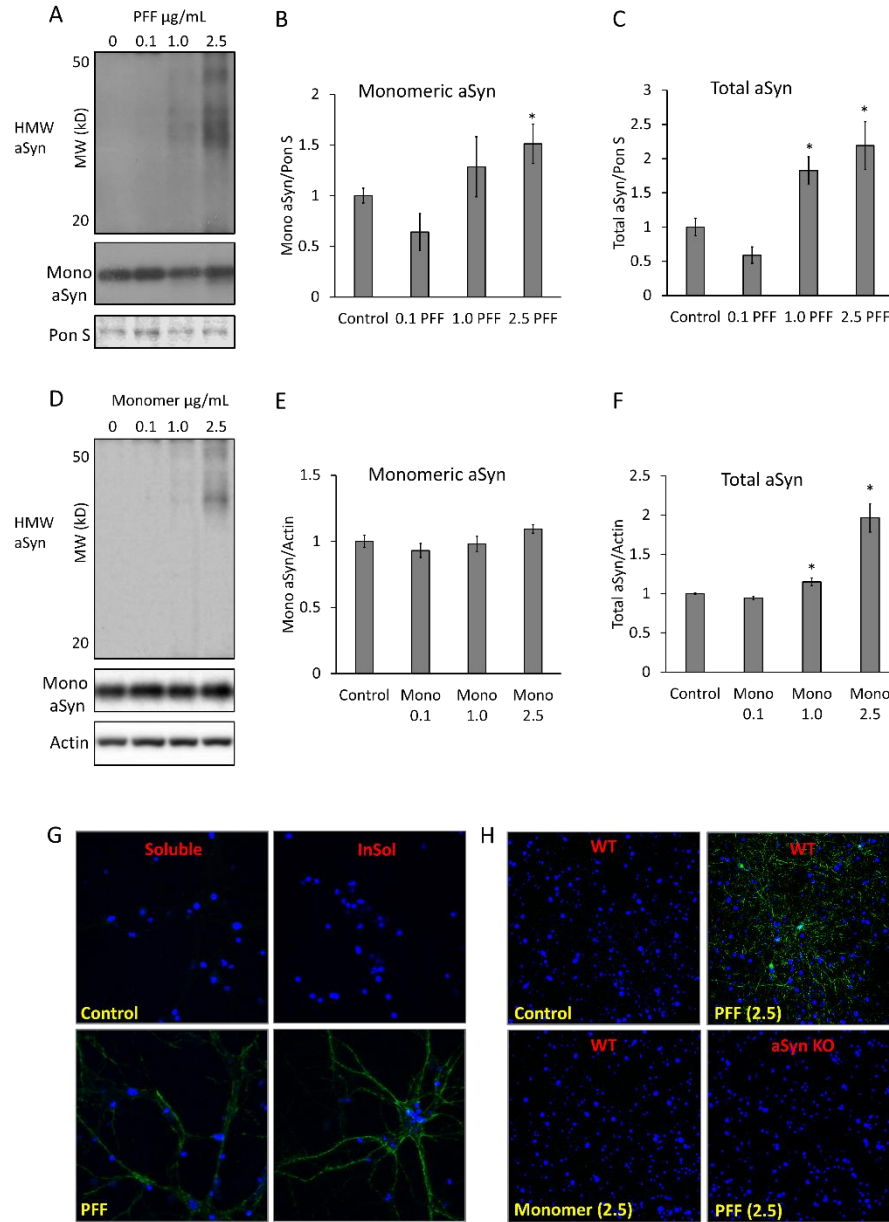
Figure 1: PFFs induce high molecular weight (HMW) and insoluble aggregates. (**A**) Western blot analysis of total monomeric and HMW aSyn from primary cortical neurons treated for 14 days with PFFs. (**B, C**) Quantification of western blots from A. (**D**) Western blot analysis of total and monomeric aSyn of primary cortical neurons exposed to aSyn monomer for 14 days. (**E, F**) Quantification of western blots D. Data represent mean ± SEM (n=3). *p<0.05 compared to control; the Student t-test. (**G**) Cortical neurons exposed to 2.5 µg/mL PFF for 14 days and then probed for p-aSyn (green) in the presence (InSol) or absence (Soluble) of 1% Triton X-100 and counter stained with Hoechst (blue). Images were taken at 63x magnification. (**H**) Wildtype or aSyn knockout neurons exposed to vehicle, PFF, or aSyn Monomer at 2.5 µg/mL for 14 days and then probed for 1% Triton X-100 insoluble p-aSyn (green) and counterstained with nuclear dye Hoechst (blue), 40x magnification.

insoluble in 1% Triton X-100 was significantly increased in response to 2.5 µg/mL PFF.

Under the same condition, exposure of cells to 2.5 µg/mL of aSyn monomer resulted in

no p-aSyn accumulation as demonstrated by immunocytochemistry analyses. aSyn

knockout cells exposed to 2.5 µg/mL PFFs also resulted in no insoluble p-aSyn under the

same condition indicating endogenous aSyn is required for accumulation of insoluble p-

aSyn (**Figure 1 H**).

Effects of PFFs on autophagy markers

Previous studies have demonstrated that mouse primary hippocampal neurons

exposed to 5 µg PFFs for 14 days exhibit increased LC3-II and levels of Triton X-100

insoluble p62 [105]. To determine whether this occurs at a lower concentration with

primary neurons from a different brain region, we performed western blot analyses of

LC3 and p62 after exposing primary cortical neurons to PFFs for 14 days (**Figure 2**). We

found that increasing concentrations of PFFs up to 2.5 µg did not significantly change

LC3-II or total levels of soluble p62 (**Figure 2 A-D**). The levels of LC3-II were

confirmed by immunocytochemistry, where LC3-II puncta per cell were counted and no

significant difference was observed between control and cells exposed to PFFs (**Figure 2

E, F**). Nor did we observe changes in either p62 or LC3-II in cells exposed to non-

aggregated aSyn monomer for 14 days (**Figure 2 G-J**).

Effects of trehalose on neuronal autophagy

Previous studies have demonstrated that autophagy induction by starvation or

rapamycin post PFF transduction did not decrease PFF-induced intracellular aSyn
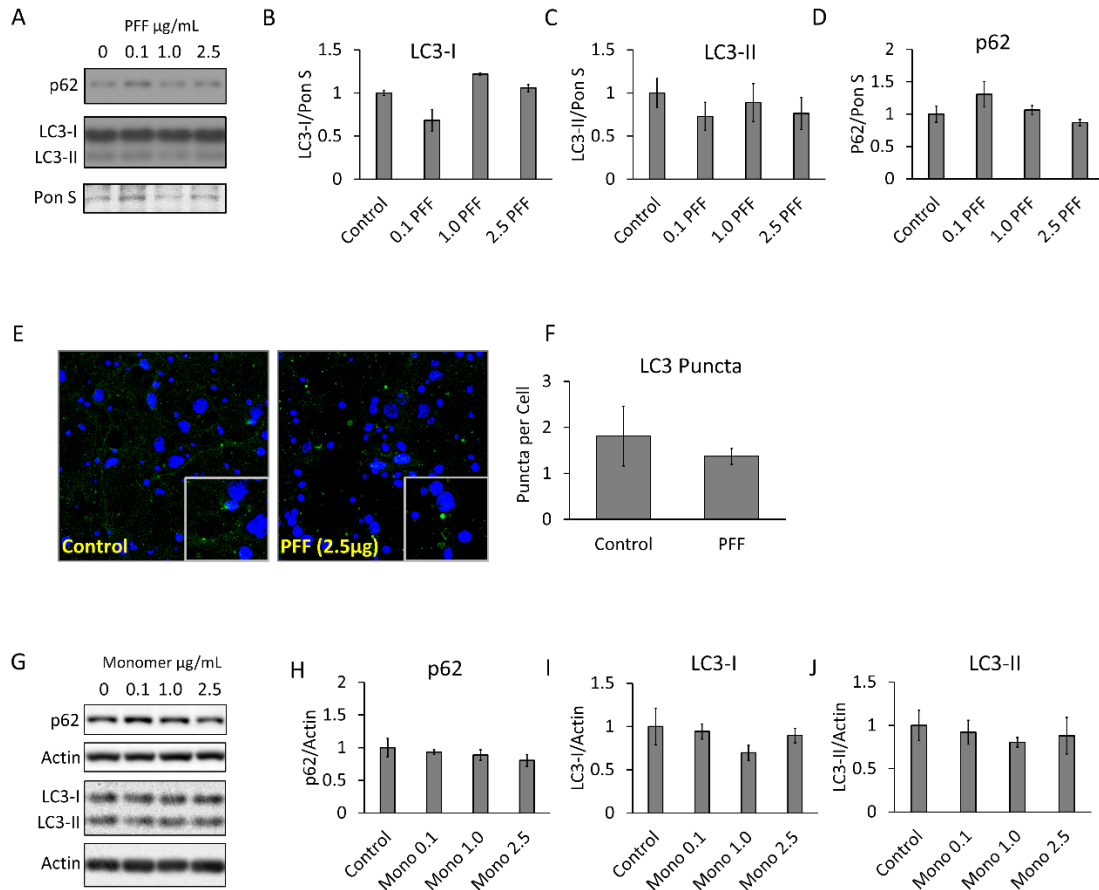
Figure 2: PFFs do not significantly alter the levels of autophagosomal protein LC3-II or autophagy adaptor/substrate protein p62. (**A**) Western blot analysis of LC3-I, LC3-II, and p62 from primary cortical neurons exposed to PFFs for 14 days. (**B-D**) Quantification of western blots from A. (**E**) Immunocytochemistry of cells exposed for 14 days to 2.5 µg/mL PFFs and probed for LC3 (green) and counterstained with nuclear dye Hoechst (blue). Images were taken at 63x. (**F**) Quantification of images from E. (**G**) Western blot analysis of LC3-I, LC3-II, and p62 from primary cortical neurons exposed to aSyn monomer for 14 days. (**H-J**) Quantification of western blots from F. Data represent mean ± SEM (n=3). *$p<0.05$ compared to control; the Student t-test.

aggregations and only exacerbated cell death [105]. Here we investigated whether induction of autophagy using trehalose attenuates PFF-induced aSyn accumulation thus enhancing neuronal survival. We exposed neurons to 25 mM trehalose for 14 days and found significant increases in LC3 puncta as assessed by immunocytochemistry analyses (**Figure 3 A, B**).
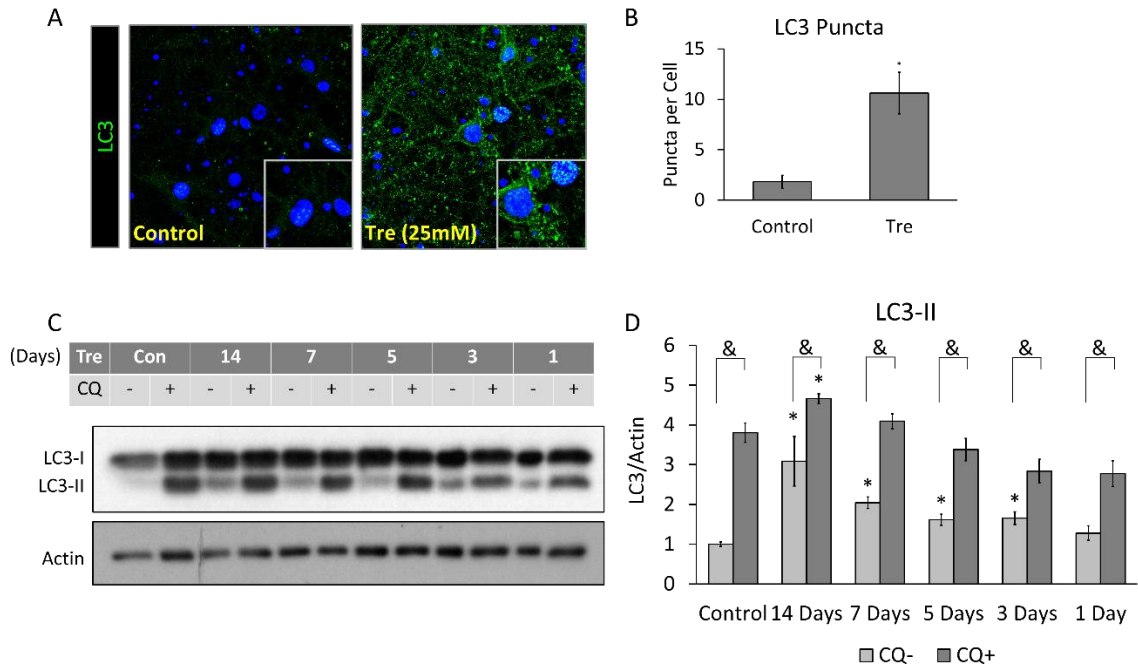
Figure 3: Trehalose increases LC3-II and autophagic flux. (**A**) Immunocytochemistry of cells exposed for 14 days to 2.5 µg/mL PFFs and probed for LC3 (green) and counterstained with nuclear dye Hoechst (blue). Images were taken at 63x. (**B**) Quantification of images from A. (**C**) Autophagic flux analysis of neurons exposed for up to 14 days to PFF with and without trehalose and then to 40 µM chloroquine (CQ) 5 hours before protein collection. Control (Con) was 14 days without Trehalose. (**D**) Quantification of western blot G. Data represent mean ± SEM (n=3). *p<0.05 compared to control; the Student t-test.

To determine if autophagic flux through the autophagy pathway was increased, we exposed cells from 1 to 14 days with 25 mM trehalose, and then with 40 µM Chloroquine (CQ) for 5 hours which prevents lysosomal degradation of autophagosomes. We found that trehalose alone significantly increased LC3-II beginning at 3 days that continued to increase until the conclusion of the experiment at 14 days. CQ induced significant increases in LC3-II over non-CQ treated neurons for all time points. However, only at 14 days did the trehalose and CQ treated cells exhibit significantly more LC3-II than the CQ only control cells, indicating increased autophagic flux at 14 days (**Figure 3 C, D**).

Effects of trehalose on aSyn protein aggregation and autophagy

To determine if trehalose impacts PFF-induced aSyn aggregation, we added 25 mM trehalose to cells at the time of PFF exposure and performed immunocytochemistry of 1% Triton X-100 insoluble p-aSyn over a range of PFF concentrations with and without trehalose for 14 days. Without trehalose, there was a strong trend toward increased p-aSyn at 0.1 µg/mL that became significant at 1.0 µg/mL and remained at similar levels at 2.5 µg/mL. In the presence of trehalose, similar trends of p-aSyn were observed with significant increases seen at 1.0 µg/mL and continuing to 2.5 µg/mL similar to cells without trehalose. No statistical differences were observed for cells exposed to PFFs with or without trehalose over a range of PFF concentrations, indicating that trehalose failed to remove p-aSyn aggregates (**Figure 4 A, B**). To further confirm these findings, we measured total aSyn in the presence or absence of both trehalose and PFFs by western blot. Trehalose exposure alone for 14 days did not change endogenous aSyn levels, while at 1.0 µg/mL (**Figure 4 C-E**) or 2.5 µg/mL (**Figure 4 F, G**) PFFs significantly increased total high molecular weight aSyn, even in the presence of trehalose, again suggesting trehalose fails to remove PFF induced aggregations. Noting that trehalose alone increases LC3-II (**Figure 3**), we measured whether this is still the case in the presence of PFF by western blot analyses lysates from cells exposed for 14 days to 25 mM trehalose, 2.5 µg/mL PFFs, or both. No significant changes were noted in LC3-I. However, we again observed increases in LC3-II with trehalose alone but not PFF alone. LC3-II remained elevated in the presence of both trehalose and PFFs at similar levels as trehalose alone (**Figure 4 F, H, I**).
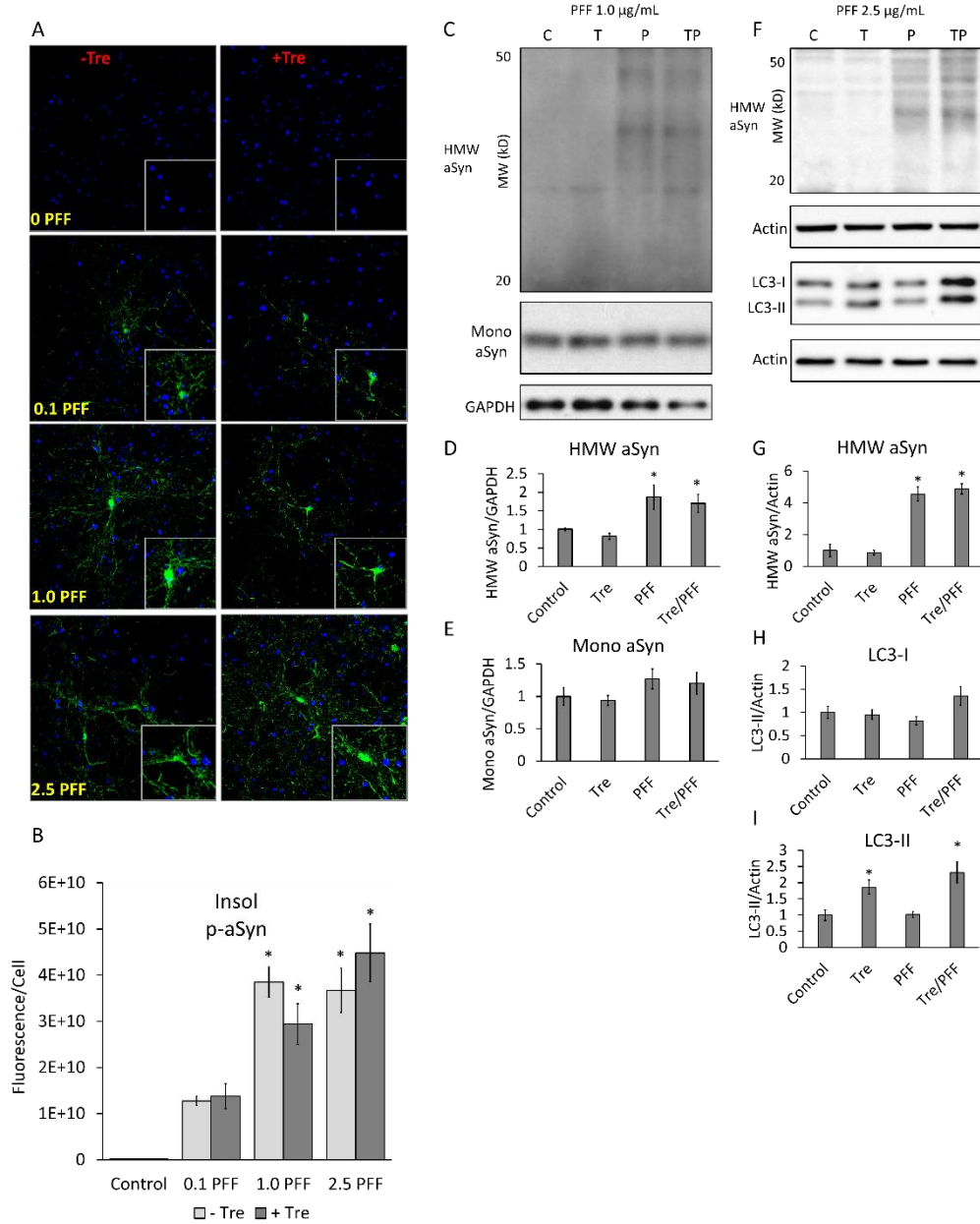
Figure 4: Trehalose fails to remove PFF-induced aggregations. (**A**) ICC of primary cortical mouse neurons exposed to PFFs (0, 0.1, 1.0, 2.5 µg/mL) ± 25 mM trehalose for 14 days and probed for 1% TX-100 insoluble phosphorylated aSyn (green) and counterstained with nuclear dye Hoechst (blue), 40x magnification. (**B**) Quantification of total fluorescence from PFF exposed cells normalized to nuclei per field. Data represent mean ± SEM (n=3). *p<0.05 to control; 2-way ANOVA. (**C**) Western blot analysis of cortical neurons exposed for 14 days to 1 µg/mL PFFs ± 25 mM trehalose. (**D, E**) Quantification of western blots C. (**F**) Western blot analysis of cortical neurons exposed for 14 days to 2.5 µg/mL PFFs ± 25 mM trehalose. (**G-I**) Quantification of western blots F. Data represent mean ± SEM (n=3-4). *p<0.05 compared to control; the Student t-test. C=Control, T=Trehalose, P=PFF, TP=Both.

Trehalose impacts cell viability

Although trehalose does not appear to remove aSyn aggregations, it may help remove toxic species of aSyn that are below detection sensitivity. Alternatively, it may physically interact with the aSyn aggregates reducing their toxicity or assisting in clearing cellular organelles damaged by aSyn, and thus attenuate cell death. To test whether trehalose alone alters the basal viability of neurons in culture, we exposed primary neurons to 3 different concentrations of trehalose over a 15-day period. We saw no change in cell viability at 1 mM but beginning at 10 mM and continuing to 25 mM we saw significant increases in cell viability with trehalose exposure alone (**Figure 5 A**). Next we determined if the enhancement of viability was specific to trehalose alone or if another disaccharide could have similar effect. We thus compared cell viability after exposing cells to either trehalose or a similar disaccharide, sucrose, for 14 days both at 25 mM concentrations. Sucrose had no impact on cell viability while 25 mM trehalose increased the number of surviving cells (**Figure 5 B**).

It is currently unknown whether trehalose will increase glial cell proliferation in neuronal culture, even while using Neurobasal medium without serum. To rule out the possible effects of trehalose inducing glial proliferation, we used a glial cell proliferation inhibitor, cytosine arabinoside (AraC). As before, trehalose increased cell viability at 10 and 25 mM. At 10 mM trehalose, AraC slightly blunted cell viability but still trended upwards. At 25 mM trehalose, AraC did not blunt cell viability, indicating that glial proliferation is not responsible for the enhanced viability in response to trehalose (**Figure 5 C**). Furthermore, we confirmed this finding by comparing the number of GFAP positive cells to the total number of nuclei and determined that only approximately 5% of

cultures stained positive for GFAP and that this number did not change with Trehalose or PFF exposure (**Figure 6**).

To determine if PFFs induce cell death and are more toxic than monomeric aSyn, we compared cells exposed to both 2.5µg/mL aSyn monomer and PFFs for 14 days. We found that PFFs induced significant cell loss, while treatment with aSyn monomer had no effect on cell viability, indicating that aSyn protein in its monomeric state is not sufficient to decrease viability (**Figure 5 D**). Additionally, cells from aSyn KO mice exposed to PFFs did not show any decrease in cell viability, further demonstrating that endogenous aSyn is required to potentiate cell toxicity in response to PFFs (**Figure 5 E**). To determine if trehalose would enhance cell survival in the presence of PFFs, we exposed cells for a period of 14 days to 3 concentrations of PFFs with or without 25 mM trehalose. Using an MTT based cell death assay, we measured the effect of PFFs on cell viability. We observed that at 2.5 µg/mL PFFs decreased cell viability. In cells exposed to trehalose, there was an increase in basal cell viability after 14 days as observed above, and an increase in cell viability after 2.5 µg/mL PFF+trehalose compared to the same concentration of PFF -trehalose (**Figure 5 F**). Cell survival is comparable in +trehalose+PFF compared to –PFF-trehalose. However, in the presence of trehalose, PFFs still induced cell death compared to +trehalose+PFF indicating that PFF toxicity still persists.
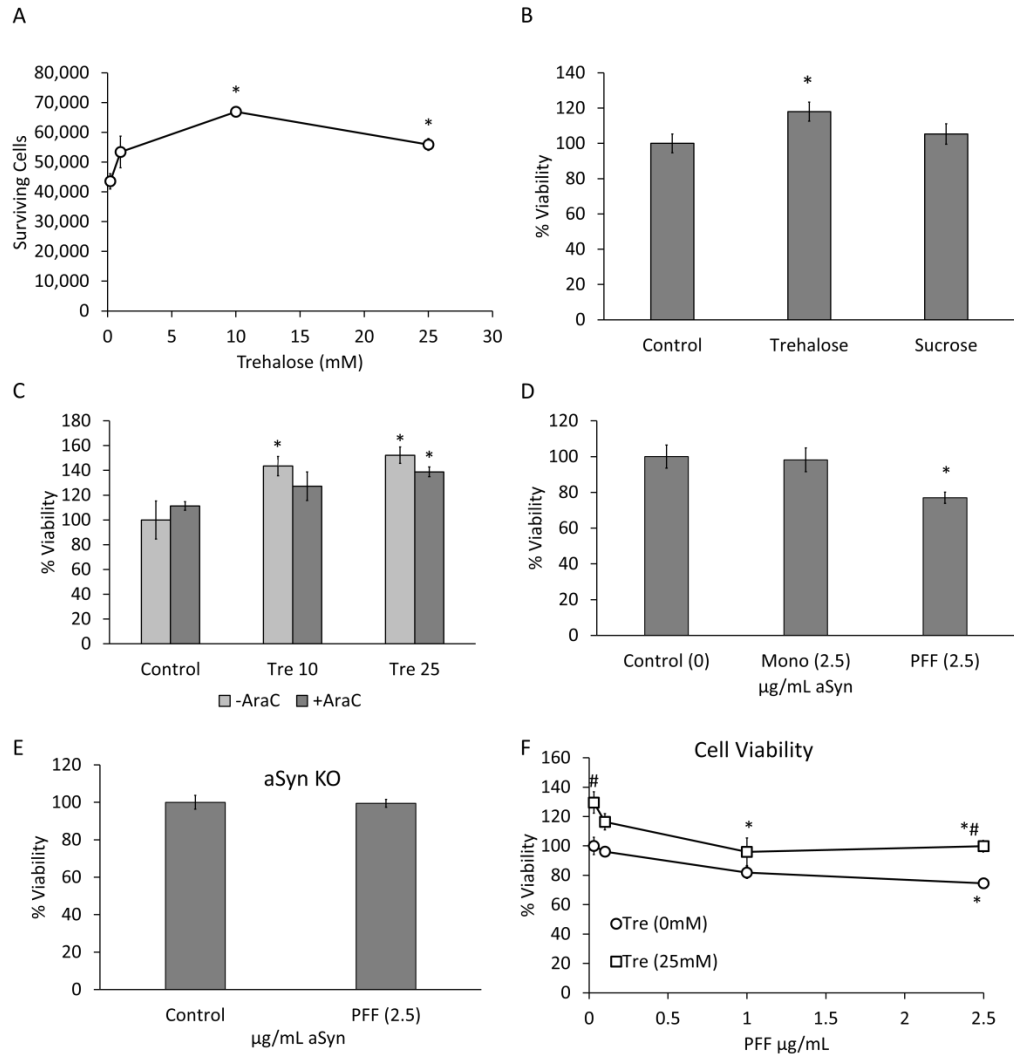
Figure 5: Effects of trehalose on cell viability. (**A**) Viability of primary cortical neurons exposed to 1, 10, or 25 mM trehalose for 15 days was determined by trypan blue exclusion assays and plotted. *$p<0.05$ (n≥3). (**B**) Viability of primary cortical neurons exposed to either 25 mM trehalose or 25 mM sucrose for 14 days was determined by trypan blue exclusion assays. Data represent mean ± SEM (n≥3). *$p<0.05$ compared to control. (**C**) Viability of primary neurons exposed to trehalose in the presence or absence of 2.5 µM cytosine arabinoside (AraC) was determined by trypan blue exclusion. Data represent mean ± SEM (n≥3). *$p<0.05$ compared to control. (**D**) Viability of primary cortical neurons treated with 2.5 µg/mL aSyn monomer or PFF for 14 days was determined by MTT. Data represent mean ± SEM (n=5). *$p<0.05$ compared to control; 1-way ANOVA. (**E**) Viability of aSyn KO neurons exposed to control or 2.5 µg/mL PFF for 14 days was determined by MTT. Data represent mean ± SEM (n=6). Student t-test. (**F**) Viability of primary neurons exposed to PFFs plus or minus 25 mM trehalose for 14 days was determined by MTT. Data represent mean ± SEM (n=5). *$p<0.05$ compared to respective control (no PFFs). #$p<0.05$ between + and - trehalose treated cells; 2-way ANOVA.
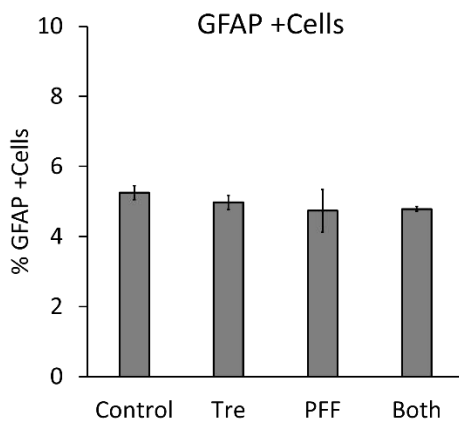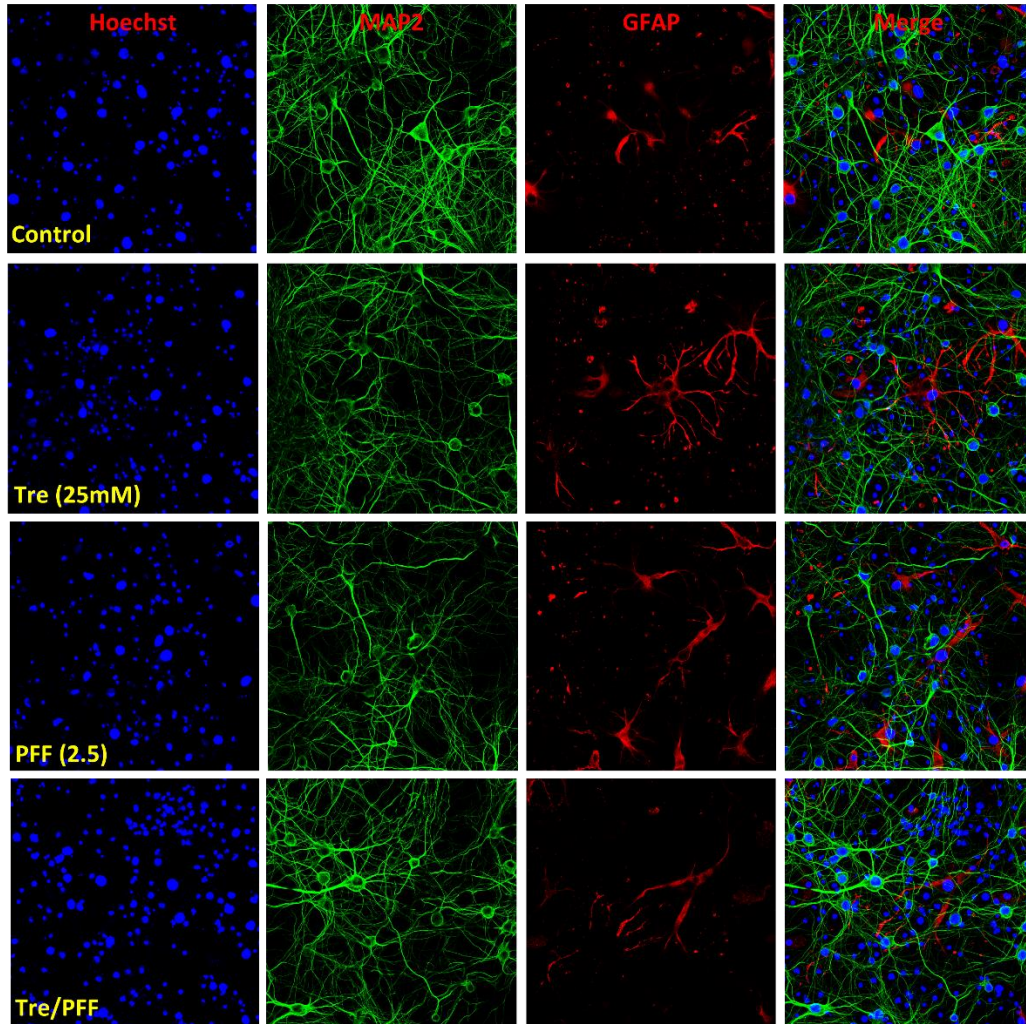
Figure 6: Assessment of cell culture population. Primary cortical neurons exposed to control, 25mM trehalose, 2.5 µg/mL PFFs, or both for 14 days were probed for MAP2, GFAP and counterstained with nuclear dye Hoechst (blue), 40x magnification. GFAP positive cells were quantified and normalized to total cell number determined by nuclear dye. Data represent mean ± SEM (n=3).

DISCUSSION

In this study we have shown that exogenously applied aSyn pre-formed fibrils (PFFs) induce significant protein aggregation in primary neurons (**Figure 1 A-C, G**) consistent with prior reports [193, 246]. The addition of aSyn monomer does not induce S129 phosphorylated insoluble inclusions in primary neurons (**Figure 1 D-F, H**). Furthermore, endogenous aSyn is required for the propagation of PFFs as aSyn KO neurons exposed to 2.5 µg/mL PFFs do not accumulate insoluble S129 phosphorylated aSyn inclusions (**Figure 1 H**).

In our study, PFFs did not change levels of p62 and LC3-II as previous studies have shown (**Figure 2 A-D**). This is likely due to a lower amount of PFFs added, and that in our system we used cortical neurons where Lewy body pathology occurs later in Parkinson's disease [32]. Additionally, our cultures were isolated from postnatal mice opposed to embryonic cultures, thus it is possible that a higher threshold is required for PFFs to attenuate autophagy. By these measures our model used a less severe exposure to PFFs and concurrently we observed a less severe phenotype.

Most studies in cell cultures use acute high doses of ≥100 mM trehalose, demonstrating in the short term that trehalose enhances autophagy. In these models, up-regulation of autophagy was implicated as being protective [106, 262]. However, in animal models, chronic trehalose exposure is necessary, and may also be for future patients. To determine the effects of chronic lower concentrations of trehalose in culture, we for the first time show a low concentration of 25 mM trehalose over a 14-day period enhances autophagic flux and increases basal cell viability. And while trehalose in the presence of PFFs was unable to enhance viability to that of cells exposed only to

trehalose, it was able to restore viability to the level of untreated controls (**Figure 5 F**). This protective effect is intriguing especially that the survival of the minor population of astrocytes was not changed by either PFF or trehalose.

It is currently unclear how trehalose enhances cell survival. Trehalose increased LC3-II in the absence and presence of PFF (**Figure 4 I-K**). Nonetheless, trehalose has been shown to alter the formation of A53T fibrils, tau fibrils, amyloid-beta and polyQ proteins [257, 258, 262-264], and thus is proposed to act as a molecular chaperone. In yeast, it has been shown that under the protein misfolding and aggregation stress of desiccation, trehalose is essential for maintaining viability by stabilizing cellular proteins, similar in function to HSP104 [265]. It also can interact in synergy with existing chaperones, as is the case with its interaction with p26 to maintain functional citrate synthase protein during heat shock *in vitro* [266]. Furthermore, unlike rapamycin, trehalose did not exacerbate PFF toxicity. Additionally, trehalose has been shown effective in ameliorating symptoms in an A53T AAV rat model of PD administered via drinking water, suggesting that trehalose may also protect against PFF-induced neurodegeneration in animal models [267]. Nonetheless, this study corroborates previous work that PFFs seem to resist degradation even with enhancement of macroautophagy. Future studies are still urgently needed to identify novel pathways that promote aSyn degradation and enhance neuronal survival in response to exposure to aSyn fibrils.

THE ROLE OF AUTOPHAGY, MITOPHAGY AND LYSOSOMAL FUNCTIONS IN
MODULATING BIOENERGETICS AND SURVIVAL IN THE CONTEXT OF
REDOX AND PROTEOTOXIC DAMAGE: IMPLICATIONS FOR
NEURODEGENERATIVE DISEASE

by

MATTHEW REDMANN, VICTOR DARLEY-USMAR, AND JIANHUA ZHANG

CHAPTER 5

DISCUSSION AND FUTURE DIRECTIONS

INTRODUCTION

The studies in this dissertation have focused on the impact of autophagy regulation on key aspects of mitochondrial function and protein aggregation as they relate to aging and Parkinson's disease (**Figure 1**). Chapter 3 focused on the interplay between autophagy and mitochondria. Evidence was provided that if the lysosome is inhibited and autophagy halted in neurons, damaged mitochondria will accumulate. This was evidenced by increased mtDNA damage, decreased basal, maximal, ATP-linked, and reserve capacity parameters of oxygen consumption. This finding also held true in permeabilized neurons where complex I, II, and IV activities were decreased. We also found alterations in TCA cycle intermediates. This chapter demonstrates the importance of autophagy in maintaining mitochondrial health and function. As damaged mitochondria accumulate in aging and PD brains, insufficient autophagy may contribute to their progression.

Chapter 4 focused on the interplay between autophagy and protein aggregation. We observed that PFFs induce insoluble S129 phosphorylated aSyn aggregations. However, despite that trehalose induced autophagy in primary cortical mouse neurons over a 14 d time period and increased autophagic flux, it failed in preventing or removing aSyn accumulations, and failed to rescue neurons from PFF toxicity. This suggests that PFFs might be evading autophagy processes and autophagic degradation. This point will be discussed in more detail below.

Therefore, although we have gained insights into how autophagy interplays with mitochondrial and protein homeostasis, neuronal function and survival, there are still unanswered questions regarding neuronal function and neurodegeneration and how autophagy may provide strategies for therapeutics. In this chapter, I will further discuss the role of autophagy, mitophagy, and lysosomal function in modulating bioenergetics and survival in the context of aging and neurodegenerative disease, primarily Parkinson's disease, as well as future directions that will address unanswered questions.
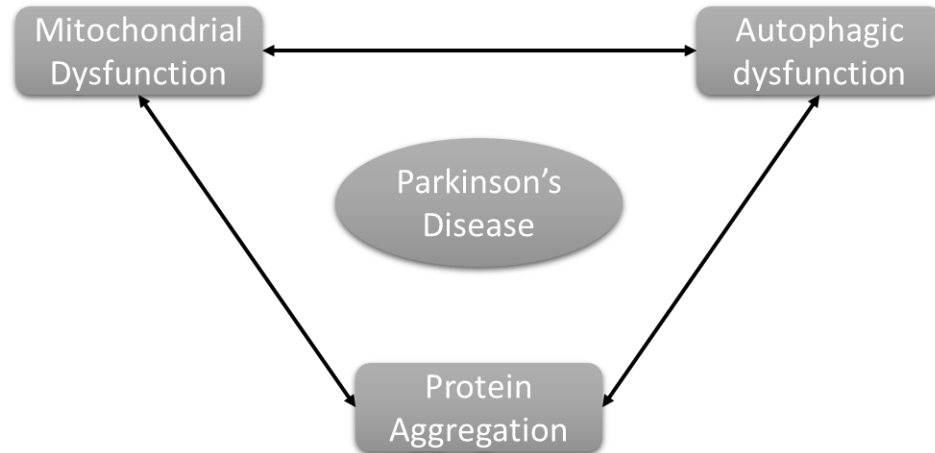
Figure 1: Diagram of the 3 main intracellular deficits observed in Parkinson's disease. aSyn gene triplication and mutations are disease causing in a small subset of familial PD. Parkin and PINK1 recessive mutations are also disease-causing. Nonetheless, in sporadic PD, it is currently unknown which deficit is strictly disease-causing as evidence for the interplay of mitochondrial dysfunction, autophagic dysfunction, and protein aggregation are all present.

AUTOPHAGY AND MITOCHONDRIAL HOMEOSTASIS

Mitochondrial dysfunction has been reported to occur in widespread brain areas, including both the substantia nigra and the cortex in Parkinson's disease brains [172, 231, 268, 269]. Mitochondrial DNA mutations and electron transport chain deficits have been

detected in Alzheimer's and Parkinson's diseases with these deficits undoubtedly contributing to disease progression [268, 270-277]. Although the alteration of mitochondrial morphology and the extent of decreased respiratory chain activity varies in tissues and isolated mitochondria among these diseases, they are nonetheless prevalent [278]. How mitochondrial dysfunction is produced in patients is unclear. Together with mitochondrial dysfunction, oxidative and nitrative stress are also pronounced in neurodegenerative diseases and aging, and contribute to the initiation and progression of neurodegeneration [268, 270-277]. Environmental toxins such as rotenone and paraquat that damage mitochondria have been shown to induce dopaminergic degeneration in animal models and increase Parkinson's disease risk in humans [279-281]. Also of importance, aSyn can target to mitochondria via a N-terminal sequence, decrease complex I activity and increase the production of reactive oxygen species linking aSyn protein aggregation to mitochondrial function in disease progression [65, 66, 282-288].

Some prior studies have investigated the effects of bypassing complex I blockade via supplying a toxin-resistant subunit, enhancing complex II activities, stabilizing mitochondrial membrane potential [289-291], or enhancing reactive oxygen species clearance [292-295] in various animal models. However, clinical trials based on these approaches have had limited success. Focusing on specific mitochondrial complexes will likely be ineffective at attenuating cellular aging or death from PD. The limitations include the possibilities of perturbing cellular bioenergetics and redox signaling, and the inability to reverse already propagated damage to organelles or mitigating already existing toxic protein inclusions. Fruitful avenues will likely still need to focus on enhancing overall autophagic function to eliminate protein aggregates and restore

mitochondrial function through mitophagy. This can likely be done through promoting lysosome function.

Degradation of dysfunctional mitochondria is carried out by the autophagy-lysosomal pathway. A deficiency in the autophagy protein Atg7 has been shown to cause mitochondrial dysfunction, both in isolated mitochondria from skeletal muscle and in cultured embryonic fibroblasts. Furthermore, intracellular ROS levels are increased in autophagy gene Atg7 knockout cells [208]. Parkin knockout results in aberrant mitochondrial morphology and activities [296]. Autophagy inhibition has been shown to exacerbate neuronal injury in multiple animal models, including the rotenone model of PD, where injection into rats or oral administration in mice leads to aSyn accumulation and neurodegeneration [297, 298]. In a rat primary cortical neuron context, it has been found that rotenone as low as 10 nM induced immediate mitochondrial respiratory inhibition and inhibited autophagic flux. Interestingly, the autophagy stimulator rapamycin attenuated cell death while autophagy inhibition by 3MA exacerbated cell death [195]. Autophagy inhibition is also deleterious in instances of oxidative damage to mitochondria by nitric oxide where the addition of 3MA exacerbates injury [235]. Indeed, our studies have shown that proper mitophagy is essential for maintaining proper functioning mitochondria (**Figure 5-2**).

In our studies it is clear that autophagy blockade through lysosomal inhibition is deleterious to mitochondrial health. This is supported by previously published studies from other groups, as discussed above. The molecular underpinnings of this decline have yet to be fully investigated. However, it is likely that given the observations of overall decreased mitochondrial function and health that reactive damage is in part responsible.
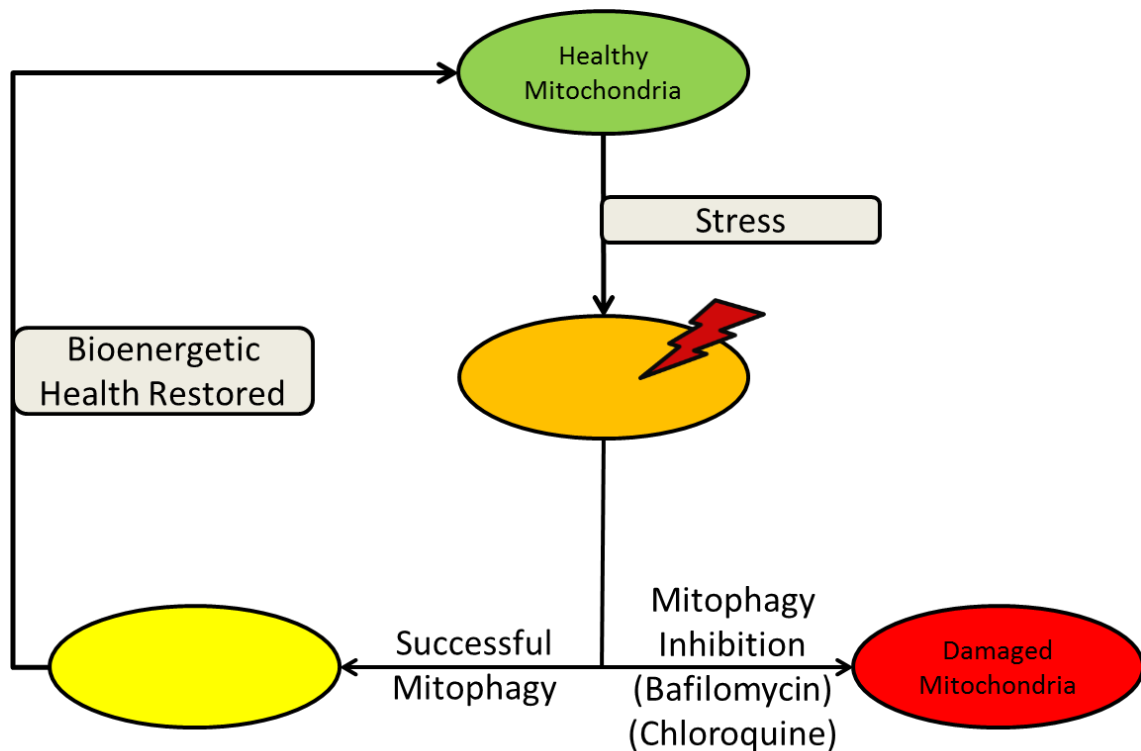
Figure 2: Schematic of maintaining mitochondrial health. During normal autophagy processing, damaged mitochondria can be recycled through the lysosome. When stress is incurred, successful mitophagy is required to maintain mitochondrial health. When lysosome function is inhibited by bafilomycin or chloroquine, mitophagy fails and mitochondrial deficits accrue.

In our studies we observed no changes in the levels of mitochondrial ETC proteins. However, their specific activities were decreased even when their substrates were not rate limiting. This suggests that the ETC protein components that remain are not functioning correctly. Whether this is due to oxidative damage or inappropriate assembly will need to be further investigated. Additionally, key components of the TCA cycle were altered, specifically those downstream of citrate synthase or those linked to glutaminolysis. In the case of citrate synthase, the apparent discrepancy between levels of activity and protein levels is even more stark, where protein levels are increased but function and metabolite levels are significantly diminished. This again suggests that these proteins are not

functioning correctly or are otherwise being inhibited. Whether levels of TCA

metabolites and/or citrate synthase activities are decreased in PD brains will need to be

investigated in future studies to provide a better understanding of disease mechanisms.

Mitochondria are both producers and targets of oxidative damage and it is

possible that ETC and TCA components are accumulating reactive species damage that is

failing to be cleared by mitophagy, given lysosomal inhibition. Indeed, several

components of both the ETC and TCA are sensitive to oxidative damage. Citrate synthase

has been shown to be sensitive to peroxyl radicals that can cause its inactivation [299].

Additionally, aconitase has been shown to sensitive to oxidative damage during aging

that resulted in a reduction in its activity [300]. If indeed, oxidative damage to

mitochondrial proteins is responsible for the observed mitochondrial dysfunction,

reducing this stress would conceivably ameliorate these deficits, for example by using

N-acetylcysteine, which is a precursor of glutathione and may attenuate modification of

cysteines by oxidants or vitamin E [301]. Nonetheless, caution needs to be heeded, as

several clinical trials based on antioxidant strategies have failed, indicating antioxidants

may be too specific for the vast spectrum of damage that occurs [69]. Furthermore,

antioxidants are unable to remove damage that has already been propagated. And indeed,

this is what makes autophagy enhancement attractive, because it potentially can be useful

to clear damage induced by a diverse range of oxidants and thus reverse disease

phenotypes.

It is also possible that restoring flow through the TCA cycle could be beneficial as

well. This could be accomplished by providing substrates at key steps of the cycle that

appear to be inhibited. Adding in additional substrates like citrate, cis-aconitate, or

isocitrate at the citrate synthase and aconitase steps may allow for a restoration of downstream intermediates, in effect "jump starting" the TCA cycle back to proper function. This in turn would also provide substrates for the ETC and possibly for anti-oxidant defense.

In Parkinson's disease, mitochondrial dysfunction and oxidative damage are cellular characteristics of the disease. It is very possible that in PD tissue, cellular deficits are occurring that are similar to what we have observed in our work. As such, some of the antioxidant or TCA cycle supplementation therapies discussed above may be beneficial in disease treatment. However, early intervention is likely to be key to therapeutic success. In our studies only 24 hours of autophagy inhibition lead to decreases in mitochondrial health. Furthermore, utilizing ROS scavengers late in the disease course has been shown less than effective [302].

Taken together, autophagy plays an important role in mitochondrial quality control and neuronal survival and therapeutic approaches should seek to restore this beneficial pathway or mitigate the effects of its decline on mitochondria.

AUTOPHAGY AND PROTEOTOXICITY

In addition to mitochondrial dysfunction, accumulation of aSyn is an important feature of PD, dementia with Lewy bodies and multiple systems atrophy [18, 243, 244]. The role of autophagy and lysosomal mediated protein degradation pathways in neurons have been evidenced in several ways. Human patients who lack functional Cathepsin D develop congenital neuronal ceroid-lipofuscinosis (NCL), a disease that results in rapid neurodegeneration and death within hours to weeks after birth [303]. Cathepsin D

knockout mice have been found to exhibit a similar phenotype, ultimately leading to death at approximately p25 [304].

Studies from our own laboratory have previously demonstrated the cathepsin D knockout mice exhibit significant aSyn accumulation [259, 305-307]. In contrast, it has been shown that overexpression of wildtype cathepsin D, but not cathepsin B, L, or mutant cathepsin D, decrease aSyn toxicity in worms *in vivo* and mammalian cells *in vitro* [259]. In addition to cathepsin D, cathepsins B and L also protect against mutant huntingtin-induced neuron death, while inhibition of autophagy-lysosomal functions by E64 or pepstatin A exacerbated mutant huntingtin-induced neuron death [308]. Interestingly, lysosomal inhibition by the lysosomotropic agent chloroquine or the lysosomal protease cathepsin D inhibitor pepstatin A have both been shown to increase the formation of reactive species as well [309-313]. These observations indicate that lysosomal function and efficiency are crucial in normal cellular function, and that its enhancement may be beneficial in promoting the removal of toxic long-lived proteins. Thus future studies may need to examine whether overexpression of cathepsin D may attenuate aSyn accumulation in animal models to demonstrate proof of principle for a cathepsin D based therapeutic development.

One critical issue for aSyn pathology is that it can leave the cell and seed aggregations in neighboring cells, acting in a prion-like fashion. Recent work demonstrated that preformed aSyn fibrils can be taken up into neurons and seed the formation of endogenous aSyn aggregates that resemble many aspects of Lewy body and Lewy neurite pathologies, including forming insoluble, ubiquitinated and phosphorylated high molecular weight species that further amplify disease pathogenesis [193, 245, 246].

How aSyn leaves the cell and seeds aggregations elsewhere is still unclear, but exosomal or exocytosis-mediated mechanisms, along with direct diffusion through plasma membranes, have been proposed [314, 315]. Future studies need to define this propagation mechanism to better design strategies for prevention and treatment of aSyn spread.

The spread of aSyn is worsened by autophagic decline, a pattern observed in PD models and aging models [245]. A decrease in lysosomal function promotes the release of aSyn from the cell, and that aSyn can seed further aggregation in a new population of cells [35]. This presents an important mechanism for disease progression and warrants serious consideration for therapeutic development.

One of the major regulators of macroautophagy is the mammalian target of rapamycin (mTOR). Activation of autophagy by rapamycin and its derivatives, via inhibition of mTOR, has shown to be beneficial in cell and animal models as treatments for neurodegenerative diseases [248]. However, mTOR inhibition also leads to decreased protein synthesis, and the side effects associated with rapamycin use in humans has limited its use clinically, especially over the long term. Furthermore, rapamycin fails to clear intracellular aggregates that are resultant from preformed aSyn fibril exposure and ultimately exacerbating cell death [105].

Since rapamycin may not be the best strategy to prevent aSyn spread, mTOR independent autophagy activators such as trehalose were explored in the context of aSyn propagation and were employed in the studies encompassed in this dissertation. Trehalose is considered safe for human use at doses up to 50 g in drinking water [106] and although no epidemiology studies have been performed to specifically correlate its consumption

with PD incidence, trehalose has been shown to activate autophagy and decrease aSyn aggregates in PC12 cells [250], decrease Tau accumulation in mice [255], and decrease neurodegeneration in amyotrophic lateral sclerosis [256], Huntington's [257], and Alzheimer's [258] disease models. One potential mechanism of trehalose action may be activation of the transcription factor TFEB which activates more than 30 autophagy and lysosomal genes; however other mechanisms may also contribute to its action [107, 251, 252]. Modulation of TFEB directly has also shown promise in neuroprotection in certain models, where its genetic overexpression of pharmacologic induction has been shown to promote aSyn degradation, again demonstrating the importance of the lysosome in mitigating cellular stress through autophagy [316, 317]. Trehalose has been shown to be safe with no use limits in Korea and Taiwan, up to 5% in food in UK, and in 2000 the US FDA gave a letter of no objection to a Generally Regarded as Safe (GRAS) notice for human consumption [254]. In drinking water at a concentration of 1-5%, at several age groups from 3 weeks to 4 months, trehalose has been shown to be beneficial in increasing autophagy, while decreasing the accumulation of Tau and dopaminergic neuron death, and improving behavioral performance in *Parkin* knockout mice overexpressing human mutated Tau protein [255-258]. However, in our studies in primary neurons, trehalose was ineffective in attenuating aSyn accumulation in response to PFFs and in attenuating PFF induced cell death. It is still unclear whether autophagy enhancement with trehalose treatment is insufficient and whether the use of more powerful autophagy enhancers could be more neuroprotective against PFF induced cell death.

Both trehalose and rapamycin have been found neuroprotective in several experimental models [318-321]. However, our study demonstrated that autophagy

induction by trehalose seems ineffective in removing PFF-induced aggregations or preventing PFF-induced cell death. These observations could be resultant from several factors. One possible explanation for this is that the PFFs themselves exact a more severe neurodegenerative phenotype on the cells than other models of aSyn overexpression, since overexpressed aSyn protein may be still susceptible to autophagic degradation and may not be toxic. This appears to be substantiated by the literature cited above, where trehalose seems effective in reducing the amount of aggregated proteins in neurodegenerative disease overexpression models, as opposed to fibril models. It seems apparent that PFF induced aggregations are more toxic than having non-aggregated aSyn present in the cell. In our studies, the PFFs themselves do not appear toxic without endogenous aSyn based on observations in aSyn knockout mice, but aggregates in WT neurons fail to be cleared and induce cell death thus suggesting a resistance to clearance by autophagy. And indeed, merely adding additional aSyn to the cell in monomer form is ineffective at inducing a Parkinson's like cellular phenotype, this in essence is what other commonly used overexpression models do. It is conceivable that if we utilized other more commonly used overexpression models trehalose would have been successful in clearing those aggregates. Thus trehalose may still be useful to mitigate certain aspect of PD pathology in cells where aSyn is overabundant.

In regards to why PFF induced aggregations are not cleared by trehalose in our studies, two likely scenarios exist, one where aSyn aggregates fail to make it properly into the autophagosome. The second, aSyn aggregations make it physically into the autophagosome, but fusion with the lysosome is inhibited. In both scenarios, the dose and duration of trehalose treatment as well as combinatorial treatment of autophagy

enhancers at multiple stages of the autophagy process may still require further investigation.

In this first scenario, the properties of aSyn that allow it to interact with lipid membranes may be causing failure of the autophagosome to form or properly nucleate [322, 323]. It has been shown that the curvature of autophagosomes is important for their function [324]. In the case of PFF exposure and accumulation of aSyn, an overabundance of this protein may allow it to interact with the lipid membranes of autophagosomes thus altering the curvature of the membrane and preventing proper autophagosome formation. It is even conceivable that this mechanism would be applicable in scenario two discussed below.

In the second scenario, aggregates make it to the autophagosome, but the clearance of autophagosomes is otherwise inhibited. aSyn has been shown to interact with SNARE proteins, thus providing an avenue in which aSyn could interact with these proteins blocking their function and preventing successful autophagosome and lysosome docking [325]. Intriguingly, aSyn has also been to undermine lysosomal integrity, inducing lysosomal rupturing [326]. If aSyn is indeed causing rupture or even permeabilizing the lysosome to the point of decreased acidity, this may alter lysosome/autophagosome fusion as it has been shown that lysosomes with increased pH tend not to fuse with autophagosomes [327]. The lysosome is the rate-limiting step of autophagy in neurons and the reasons for autophagic failure might be due to autophagosome and lysosome fusion inhibition [328]. If aSyn is causing "leaky" lysosomes with increased pH, this could potentially explain why a previously published report observed that after PFF treatment, lysosomes and autophagosomes seem to co-

localize but do not seem to fuse [105]. In the scenarios when lysosomes are

dysfunctional due to PFF exposure, it is possible that mitochondrial dysfunction also

occurs, leading to cell death (**Figure 3**). This would be similar to Chapter 3 where

lysosomal inhibition with bafilomycin or chloroquine induced mitochondrial deficits. At

the concentrations that were used over a 24 h period, lysosomal inhibitors caused no
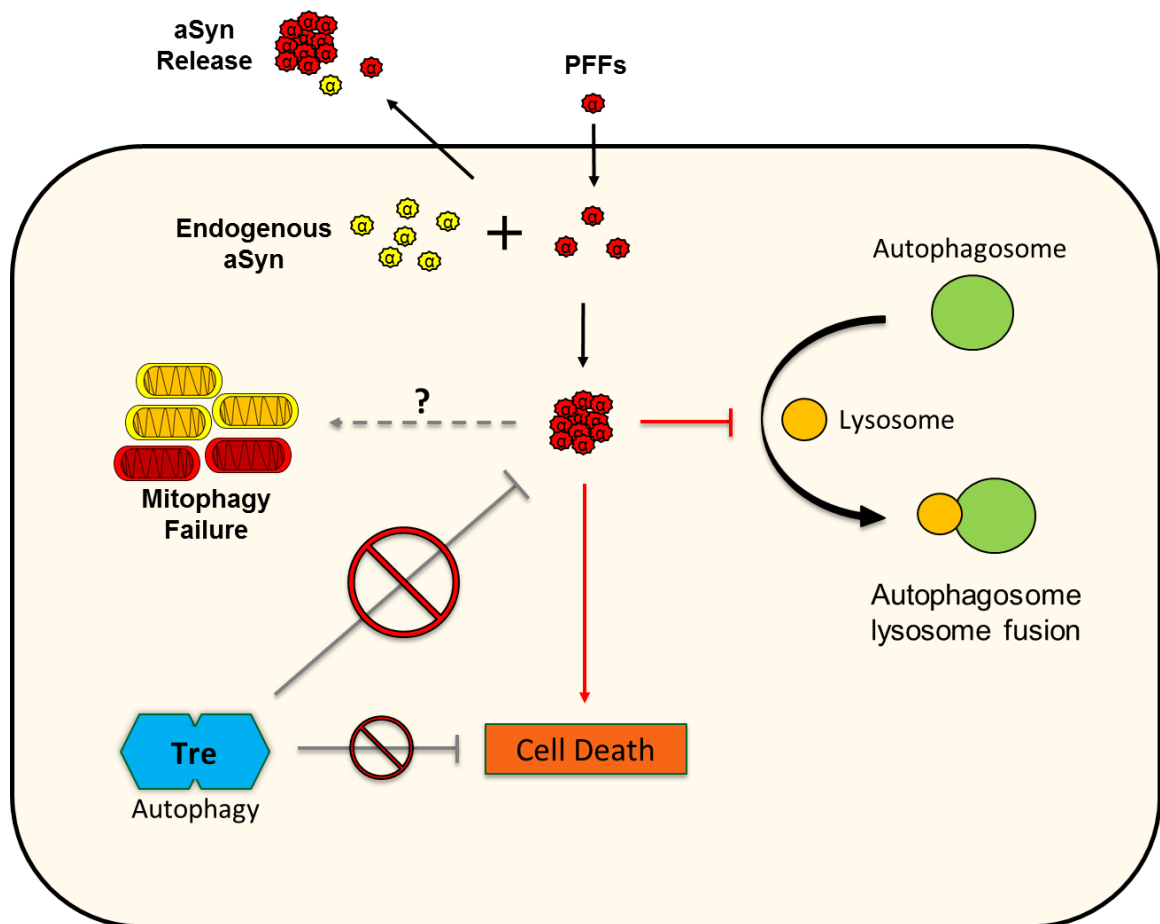
Figure 3: Interplay between PFFs and cellular machinery. aSyn PFFs (red circles) recruit
endogenous aSyn (yellow circles) to form aggregates and induce neuron death. aSyn
aggregations may interact with mitochondria and cause decreased mitochondrial function.
PFFs resist aggregation by autophagy and might inhibit autophagosome lysosome fusion.
Aggregates can also be released and propagate to neighboring cells and further
pathological damage to the brain. Treatment with trehalose fails to remove aggregates or
prevent cell death.

observable cell death, however lysosomal inhibition over a 14 d period as done with PFF

treatment could be sufficient to induce the cell death that was observed.

Although it is becoming increasingly apparent that aSyn fibrils do have properties

that separate them apart from other aSyn overexpression models, further investigation of

how aSyn fibrils interact with autophagosomes and lysosomes is warranted. And indeed,

if PFFs are autophagy resistant entities, the mechanisms that underlie this resistance need

to be investigated further.

CONCLUSIONS

In this dissertation we have provided additional observations that autophagy is

necessary for mitochondrial homeostasis and its inhibition results in increased

mitochondrial damage and a decrease in mitochondrial function. This provides evidence

for the importance of autophagy in maintaining healthy mitochondria and suggests that

enhancing autophagic capabilities might be an area worth pursuing as a therapy.

Furthermore, we discussed the likelihood of reactive species damage under the stress of

autophagy inhibition and that mitigating this stress or restoring TCA cycle intermediates

may be beneficial. Whether autophagy or mitophagy enhancement strategies are

sufficient to confer protection of neuronal mitochondrial health is a key area of research

in aging and neurodegenerative disease. Furthermore, our observations that autophagy

enhancement by trehalose is ineffective in removing aSyn aggregates and protecting

against toxicity suggest that either PFF induced aSyn aggregates fail to be encapsulated

by autophagosomes or otherwise block lysosome autophagosome fusion. The PFF model

seems unique in its formation of aSyn inclusions that seem entirely resistant to trehalose

enhanced autophagy when compared to other aSyn overexpression models. Indeed, it is

likely that trehalose may still be effective in these other models or *in vivo*. Nonetheless,

understanding the relationship between aSyn and autophagy machinery will be crucial in

identifying specific targets for therapeutic modulation.

REFERENCES

1.   Martin, I., V.L. Dawson, and T.M. Dawson, *Recent advances in the genetics of Parkinson's disease.* Annu Rev Genomics Hum Genet, 2011. **12**: p. 301-25.
2.   Parkinson, J., *An essay on the shaking palsy. 1817.* J Neuropsychiatry Clin Neurosci, 2002. **14**(2): p. 223-36; discussion 222.
3.   Spillantini, M.G., *Parkinson's disease, dementia with Lewy bodies and multiple system atrophy are alpha-synucleinopathies.* Parkinsonism Relat Disord, 1999. **5**(4): p. 157-62.
4.   Spillantini, M.G. and M. Goedert, *The alpha-synucleinopathies: Parkinson's disease, dementia with Lewy bodies, and multiple system atrophy.* Ann N Y Acad Sci, 2000. **920**: p. 16-27.
5.   Louis, E.D., et al., *Progression of parkinsonian signs in Parkinson disease.* Arch Neurol, 1999. **56**(3): p. 334-7.
6.   Haehner, A., et al., *Prevalence of smell loss in Parkinson's disease--a multicenter study.* Parkinsonism Relat Disord, 2009. **15**(7): p. 490-4.
7.   Savica, R., et al., *Medical records documentation of constipation preceding Parkinson disease: A case-control study.* Neurology, 2009. **73**(21): p. 1752-8.
8.   Singaram, C., et al., *Dopaminergic defect of enteric nervous system in Parkinson's disease patients with chronic constipation.* Lancet, 1995. **346**(8979): p. 861-4.
9.   Parkinson Progression Marker, I., *The Parkinson Progression Marker Initiative (PPMI).* Prog Neurobiol, 2011. **95**(4): p. 629-35.
10.   Block, G., et al., *Comparison of immediate-release and controlled release carbidopa/levodopa in Parkinson's disease. A multicenter 5-year study. The CR First Study Group.* Eur Neurol, 1997. **37**(1): p. 23-7.
11.   Lieberman, A., et al., *Comparison of dopa decarboxylase inhibitor (carbidopa) combined with levodopa and levodopa alone in Parkinson's disease.* Neurology, 1975. **25**(10): p. 911-6.
12.   Koller, W.C., et al., *Immediate-release and controlled-release carbidopa/levodopa in PD: a 5-year randomized multicenter study. Carbidopa/Levodopa Study Group.* Neurology, 1999. **53**(5): p. 1012-9.
13.   Goldenberg, M.M., *Medical management of Parkinson's disease.* P T, 2008. **33**(10): p. 590-606.
14.   Factor, S.A. and W.J. Weiner, *Parkinson's disease : diagnosis and clinical management.* 2nd ed. 2008, New York: Demos. xxviii, 819 p., 8 p. of plates.
15.   Cotzias, G.C., *L-Dopa for Parkinsonism.* N Engl J Med, 1968. **278**(11): p. 630.
16.   Cotzias, G.C., P.S. Papavasiliou, and R. Gellene, *Experimental treatment of parkinsonism with L-Dopa.* Neurology, 1968. **18**(3): p. 276-7.
17.   Yahr, M.D., et al., *L-Dopa (L-3,4-dihydroxyphenylanine)--its clinical effects in parkinsonism.* Trans Am Neurol Assoc, 1968. **93**: p. 56-63.

18. Spillantini, M.G., et al., *Alpha-synuclein in Lewy bodies.* Nature, 1997. **388**(6645): p. 839-40.

19. Outeiro, T.F. and S. Lindquist, *Yeast cells provide insight into alpha-synuclein biology and pathobiology.* Science, 2003. **302**(5651): p. 1772-5.

20. Davidson, W.S., et al., *Stabilization of alpha-synuclein secondary structure upon binding to synthetic membranes.* J Biol Chem, 1998. **273**(16): p. 9443-9.

21. Jensen, M.B., et al., *Membrane curvature sensing by amphipathic helices: a single liposome study using alpha-synuclein and annexin B12.* J Biol Chem, 2011. **286**(49): p. 42603-14.

22. Varkey, J., et al., *Membrane curvature induction and tubulation are common features of synucleins and apolipoproteins.* J Biol Chem, 2010. **285**(42): p. 32486-93.

23. Fujiwara, H., et al., *alpha-Synuclein is phosphorylated in synucleinopathy lesions.* Nat Cell Biol, 2002. **4**(2): p. 160-4.

24. Greten-Harrison, B., et al., *alphabetagamma-Synuclein triple knockout mice reveal age-dependent neuronal dysfunction.* Proc Natl Acad Sci U S A, 2010. **107**(45): p. 19573-8.

25. Abeliovich, A., et al., *Mice lacking alpha-synuclein display functional deficits in the nigrostriatal dopamine system.* Neuron, 2000. **25**(1): p. 239-52.

26. Specht, C.G. and R. Schoepfer, *Deletion of the alpha-synuclein locus in a subpopulation of C57BL/6J inbred mice.* BMC Neurosci, 2001. **2**: p. 11.

27. Bucciantini, M., et al., *Prefibrillar amyloid protein aggregates share common features of cytotoxicity.* J Biol Chem, 2004. **279**(30): p. 31374-82.

28. Kayed, R., et al., *Common structure of soluble amyloid oligomers implies common mechanism of pathogenesis.* Science, 2003. **300**(5618): p. 486-9.

29. Osterberg, V.R., et al., *Progressive aggregation of alpha-synuclein and selective degeneration of lewy inclusion-bearing neurons in a mouse model of parkinsonism.* Cell Rep, 2015. **10**(8): p. 1252-60.

30. Zatloukal, K., et al., *p62 Is a common component of cytoplasmic inclusions in protein aggregation diseases.* Am J Pathol, 2002. **160**(1): p. 255-63.

31. Kuzuhara, S., et al., *Lewy bodies are ubiquitinated. A light and electron microscopic immunocytochemical study.* Acta Neuropathol, 1988. **75**(4): p. 345-53.

32. Braak, H., et al., *Staging of brain pathology related to sporadic Parkinson's disease.* Neurobiol Aging, 2003. **24**(2): p. 197-211.

33. Braak, H., et al., *Gastric alpha-synuclein immunoreactive inclusions in Meissner's and Auerbach's plexuses in cases staged for Parkinson's disease-related brain pathology.* Neurosci Lett, 2006. **396**(1): p. 67-72.

34. Li, J.Y., et al., *Lewy bodies in grafted neurons in subjects with Parkinson's disease suggest host-to-graft disease propagation.* Nat Med, 2008. **14**(5): p. 501-3.

35. Alvarez-Erviti, L., et al., *Lysosomal dysfunction increases exosome-mediated alpha-synuclein release and transmission.* Neurobiol Dis, 2011. **42**(3): p. 360-7.

36. Marques, O. and T.F. Outeiro, *Alpha-synuclein: from secretion to dysfunction and death.* Cell Death Dis, 2012. **3**: p. e350.

37.   Chartier-Harlin, M.C., et al., *Alpha-synuclein locus duplication as a cause of familial Parkinson's disease.* Lancet, 2004. **364**(9440): p. 1167-9.

38.   Singleton, A.B., et al., *alpha-Synuclein locus triplication causes Parkinson's disease.* Science, 2003. **302**(5646): p. 841.

39.   Polymeropoulos, M.H., et al., *Mutation in the alpha-synuclein gene identified in families with Parkinson's disease.* Science, 1997. **276**(5321): p. 2045-7.

40.   Kruger, R., et al., *Ala30Pro mutation in the gene encoding alpha-synuclein in Parkinson's disease.* Nat Genet, 1998. **18**(2): p. 106-8.

41.   Zarranz, J.J., et al., *The new mutation, E46K, of alpha-synuclein causes Parkinson and Lewy body dementia.* Ann Neurol, 2004. **55**(2): p. 164-73.

42.   Appel-Cresswell, S., et al., *Alpha-synuclein p.H50Q, a novel pathogenic mutation for Parkinson's disease.* Mov Disord, 2013. **28**(6): p. 811-3.

43.   Lesage, S., et al., *G51D alpha-synuclein mutation causes a novel parkinsonian-pyramidal syndrome.* Ann Neurol, 2013. **73**(4): p. 459-71.

44.   Chen, L. and M.B. Feany, *Alpha-synuclein phosphorylation controls neurotoxicity and inclusion formation in a Drosophila model of Parkinson disease.* Nat Neurosci, 2005. **8**(5): p. 657-63.

45.   Chen, L., et al., *Tyrosine and serine phosphorylation of alpha-synuclein have opposing effects on neurotoxicity and soluble oligomer formation.* J Clin Invest, 2009. **119**(11): p. 3257-65.

46.   Li, J.Q., L. Tan, and J.T. Yu, *The role of the LRRK2 gene in Parkinsonism.* Mol Neurodegener, 2014. **9**: p. 47.

47.   Trinh, J. and M. Farrer, *Advances in the genetics of Parkinson disease.* Nat Rev Neurol, 2013. **9**(8): p. 445-54.

48.   Lubbe, S. and H.R. Morris, *Recent advances in Parkinson's disease genetics.* J Neurol, 2014. **261**(2): p. 259-66.

49.   Deas, E., N.W. Wood, and H. Plun-Favreau, *Mitophagy and Parkinson's disease: the PINK1-parkin link.* Biochim Biophys Acta, 2011. **1813**(4): p. 623-33.

50.   Ariga, H., et al., *Neuroprotective function of DJ-1 in Parkinson's disease.* Oxid Med Cell Longev, 2013. **2013**: p. 683920.

51.   Irrcher, I., et al., *Loss of the Parkinson's disease-linked gene DJ-1 perturbs mitochondrial dynamics.* Hum Mol Genet, 2010. **19**(19): p. 3734-46.

52.   Abramov, A.Y., et al., *Bioenergetic consequences of PINK1 mutations in Parkinson disease.* PLoS One, 2011. **6**(10): p. e25622.

53.   Imaizumi, Y., et al., *Mitochondrial dysfunction associated with increased oxidative stress and alpha-synuclein accumulation in PARK2 iPSC-derived neurons and postmortem brain tissue.* Mol Brain, 2012. **5**: p. 35.

54.   Klein, C. and A. Westenberger, *Genetics of Parkinson's disease.* Cold Spring Harb Perspect Med, 2012. **2**(1): p. a008888.

55.   Butterfield, P.G., et al., *Environmental antecedents of young-onset Parkinson's disease.* Neurology, 1993. **43**(6): p. 1150-8.

56.   Gorell, J.M., et al., *The risk of Parkinson's disease with exposure to pesticides, farming, well water, and rural living.* Neurology, 1998. **50**(5): p. 1346-50.

57.   Wang, A., et al., *Parkinson's disease risk from ambient exposure to pesticides.* Eur J Epidemiol, 2011. **26**(7): p. 547-55.

58.   Schapira, A.H., *Mitochondrial dysfunction in Parkinson's disease.* Cell Death Differ, 2007. **14**(7): p. 1261-6.

59.   Greenamyre, J.T., et al., *Mitochondrial dysfunction in Parkinson's disease.* Biochem Soc Symp, 1999. **66**: p. 85-97.

60.   Winklhofer, K.F. and C. Haass, *Mitochondrial dysfunction in Parkinson's disease.* Biochim Biophys Acta, 2010. **1802**(1): p. 29-44.

61.   Schapira, A.H., et al., *Mitochondrial complex I deficiency in Parkinson's disease.* J Neurochem, 1990. **54**(3): p. 823-7.

62.   Schapira, A.H., et al., *Mitochondrial complex I deficiency in Parkinson's disease.* Lancet, 1989. **1**(8649): p. 1269.

63.   Tanner, C.M., et al., *Rotenone, paraquat, and Parkinson's disease.* Environ Health Perspect, 2011. **119**(6): p. 866-72.

64.   Bove, J., et al., *Toxin-induced models of Parkinson's disease.* NeuroRx, 2005. **2**(3): p. 484-494.

65.   Devi, L., et al., *Mitochondrial import and accumulation of alpha-synuclein impair complex I in human dopaminergic neuronal cultures and Parkinson disease brain.* J Biol Chem, 2008. **283**(14): p. 9089-100.

66.   Chinta, S.J., et al., *Mitochondrial alpha-synuclein accumulation impairs complex I function in dopaminergic neurons and results in increased mitophagy in vivo.* Neurosci Lett, 2010. **486**(3): p. 235-9.

67.   Klivenyi, P., et al., *Mice lacking alpha-synuclein are resistant to mitochondrial toxins.* Neurobiol Dis, 2006. **21**(3): p. 541-8.

68.   Drolet, R.E., et al., *Mice lacking alpha-synuclein have an attenuated loss of striatal dopamine following prolonged chronic MPTP administration.* Neurotoxicology, 2004. **25**(5): p. 761-9.

69.   Giordano, S., V. Darley-Usmar, and J. Zhang, *Autophagy as an essential cellular antioxidant pathway in neurodegenerative disease.* Redox Biol, 2014. **2**: p. 82-90.

70.   de Duve, C., *The lysosome turns fifty.* Nat Cell Biol, 2005. **7**(9): p. 847-9.

71.   De Duve, C., et al., *Tissue fractionation studies. 6. Intracellular distribution patterns of enzymes in rat-liver tissue.* Biochem J, 1955. **60**(4): p. 604-17.

72.   Klionsky, D.J., *Autophagy revisited: a conversation with Christian de Duve.* Autophagy, 2008. **4**(6): p. 740-3.

73.   Ohsumi, Y., *Historical landmarks of autophagy research.* Cell Res, 2014. **24**(1): p. 9-23.

74.   Ganschow, R.E. and R.T. Schimke, *Independent genetic control of the catalytic activity and the rate of degradation of catalase in mice.* J Biol Chem, 1969. **244**(17): p. 4649-58.

75.   Kalish, F., N. Chovick, and J.F. Dice, *Rapid in vivo degradation of glycoproteins isolated from cytosol.* J Biol Chem, 1979. **254**(11): p. 4475-81.

76.   Klionsky, D.J. and S.D. Emr, *Autophagy as a regulated pathway of cellular degradation.* Science, 2000. **290**(5497): p. 1717-21.

77.   Li, W.W., J. Li, and J.K. Bao, *Microautophagy: lesser-known self-eating.* Cell Mol Life Sci, 2012. **69**(7): p. 1125-36.

78.   Mijaljica, D., M. Prescott, and R.J. Devenish, *Microautophagy in mammalian cells: revisiting a 40-year-old conundrum.* Autophagy, 2011. **7**(7): p. 673-82.

79. Martinez-Vicente, M., et al., *Dopamine-modified alpha-synuclein blocks chaperone-mediated autophagy.* J Clin Invest, 2008. **118**(2): p. 777-88.

80. Orenstein, S.J., et al., *Interplay of LRRK2 with chaperone-mediated autophagy.* Nat Neurosci, 2013. **16**(4): p. 394-406.

81. Wang, Y., et al., *Synergy and antagonism of macroautophagy and chaperone-mediated autophagy in a cell model of pathological tau aggregation.* Autophagy, 2010. **6**(1): p. 182-3.

82. Anglade, P., et al., *Apoptosis and autophagy in nigral neurons of patients with Parkinson's disease.* Histol Histopathol, 1997. **12**(1): p. 25-31.

83. Olanow, C.W. and P. Brundin, *Parkinson's disease and alpha synuclein: is Parkinson's disease a prion-like disorder?* Mov Disord, 2013. **28**(1): p. 31-40.

84. Zoncu, R., A. Efeyan, and D.M. Sabatini, *mTOR: from growth signal integration to cancer, diabetes and ageing.* Nat Rev Mol Cell Biol, 2011. **12**(1): p. 21-35.

85. Zhang, J., *Teaching the basics of autophagy and mitophagy to redox biologists--mechanisms and experimental approaches.* Redox Biol, 2015. **4**: p. 242-59.

86. Bove, J., M. Martinez-Vicente, and M. Vila, *Fighting neurodegeneration with rapamycin: mechanistic insights.* Nat Rev Neurosci, 2011. **12**(8): p. 437-52.

87. Webb, J.L., et al., *Alpha-Synuclein is degraded by both autophagy and the proteasome.* J Biol Chem, 2003. **278**(27): p. 25009-13.

88. Kuusisto, E., A. Salminen, and I. Alafuzoff, *Ubiquitin-binding protein p62 is present in neuronal and glial inclusions in human tauopathies and synucleinopathies.* Neuroreport, 2001. **12**(10): p. 2085-90.

89. McManus, S. and S. Roux, *The adaptor protein p62/SQSTM1 in osteoclast signaling pathways.* J Mol Signal, 2012. **7**: p. 1.

90. Dodson, M., et al., *KEAP1-NRF2 signalling and autophagy in protection against oxidative and reductive proteotoxicity.* Biochem J, 2015. **469**(3): p. 347-55.

91. Zhang, N.Y., Z. Tang, and C.W. Liu, *alpha-Synuclein protofibrils inhibit 26 S proteasome-mediated protein degradation: understanding the cytotoxicity of protein protofibrils in neurodegenerative disease pathogenesis.* J Biol Chem, 2008. **283**(29): p. 20288-98.

92. McNaught, K.S., et al., *Failure of the ubiquitin-proteasome system in Parkinson's disease.* Nat Rev Neurosci, 2001. **2**(8): p. 589-94.

93. McNaught, K.S., et al., *Altered proteasomal function in sporadic Parkinson's disease.* Exp Neurol, 2003. **179**(1): p. 38-46.

94. McNaught, K.S. and P. Jenner, *Proteasomal function is impaired in substantia nigra in Parkinson's disease.* Neurosci Lett, 2001. **297**(3): p. 191-4.

95. Ebrahimi-Fakhari, D., P.J. McLean, and V.K. Unni, *Alpha-synuclein's degradation in vivo: opening a new (cranial) window on the roles of degradation pathways in Parkinson disease.* Autophagy, 2012. **8**(2): p. 281-3.

96. Hara, T., et al., *Suppression of basal autophagy in neural cells causes neurodegenerative disease in mice.* Nature, 2006. **441**(7095): p. 885-9.

97. Komatsu, M., et al., *Loss of autophagy in the central nervous system causes neurodegeneration in mice.* Nature, 2006. **441**(7095): p. 880-4.

98. Nishiyama, J., et al., *Aberrant membranes and double-membrane structures accumulate in the axons of Atg5-null Purkinje cells before neuronal death.* Autophagy, 2007. **3**(6): p. 591-6.

99. Maday, S., K.E. Wallace, and E.L. Holzbaur, *Autophagosomes initiate distally and mature during transport toward the cell soma in primary neurons.* J Cell Biol, 2012. **196**(4): p. 407-17.

100. Son, J.H., et al., *Neuronal autophagy and neurodegenerative diseases.* Exp Mol Med, 2012. **44**(2): p. 89-98.

101. Maday, S. and E.L. Holzbaur, *Compartment-Specific Regulation of Autophagy in Primary Neurons.* J Neurosci, 2016. **36**(22): p. 5933-45.

102. Tsang, C.K., et al., *Targeting mammalian target of rapamycin (mTOR) for health and diseases.* Drug Discov Today, 2007. **12**(3-4): p. 112-24.

103. Jiang, J., et al., *Rapamycin protects the mitochondria against oxidative stress and apoptosis in a rat model of Parkinson's disease.* Int J Mol Med, 2013. **31**(4): p. 825-32.

104. Ravikumar, B., R. Duden, and D.C. Rubinsztein, *Aggregate-prone proteins with polyglutamine and polyalanine expansions are degraded by autophagy.* Hum Mol Genet, 2002. **11**(9): p. 1107-17.

105. Tanik, S.A., et al., *Lewy body-like alpha-synuclein aggregates resist degradation and impair macroautophagy.* J Biol Chem, 2013. **288**(21): p. 15194-210.

106. Sarkar, S., et al., *Trehalose, a novel mTOR-independent autophagy enhancer, accelerates the clearance of mutant huntingtin and alpha-synuclein.* J Biol Chem, 2007. **282**(8): p. 5641-52.

107. Sardiello, M., et al., *A gene network regulating lysosomal biogenesis and function.* Science, 2009. **325**(5939): p. 473-7.

108. Wu, Y.T., et al., *Dual role of 3-methyladenine in modulation of autophagy via different temporal patterns of inhibition on class I and III phosphoinositide 3-kinase.* J Biol Chem, 2010. **285**(14): p. 10850-61.

109. Hook, G., V. Hook, and M. Kindy, *The cysteine protease inhibitor, E64d, reduces brain amyloid-beta and improves memory deficits in Alzheimer's disease animal models by inhibiting cathepsin B, but not BACE1, beta-secretase activity.* J Alzheimers Dis, 2011. **26**(2): p. 387-408.

110. Newmeyer, D.D. and S. Ferguson-Miller, *Mitochondria: releasing power for life and unleashing the machineries of death.* Cell, 2003. **112**(4): p. 481-90.

111. Mitchell, T., et al., *Convergent mechanisms for dysregulation of mitochondrial quality control in metabolic disease: implications for mitochondrial therapeutics.* Biochem Soc Trans, 2013. **41**(1): p. 127-33.

112. Dodson, M., et al., *Inhibition of glycolysis attenuates 4-hydroxynonenal-dependent autophagy and exacerbates apoptosis in differentiated SH-SY5Y neuroblastoma cells.* Autophagy, 2013. **9**(12).

113. Greenamyre, J.T., et al., *Complex I and Parkinson's disease.* IUBMB Life, 2001. **52**(3-5): p. 135-41.

114. Shavali, S., et al., *Mitochondrial localization of alpha-synuclein protein in alpha-synuclein overexpressing cells.* Neurosci Lett, 2008. **439**(2): p. 125-8.

115. Mizuno, Y., et al., *An immunohistochemical study on alpha-ketoglutarate dehydrogenase complex in Parkinson's disease.* Ann Neurol, 1994. **35**(2): p. 204-10.

116. Mizuno, Y., T. Saitoh, and N. Sone, *Inhibition of mitochondrial alpha-ketoglutarate dehydrogenase by 1-methyl-4-phenylpyridinium ion.* Biochem Biophys Res Commun, 1987. **143**(3): p. 971-6.

117. Lee, J., S. Giordano, and J. Zhang, *Autophagy, mitochondria and oxidative stress: cross-talk and redox signalling.* Biochem J, 2012. **441**(2): p. 523-40.

118. Zhang, J., *Autophagy and Mitophagy in Cellular Damage Control.* Redox Biol, 2013. **1**(1): p. 19-23.

119. Lemasters, J.J., *Selective mitochondrial autophagy, or mitophagy, as a targeted defense against oxidative stress, mitochondrial dysfunction, and aging.* Rejuvenation Res, 2005. **8**(1): p. 3-5.

120. Twig, G. and O.S. Shirihai, *The interplay between mitochondrial dynamics and mitophagy.* Antioxid Redox Signal, 2011. **14**(10): p. 1939-51.

121. Mao, K., et al., *The scaffold protein Atg11 recruits fission machinery to drive selective mitochondria degradation by autophagy.* Dev Cell, 2013. **26**(1): p. 9-18.

122. Kim, I. and J.J. Lemasters, *Mitochondrial degradation by autophagy (mitophagy) in GFP-LC3 transgenic hepatocytes during nutrient deprivation.* Am J Physiol Cell Physiol, 2011. **300**(2): p. C308-17.

123. Twig, G., et al., *Fission and selective fusion govern mitochondrial segregation and elimination by autophagy.* EMBO J, 2008. **27**(2): p. 433-46.

124. Rambold, A.S., et al., *Tubular network formation protects mitochondria from autophagosomal degradation during nutrient starvation.* Proc Natl Acad Sci U S A, 2011. **108**(25): p. 10190-5.

125. Olichon, A., et al., *Loss of OPA1 perturbates the mitochondrial inner membrane structure and integrity, leading to cytochrome c release and apoptosis.* J Biol Chem, 2003. **278**(10): p. 7743-6.

126. Duvezin-Caubet, S., et al., *Proteolytic processing of OPA1 links mitochondrial dysfunction to alterations in mitochondrial morphology.* J Biol Chem, 2006. **281**(49): p. 37972-9.

127. Narendra, D., et al., *Parkin is recruited selectively to impaired mitochondria and promotes their autophagy.* J Cell Biol, 2008. **183**(5): p. 795-803.

128. Shen, Q., et al., *Mutations in Fis1 disrupt orderly disposal of defective mitochondria.* Mol Biol Cell, 2014. **25**(1): p. 145-59.

129. Elmore, S.P., et al., *The mitochondrial permeability transition initiates autophagy in rat hepatocytes.* FASEB J, 2001. **15**(12): p. 2286-7.

130. Michiorri, S., et al., *The Parkinson-associated protein PINK1 interacts with Beclin1 and promotes autophagy.* Cell Death Differ, 2010. **17**(6): p. 962-74.

131. Jin, S.M., et al., *Mitochondrial membrane potential regulates PINK1 import and proteolytic destabilization by PARL.* J Cell Biol, 2010. **191**(5): p. 933-42.

132. Geisler, S., et al., *PINK1/Parkin-mediated mitophagy is dependent on VDAC1 and p62/SQSTM1.* Nat Cell Biol, 2010. **12**(2): p. 119-31.

133. Narendra, D., et al., *p62/SQSTM1 is required for Parkin-induced mitochondrial clustering but not mitophagy; VDAC1 is dispensable for both.* Autophagy, 2010. **6**(8): p. 1090-106.

134. Vives-Bauza, C., et al., *PINK1-dependent recruitment of Parkin to mitochondria in mitophagy.* Proc Natl Acad Sci U S A, 2010. **107**(1): p. 378-83.

135. Gegg, M.E., et al., *Mitofusin 1 and mitofusin 2 are ubiquitinated in a PINK1/parkin-dependent manner upon induction of mitophagy.* Hum Mol Genet, 2010. **19**(24): p. 4861-70.

136. Poole, A.C., et al., *The mitochondrial fusion-promoting factor mitofusin is a substrate of the PINK1/parkin pathway.* PLoS One, 2010. **5**(4): p. e10054.

137. Rakovic, A., et al., *Mutations in PINK1 and Parkin impair ubiquitination of Mitofusins in human fibroblasts.* PLoS One, 2011. **6**(3): p. e16746.

138. Ziviani, E., R.N. Tao, and A.J. Whitworth, *Drosophila parkin requires PINK1 for mitochondrial translocation and ubiquitinates mitofusin.* Proc Natl Acad Sci U S A, 2010. **107**(11): p. 5018-23.

139. Tanaka, A., et al., *Proteasome and p97 mediate mitophagy and degradation of mitofusins induced by Parkin.* J Cell Biol, 2010. **191**(7): p. 1367-80.

140. Yoshii, S.R., et al., *Parkin mediates proteasome-dependent protein degradation and rupture of the outer mitochondrial membrane.* J Biol Chem, 2011. **286**(22): p. 19630-40.

141. Chan, N.C., et al., *Broad activation of the ubiquitin-proteasome system by Parkin is critical for mitophagy.* Hum Mol Genet, 2011. **20**(9): p. 1726-37.

142. Okatsu, K., et al., *Mitochondrial hexokinase HKI is a novel substrate of the Parkin ubiquitin ligase.* Biochem Biophys Res Commun, 2012. **428**(1): p. 197-202.

143. Sarraf, S.A., et al., *Landscape of the PARKIN-dependent ubiquitylome in response to mitochondrial depolarization.* Nature, 2013. **496**(7445): p. 372-6.

144. Lee, S.J., A.B. Hwang, and C. Kenyon, *Inhibition of respiration extends C. elegans life span via reactive oxygen species that increase HIF-1 activity.* Curr Biol, 2010. **20**(23): p. 2131-6.

145. Van Humbeeck, C., et al., *Parkin interacts with Ambra1 to induce mitophagy.* J Neurosci, 2011. **31**(28): p. 10249-61.

146. Murata, H., et al., *SARM1 and TRAF6 bind to and stabilize PINK1 on depolarized mitochondria.* Mol Biol Cell, 2013. **24**(18): p. 2772-84.

147. Thomas, K.J., et al., *DJ-1 acts in parallel to the PINK1/parkin pathway to control mitochondrial function and autophagy.* Hum Mol Genet, 2011. **20**(1): p. 40-50.

148. Joselin, A.P., et al., *ROS-dependent regulation of Parkin and DJ-1 localization during oxidative stress in neurons.* Hum Mol Genet, 2012. **21**(22): p. 4888-903.

149. McCoy, M.K. and M.R. Cookson, *DJ-1 regulation of mitochondrial function and autophagy through oxidative stress.* Autophagy, 2011. **7**(5): p. 531-2.

150. Rakovic, A., et al., *Phosphatase and tensin homolog (PTEN)-induced putative kinase 1 (PINK1)-dependent ubiquitination of endogenous Parkin attenuates mitophagy: study in human primary fibroblasts and induced pluripotent stem cell-derived neurons.* J Biol Chem, 2013. **288**(4): p. 2223-37.

151. Rakovic, A., et al., *Effect of endogenous mutant and wild-type PINK1 on Parkin in fibroblasts from Parkinson disease patients.* Hum Mol Genet, 2010. **19**(16): p. 3124-37.

152. Van Laar, V.S., et al., *Bioenergetics of neurons inhibit the translocation response of Parkin following rapid mitochondrial depolarization.* Hum Mol Genet, 2011. **20**(5): p. 927-40.

153. Cai, Q., et al., *Spatial parkin translocation and degradation of damaged mitochondria via mitophagy in live cortical neurons.* Curr Biol, 2012. **22**(6): p. 545-52.

154. Haskin, J., et al., *AF-6 is a positive modulator of the PINK1/parkin pathway and is deficient in Parkinson's disease.* Hum Mol Genet, 2013. **22**(10): p. 2083-96.

155. Burchell, V.S., et al., *The Parkinson's disease-linked proteins Fbxo7 and Parkin interact to mediate mitophagy.* Nat Neurosci, 2013. **16**(9): p. 1257-65.

156. Orvedahl, A., et al., *Image-based genome-wide siRNA screen identifies selective autophagy factors.* Nature, 2011. **480**(7375): p. 113-7.

157. Lefebvre, V., et al., *Genome-wide RNAi screen identifies ATPase inhibitory factor 1 (ATPIF1) as essential for PARK2 recruitment and mitophagy.* Autophagy, 2013. **9**(11): p. 1770-9.

158. Hasson, S.A., et al., *High-content genome-wide RNAi screens identify regulators of parkin upstream of mitophagy.* Nature, 2013. **504**(7479): p. 291-5.

159. Lefebvre, V., et al., *Genome-wide RNAi screen identifies ATPase inhibitory factor 1 (ATPIF1) as essential for PARK2 recruitment and mitophagy.* Autophagy, 2013. **9**(11).

160. Yamano, K., et al., *Mitochondrial Rab GAPs govern autophagosome biogenesis during mitophagy.* Elife, 2014. **3**: p. e01612.

161. Higdon, A.N., et al., *Hemin causes mitochondrial dysfunction in endothelial cells through promoting lipid peroxidation: the protective role of autophagy.* Am J Physiol Heart Circ Physiol, 2012. **302**(7): p. H1394-409.

162. Gilkerson, R.W., et al., *Mitochondrial autophagy in cells with mtDNA mutations results from synergistic loss of transmembrane potential and mTORC1 inhibition.* Hum Mol Genet, 2012. **21**(5): p. 978-90.

163. Mitchell, T., et al., *Dysfunctional mitochondrial bioenergetics and oxidative stress in Akita(+/Ins2)-derived beta-cells.* Am J Physiol Endocrinol Metab, 2013. **305**(5): p. E585-99.

164. Allen, G.F., et al., *Loss of iron triggers PINK1/Parkin-independent mitophagy.* EMBO Rep, 2013. **14**(12): p. 1127-35.

165. Melser, S., et al., *Rheb regulates mitophagy induced by mitochondrial energetic status.* Cell Metab, 2013. **17**(5): p. 719-30.

166. Liu, K., et al., *Phosphorylated AKT inhibits the apoptosis induced by DRAM-mediated mitophagy in hepatocellular carcinoma by preventing the translocation of DRAM to mitochondria.* Cell Death Dis, 2014. **5**: p. e1078.

167. Li, L., et al., *Nuclear factor high-mobility group box1 mediating the activation of Toll-like receptor 4 signaling in hepatocytes in the early stage of nonalcoholic fatty liver disease in mice.* Hepatology, 2011. **54**(5): p. 1620-30.

168. Jin, S.M. and R.J. Youle, *PINK1- and Parkin-mediated mitophagy at a glance.* J Cell Sci, 2012. **125**(Pt 4): p. 795-9.

169. McLelland, G.L., et al., *Parkin and PINK1 function in a vesicular trafficking pathway regulating mitochondrial quality control.* EMBO J, 2014. **33**(4): p. 282-95.

170. Chu, C.T., et al., *Cardiolipin externalization to the outer mitochondrial membrane acts as an elimination signal for mitophagy in neuronal cells.* Nat Cell Biol, 2013.

171. Webster, B.R., et al., *Restricted mitochondrial protein acetylation initiates mitochondrial autophagy.* J Cell Sci, 2013. **126**(Pt 21): p. 4843-9.
172. Murphy, M.P., *How mitochondria produce reactive oxygen species.* Biochem J, 2009. **417**(1): p. 1-13.
173. Zhu, J.H., et al., *Regulation of autophagy by extracellular signal-regulated protein kinases during 1-methyl-4-phenylpyridinium-induced cell death.* Am J Pathol, 2007. **170**(1): p. 75-86.
174. Bernardi, P., *Mitochondrial transport of cations: channels, exchangers, and permeability transition.* Physiol Rev, 1999. **79**(4): p. 1127-55.
175. Chen, H. and D.C. Chan, *Mitochondrial dynamics--fusion, fission, movement, and mitophagy--in neurodegenerative diseases.* Hum Mol Genet, 2009. **18**(R2): p. R169-76.
176. Yang, Z. and D.J. Klionsky, *Mammalian autophagy: core molecular machinery and signaling regulation.* Curr Opin Cell Biol, 2010. **22**(2): p. 124-31.
177. Mizushima, N., et al., *Autophagy fights disease through cellular self-digestion.* Nature, 2008. **451**(7182): p. 1069-75.
178. Kim, Y.C. and K.L. Guan, *mTOR: a pharmacologic target for autophagy regulation.* J Clin Invest, 2015. **125**(1): p. 25-32.
179. Choi, A.M., S.W. Ryter, and B. Levine, *Autophagy in human health and disease.* N Engl J Med, 2013. **368**(19): p. 1845-6.
180. Eskelinen, E.L. and P. Saftig, *Autophagy: a lysosomal degradation pathway with a central role in health and disease.* Biochim Biophys Acta, 2009. **1793**(4): p. 664-73.
181. Youle, R.J. and D.P. Narendra, *Mechanisms of mitophagy.* Nat Rev Mol Cell Biol, 2011. **12**(1): p. 9-14.
182. Kim, I., S. Rodriguez-Enriquez, and J.J. Lemasters, *Selective degradation of mitochondria by mitophagy.* Arch Biochem Biophys, 2007. **462**(2): p. 245-53.
183. Shigenaga, M.K., T.M. Hagen, and B.N. Ames, *Oxidative damage and mitochondrial decay in aging.* Proc Natl Acad Sci U S A, 1994. **91**(23): p. 10771-8.
184. Wang, C.H., et al., *Oxidative stress response elicited by mitochondrial dysfunction: implication in the pathophysiology of aging.* Exp Biol Med (Maywood), 2013. **238**(5): p. 450-60.
185. Castro Mdel, R., et al., *Aging increases mitochondrial DNA damage and oxidative stress in liver of rhesus monkeys.* Exp Gerontol, 2012. **47**(1): p. 29-37.
186. Chacko, B.K., et al., *The Bioenergetic Health Index: a new concept in mitochondrial translational research.* Clin Sci (Lond), 2014. **127**(6): p. 367-73.
187. Lesnefsky, E.J., et al., *Mitochondrial dysfunction in cardiac disease: ischemia--reperfusion, aging, and heart failure.* J Mol Cell Cardiol, 2001. **33**(6): p. 1065-89.
188. Dauer, W. and S. Przedborski, *Parkinson's disease: mechanisms and models.* Neuron, 2003. **39**(6): p. 889-909.
189. Xiong, N., et al., *Mitochondrial complex I inhibitor rotenone-induced toxicity and its potential mechanisms in Parkinson's disease models.* Crit Rev Toxicol, 2012. **42**(7): p. 613-32.
190. Fukuda, T., *Neurotoxicity of MPTP.* Neuropathology, 2001. **21**(4): p. 323-32.

191. Drechsel, D.A. and M. Patel, *Differential contribution of the mitochondrial respiratory chain complexes to reactive oxygen species production by redox cycling agents implicated in parkinsonism.* Toxicol Sci, 2009. **112**(2): p. 427-34.

192. Volpicelli-Daley, L.A., K.C. Luk, and V.M. Lee, *Addition of exogenous alpha-synuclein preformed fibrils to primary neuronal cultures to seed recruitment of endogenous alpha-synuclein to Lewy body and Lewy neurite-like aggregates.* Nat Protoc, 2014. **9**(9): p. 2135-46.

193. Volpicelli-Daley, L.A., et al., *Exogenous alpha-synuclein fibrils induce Lewy body pathology leading to synaptic dysfunction and neuron death.* Neuron, 2011. **72**(1): p. 57-71.

194. Boyer-Guittaut, M., et al., *The role of GABARAPL1/GEC1 in autophagic flux and mitochondrial quality control in MDA-MB-436 breast cancer cells.* Autophagy, 2014. **10**(6): p. 986-1003.

195. Giordano, S., et al., *Bioenergetic adaptation in response to autophagy regulators during rotenone exposure.* J Neurochem, 2014.

196. Knight-Lozano, C.A., et al., *Cigarette smoke exposure and hypercholesterolemia increase mitochondrial damage in cardiovascular tissues.* Circulation, 2002. **105**(7): p. 849-54.

197. Redmann, M., et al., *Inhibition of autophagy with bafilomycin and chloroquine decreases mitochondrial quality and bioenergetic function in primary neurons.* Redox Biol, 2016. **11**: p. 73-81.

198. Salabei, J.K., A.A. Gibb, and B.G. Hill, *Comprehensive measurement of respiratory activity in permeabilized cells using extracellular flux analysis.* Nat Protoc, 2014. **9**(2): p. 421-38.

199. Dranka, B.P., et al., *Assessing bioenergetic function in response to oxidative stress by metabolic profiling.* Free Radic Biol Med, 2011. **51**(9): p. 1621-35.

200. Dodson, M., V. Darley-Usmar, and J. Zhang, *Cellular metabolic and autophagic pathways: traffic control by redox signaling.* Free Radic Biol Med, 2013. **63**: p. 207-21.

201. Yorimitsu, T. and D.J. Klionsky, *Autophagy: molecular machinery for self-eating.* Cell Death Differ, 2005. **12 Suppl 2**: p. 1542-52.

202. Slater, A.F. and A. Cerami, *Inhibition by chloroquine of a novel haem polymerase enzyme activity in malaria trophozoites.* Nature, 1992. **355**(6356): p. 167-9.

203. Trape, J.F., et al., *Impact of chloroquine resistance on malaria mortality.* C R Acad Sci III, 1998. **321**(8): p. 689-97.

204. Kimura, T., et al., *Chloroquine in cancer therapy: a double-edged sword of autophagy.* Cancer Res, 2013. **73**(1): p. 3-7.

205. Hook, G., et al., *Cathepsin B is a New Drug Target for Traumatic Brain Injury Therapeutics: Evidence for E64d as a Promising Lead Drug Candidate.* Front Neurol, 2015. **6**: p. 178.

206. Hook, G., et al., *Brain pyroglutamate amyloid-beta is produced by cathepsin B and is reduced by the cysteine protease inhibitor E64d, representing a potential Alzheimer's disease therapeutic.* J Alzheimers Dis, 2014. **41**(1): p. 129-49.

207. Klionsky, D.J., et al., *Guidelines for the use and interpretation of assays for monitoring autophagy.* Autophagy, 2012. **8**(4): p. 445-544.

208. Wu, J.J., et al., *Mitochondrial dysfunction and oxidative stress mediate the physiological impairment induced by the disruption of autophagy.* Aging (Albany NY), 2009. **1**(4): p. 425-37.

209. Bowman, E.J., A. Siebers, and K. Altendorf, *Bafilomycins: a class of inhibitors of membrane ATPases from microorganisms, animal cells, and plant cells.* Proc Natl Acad Sci U S A, 1988. **85**(21): p. 7972-6.

210. Werner, G., et al., *Metabolic products of microorganisms. 224. Bafilomycins, a new group of macrolide antibiotics. Production, isolation, chemical structure and biological activity.* J Antibiot (Tokyo), 1984. **37**(2): p. 110-7.

211. Yoshimori, T., et al., *Bafilomycin A1, a specific inhibitor of vacuolar-type H(+)-ATPase, inhibits acidification and protein degradation in lysosomes of cultured cells.* J Biol Chem, 1991. **266**(26): p. 17707-12.

212. Yamamoto, A., et al., *Bafilomycin A1 prevents maturation of autophagic vacuoles by inhibiting fusion between autophagosomes and lysosomes in rat hepatoma cell line, H-4-II-E cells.* Cell Struct Funct, 1998. **23**(1): p. 33-42.

213. Klionsky, D.J., et al., *Does bafilomycin A1 block the fusion of autophagosomes with lysosomes?* Autophagy, 2008. **4**(7): p. 849-50.

214. Teplova, V.V., et al., *Bafilomycin A1 is a potassium ionophore that impairs mitochondrial functions.* J Bioenerg Biomembr, 2007. **39**(4): p. 321-9.

215. Zhdanov, A.V., R.I. Dmitriev, and D.B. Papkovsky, *Bafilomycin A1 activates respiration of neuronal cells via uncoupling associated with flickering depolarization of mitochondria.* Cell Mol Life Sci, 2011. **68**(5): p. 903-17.

216. Ochiai, H., et al., *Inhibitory effect of bafilomycin A1, a specific inhibitor of vacuolar-type proton pump, on the growth of influenza A and B viruses in MDCK cells.* Antiviral Res, 1995. **27**(4): p. 425-30.

217. Yeganeh, B., et al., *Suppression of influenza A virus replication in human lung epithelial cells by noncytotoxic concentrations bafilomycin A1.* Am J Physiol Lung Cell Mol Physiol, 2015. **308**(3): p. L270-86.

218. Hernandez-Breijo, B., et al., *Azathioprine desensitizes liver cancer cells to insulin-like growth factor 1 and causes apoptosis when it is combined with bafilomycin A1.* Toxicol Appl Pharmacol, 2013. **272**(3): p. 568-78.

219. Ohta, T., et al., *Bafilomycin A1 induces apoptosis in the human pancreatic cancer cell line Capan-1.* J Pathol, 1998. **185**(3): p. 324-30.

220. Lim, J.H., et al., *Bafilomycin induces the p21-mediated growth inhibition of cancer cells under hypoxic conditions by expressing hypoxia-inducible factor-1alpha.* Mol Pharmacol, 2006. **70**(6): p. 1856-65.

221. Homewood, C.A., et al., *Lysosomes, pH and the anti-malarial action of chloroquine.* Nature, 1972. **235**(5332): p. 50-2.

222. Chaanine, A.H., et al., *High-dose chloroquine is metabolically cardiotoxic by inducing lysosomes and mitochondria dysfunction in a rat model of pressure overload hypertrophy.* Physiol Rep, 2015. **3**(7).

223. Zhang, J. and V. Darley-Usmar, *Mitochondrial Dysfunction in Neurodegenerative Disease: Protein Aggregation, Autophagy, and Oxidative Stress*, in *Mitochondrial Dysfunction in Neurodegenerative Disorders*, A.K. Reeve, et al., Editors. 2012, Springer London. p. 95-111.

224. Redmann, M., et al., *Mitophagy mechanisms and role in human diseases.* Int J Biochem Cell Biol, 2014. **53**: p. 127-33.

225. Hill, B.G., et al., *Integration of cellular bioenergetics with mitochondrial quality control and autophagy.* Biol Chem, 2012. **393**(12): p. 1485-1512.

226. Butow, R.A. and N.G. Avadhani, *Mitochondrial signaling: the retrograde response.* Mol Cell, 2004. **14**(1): p. 1-15.

227. Goldenthal, M.J. and J. Marin-Garcia, *Mitochondrial signaling pathways: a receiver/integrator organelle.* Mol Cell Biochem, 2004. **262**(1-2): p. 1-16.

228. Gupta, S., *Molecular signaling in death receptor and mitochondrial pathways of apoptosis (Review).* Int J Oncol, 2003. **22**(1): p. 15-20.

229. Fetterman, J.L., et al., *Developmental exposure to second-hand smoke increases adult atherogenesis and alters mitochondrial DNA copy number and deletions in apoE(-/-) mice.* PLoS One, 2013. **8**(6): p. e66835.

230. Schneider, C.A., W.S. Rasband, and K.W. Eliceiri, *NIH Image to ImageJ: 25 years of image analysis.* Nat Methods, 2012. **9**(7): p. 671-5.

231. Schapira, A.H. and M. Gegg, *Mitochondrial contribution to Parkinson's disease pathogenesis.* Parkinsons Dis, 2011. **2011**: p. 159160.

232. Smith, M.R., et al., *Mitochondrial thiol modification by a targeted electrophile inhibits metabolism in breast adenocarcinoma cells by inhibiting enzyme activity and protein levels.* Redox Biol, 2016. **8**: p. 136-48.

233. Mizushima, N. and T. Yoshimori, *How to interpret LC3 immunoblotting.* Autophagy, 2007. **3**(6): p. 542-5.

234. Kabeya, Y., et al., *LC3, a mammalian homologue of yeast Apg8p, is localized in autophagosome membranes after processing.* EMBO J, 2000. **19**(21): p. 5720-8.

235. Benavides, G.A., et al., *Inhibition of autophagy and glycolysis by nitric oxide during hypoxia-reoxygenation impairs cellular bioenergetics and promotes cell death in primary neurons.* Free Radic Biol Med, 2013. **65**: p. 1215-28.

236. Hjelmeland, A. and J. Zhang, *Metabolic, autophagic, and mitophagic activities in cancer initiation and progression.* Biomed J, 2016. **39**(2): p. 98-106.

237. Liang, Q., et al., *Bioenergetic and autophagic control by Sirt3 in response to nutrient deprivation in mouse embryonic fibroblasts.* Biochem J, 2013. **454**(2): p. 249-57.

238. Redmann, M., V. Darley-Usmar, and J. Zhang, *The Role of Autophagy, Mitophagy and Lysosomal Functions in Modulating Bioenergetics and Survival in the Context of Redox and Proteotoxic Damage: Implications for Neurodegenerative Diseases.* Aging Dis, 2016. **7**(2): p. 150-62.

239. Wang, Z., et al., *Gut flora metabolism of phosphatidylcholine promotes cardiovascular disease.* Nature, 2011. **472**(7341): p. 57-63.

240. Wang, Z., et al., *Targeted metabolomic evaluation of arginine methylation and cardiovascular risks: potential mechanisms beyond nitric oxide synthase inhibition.* Arterioscler Thromb Vasc Biol, 2009. **29**(9): p. 1383-91.

241. Chouchani, E.T., et al., *Ischaemic accumulation of succinate controls reperfusion injury through mitochondrial ROS.* Nature, 2014. **515**(7527): p. 431-5.

242. Damier, P., et al., *The substantia nigra of the human brain. II. Patterns of loss of dopamine-containing neurons in Parkinson's disease.* Brain, 1999. **122 (Pt 8)**: p. 1437-48.

243. Baba, M., et al., *Aggregation of alpha-synuclein in Lewy bodies of sporadic Parkinson's disease and dementia with Lewy bodies.* Am J Pathol, 1998. **152**(4): p. 879-84.

244. Spillantini, M.G., et al., *Filamentous alpha-synuclein inclusions link multiple system atrophy with Parkinson's disease and dementia with Lewy bodies.* Neurosci Lett, 1998. **251**(3): p. 205-8.

245. Lee, H.J., et al., *Autophagic failure promotes the exocytosis and intercellular transfer of alpha-synuclein.* Exp Mol Med, 2013. **45**: p. e22.

246. Luk, K.C., et al., *Pathological alpha-synuclein transmission initiates Parkinson-like neurodegeneration in nontransgenic mice.* Science, 2012. **338**(6109): p. 949-53.

247. Cuervo, A.M., et al., *Autophagy and aging: the importance of maintaining "clean" cells.* Autophagy, 2005. **1**(3): p. 131-40.

248. Hochfeld, W.E., S. Lee, and D.C. Rubinsztein, *Therapeutic induction of autophagy to modulate neurodegenerative disease progression.* Acta Pharmacol Sin, 2013. **34**(5): p. 600-4.

249. Stallone, G., et al., *Management of side effects of sirolimus therapy.* Transplantation, 2009. **87**(8 Suppl): p. S23-6.

250. Lan, D.M., et al., *Effect of trehalose on PC12 cells overexpressing wild-type or A53T mutant alpha-synuclein.* Neurochem Res, 2012. **37**(9): p. 2025-32.

251. Dehay, B., et al., *Pathogenic lysosomal depletion in Parkinson's disease.* J Neurosci, 2010. **30**(37): p. 12535-44.

252. Settembre, C., et al., *TFEB links autophagy to lysosomal biogenesis.* Science, 2011. **332**(6036): p. 1429-33.

253. Sacktor, B., *Trehalase and the transport of glucose in the mammalian kidney and intestine.* Proc Natl Acad Sci U S A, 1968. **60**(3): p. 1007-14.

254. Richards, A.B., et al., *Trehalose: a review of properties, history of use and human tolerance, and results of multiple safety studies.* Food Chem Toxicol, 2002. **40**(7): p. 871-98.

255. Rodriguez-Navarro, J.A., et al., *Trehalose ameliorates dopaminergic and tau pathology in parkin deleted/tau overexpressing mice through autophagy activation.* Neurobiol Dis, 2010. **39**(3): p. 423-38.

256. Castillo, K., et al., *Trehalose delays the progression of amyotrophic lateral sclerosis by enhancing autophagy in motoneurons.* Autophagy, 2013. **9**(9): p. 1308-20.

257. Tanaka, M., et al., *Trehalose alleviates polyglutamine-mediated pathology in a mouse model of Huntington disease.* Nat Med, 2004. **10**(2): p. 148-54.

258. Liu, R., et al., *Trehalose differentially inhibits aggregation and neurotoxicity of beta-amyloid 40 and 42.* Neurobiol Dis, 2005. **20**(1): p. 74-81.

259. Qiao, L., et al., *Lysosomal enzyme cathepsin D protects against alpha-synuclein aggregation and toxicity.* Mol Brain, 2008. **1**: p. 17.

260. Shacka, J.J., et al., *Cathepsin D deficiency induces persistent neurodegeneration in the absence of Bax-dependent apoptosis.* J Neurosci, 2007. **27**(8): p. 2081-90.

261. Walls, K.C., et al., *Altered regulation of phosphatidylinositol 3-kinase signaling in cathepsin D-deficient brain.* Autophagy, 2007. **3**(3): p. 222-9.

262. Kruger, U., et al., *Autophagic degradation of tau in primary neurons and its enhancement by trehalose.* Neurobiol Aging, 2012. **33**(10): p. 2291-305.

263. Davies, J.E., S. Sarkar, and D.C. Rubinsztein, *Trehalose reduces aggregate formation and delays pathology in a transgenic mouse model of oculopharyngeal muscular dystrophy.* Hum Mol Genet, 2006. **15**(1): p. 23-31.

264. Yu, W.B., et al., *Trehalose inhibits fibrillation of A53T mutant alpha-synuclein and disaggregates existing fibrils.* Arch Biochem Biophys, 2012. **523**(2): p. 144-50.

265. Tapia, H. and D.E. Koshland, *Trehalose is a versatile and long-lived chaperone for desiccation tolerance.* Curr Biol, 2014. **24**(23): p. 2758-66.

266. Viner, R.I. and J.S. Clegg, *Influence of trehalose on the molecular chaperone activity of p26, a small heat shock/alpha-crystallin protein.* Cell Stress Chaperones, 2001. **6**(2): p. 126-35.

267. He, Q., et al., *Treatment with Trehalose Prevents Behavioral and Neurochemical Deficits Produced in an AAV alpha-Synuclein Rat Model of Parkinson's Disease.* Mol Neurobiol, 2016. **53**(4): p. 2258-68.

268. Parker, W.D., Jr., J.K. Parks, and R.H. Swerdlow, *Complex I deficiency in Parkinson's disease frontal cortex.* Brain Res, 2008. **1189**: p. 215-8.

269. Keeney, P.M., et al., *Parkinson's disease brain mitochondrial complex I has oxidatively damaged subunits and is functionally impaired and misassembled.* J Neurosci, 2006. **26**(19): p. 5256-64.

270. Malkus, K.A., E. Tsika, and H. Ischiropoulos, *Oxidative modifications, mitochondrial dysfunction, and impaired protein degradation in Parkinson's disease: how neurons are lost in the Bermuda triangle.* Mol Neurodegener, 2009. **4**: p. 24.

271. Schapira, A.H., *Mitochondria in the aetiology and pathogenesis of Parkinson's disease.* Lancet Neurol, 2008. **7**(1): p. 97-109.

272. Muller, W.E., et al., *Mitochondrial dysfunction: common final pathway in brain aging and Alzheimer's disease--therapeutic aspects.* Mol Neurobiol, 2010. **41**(2-3): p. 159-71.

273. Querfurth, H.W. and F.M. LaFerla, *Alzheimer's disease.* N Engl J Med, 2010. **362**(4): p. 329-44.

274. Santos, R.X., et al., *A synergistic dysfunction of mitochondrial fission/fusion dynamics and mitophagy in Alzheimer's disease.* J Alzheimers Dis, 2010. **20 Suppl 2**: p. S401-12.

275. Hauptmann, S., et al., *Mitochondrial dysfunction: an early event in Alzheimer pathology accumulates with age in AD transgenic mice.* Neurobiol Aging, 2009. **30**(10): p. 1574-86.

276. Crouch, P.J., et al., *Mitochondria in aging and Alzheimer's disease.* Rejuvenation Res, 2007. **10**(3): p. 349-57.

277. Moreira, P.I., M.S. Santos, and C.R. Oliveira, *Alzheimer's disease: a lesson from mitochondrial dysfunction.* Antioxid Redox Signal, 2007. **9**(10): p. 1621-30.

278. Jolly, R.D., et al., *Mitochondrial dysfunction in the neuronal ceroid-lipofuscinoses (Batten disease).* Neurochem Int, 2002. **40**(6): p. 565-71.

279. Priyadarshi, A., et al., *Environmental risk factors and Parkinson's disease: a metaanalysis.* Environ Res, 2001. **86**(2): p. 122-7.

280. Priyadarshi, A., et al., *A meta-analysis of Parkinson's disease and exposure to pesticides.* Neurotoxicology, 2000. **21**(4): p. 435-40.

281. van der Mark, M., et al., *Is pesticide use related to Parkinson disease? Some clues to heterogeneity in study results.* Environ Health Perspect, 2012. **120**(3): p. 340-7.

282. Hsu, L.J., et al., *alpha-synuclein promotes mitochondrial deficit and oxidative stress.* Am J Pathol, 2000. **157**(2): p. 401-10.

283. Martin, L.J., et al., *Parkinson's disease alpha-synuclein transgenic mice develop neuronal mitochondrial degeneration and cell death.* J Neurosci, 2006. **26**(1): p. 41-50.

284. Lin, X., et al., *Leucine-rich repeat kinase 2 regulates the progression of neuropathology induced by Parkinson's-disease-related mutant alpha-synuclein.* Neuron, 2009. **64**(6): p. 807-27.

285. Liu, G., et al., *alpha-Synuclein is differentially expressed in mitochondria from different rat brain regions and dose-dependently down-regulates complex I activity.* Neurosci Lett, 2009. **454**(3): p. 187-92.

286. Zhu, Y., et al., *alpha-Synuclein overexpression impairs mitochondrial function by associating with adenylate translocator.* Int J Biochem Cell Biol, 2011. **43**(5): p. 732-41.

287. Nakamura, K., et al., *Direct membrane association drives mitochondrial fission by the Parkinson disease-associated protein alpha-synuclein.* J Biol Chem, 2011. **286**(23): p. 20710-26.

288. Sarafian, T.A., et al., *Impairment of mitochondria in adult mouse brain overexpressing predominantly full-length, N-terminally acetylated human alpha-synuclein.* PLoS One, 2013. **8**(5): p. e63557.

289. Marella, M., et al., *Protection by the NDI1 gene against neurodegeneration in a rotenone rat model of Parkinson's disease.* PLoS One, 2008. **3**(1): p. e1433.

290. Tieu, K., et al., *D-beta-hydroxybutyrate rescues mitochondrial respiration and mitigates features of Parkinson disease.* J Clin Invest, 2003. **112**(6): p. 892-901.

291. Reeves, M.B., et al., *Complex I binding by a virally encoded RNA regulates mitochondria-induced cell death.* Science, 2007. **316**(5829): p. 1345-8.

292. Storch, A., et al., *Randomized, double-blind, placebo-controlled trial on symptomatic effects of coenzyme Q(10) in Parkinson disease.* Arch Neurol, 2007. **64**(7): p. 938-44.

293. Mejias, R., et al., *Neuroprotection by transgenic expression of glucose-6-phosphate dehydrogenase in dopaminergic nigrostriatal neurons of mice.* J Neurosci, 2006. **26**(17): p. 4500-8.

294. Ebadi, M., et al., *Metallothionein-mediated neuroprotection in genetically engineered mouse models of Parkinson's disease.* Brain Res Mol Brain Res, 2005. **134**(1): p. 67-75.

295. Yacoubian, T.A. and D.G. Standaert, *Targets for neuroprotection in Parkinson's disease.* Biochim Biophys Acta, 2009. **1792**(7): p. 676-87.

296. Mortiboys, H., et al., *Mitochondrial function and morphology are impaired in parkin-mutant fibroblasts.* Ann Neurol, 2008. **64**(5): p. 555-65.

297. Betarbet, R., et al., *Chronic systemic pesticide exposure reproduces features of Parkinson's disease.* Nat Neurosci, 2000. **3**(12): p. 1301-6.

298. Inden, M., et al., *Parkinsonian rotenone mouse model: reevaluation of long-term administration of rotenone in C57BL/6 mice.* Biol Pharm Bull, 2011. **34**(1): p. 92-6.

299. Chepelev, N.L., et al., *Oxidative modification of citrate synthase by peroxyl radicals and protection with novel antioxidants.* J Enzyme Inhib Med Chem, 2009. **24**(6): p. 1319-31.

300. Yan, L.J., R.L. Levine, and R.S. Sohal, *Oxidative damage during aging targets mitochondrial aconitase.* Proc Natl Acad Sci U S A, 1997. **94**(21): p. 11168-72.

301. Banaclocha, M.M., *Therapeutic potential of N-acetylcysteine in age-related mitochondrial neurodegenerative diseases.* Med Hypotheses, 2001. **56**(4): p. 472-7.

302. Parkinson Study, G., *Effects of tocopherol and deprenyl on the progression of disability in early Parkinson's disease.* N Engl J Med, 1993. **328**(3): p. 176-83.

303. Siintola, E., et al., *Cathepsin D deficiency underlies congenital human neuronal ceroid-lipofuscinosis.* Brain, 2006. **129**(Pt 6): p. 1438-45.

304. Saftig, P., et al., *Mice deficient for the lysosomal proteinase cathepsin D exhibit progressive atrophy of the intestinal mucosa and profound destruction of lymphoid cells.* EMBO J, 1995. **14**(15): p. 3599-608.

305. Cullen, V., et al., *Cathepsin D expression level affects alpha-synuclein processing, aggregation, and toxicity in vivo.* Mol Brain, 2009. **2**: p. 5.

306. Sevlever, D., P. Jiang, and S.H. Yen, *Cathepsin D is the main lysosomal enzyme involved in the degradation of alpha-synuclein and generation of its carboxy-terminally truncated species.* Biochemistry, 2008. **47**(36): p. 9678-87.

307. Crabtree, D., et al., *Over-expression of an inactive mutant cathepsin D increases endogenous alpha-synuclein and cathepsin B activity in SH-SY5Y cells.* J Neurochem, 2014. **128**(6): p. 950-61.

308. Liang, Q., et al., *Reduction of mutant huntingtin accumulation and toxicity by lysosomal cathepsins D and B in neurons.* Mol Neurodegener, 2011. **6**: p. 37.

309. Rouschop, K.M., et al., *Autophagy is required during cycling hypoxia to lower production of reactive oxygen species.* Radiother Oncol, 2009. **92**(3): p. 411-6.

310. Park, B.C., et al., *Chloroquine-induced nitric oxide increase and cell death is dependent on cellular GSH depletion in A172 human glioblastoma cells.* Toxicol Lett, 2008. **178**(1): p. 52-60.

311. Farombi, E.O., *Genotoxicity of chloroquine in rat liver cells: protective role of free radical scavengers.* Cell Biol Toxicol, 2006. **22**(3): p. 159-67.

312. Park, J., et al., *Reactive oxygen species mediate chloroquine-induced expression of chemokines by human astroglial cells.* Glia, 2004. **47**(1): p. 9-20.

313. Yamasaki, R., et al., *Involvement of lysosomal storage-induced p38 MAP kinase activation in the overproduction of nitric oxide by microglia in cathepsin D-deficient mice.* Mol Cell Neurosci, 2007. **35**(4): p. 573-84.

314. Desplats, P., et al., *Inclusion formation and neuronal cell death through neuron-to-neuron transmission of alpha-synuclein.* Proc Natl Acad Sci U S A, 2009. **106**(31): p. 13010-5.

315. Emmanouilidou, E., et al., *Cell-produced alpha-synuclein is secreted in a calcium-dependent manner by exosomes and impacts neuronal survival.* J Neurosci, 2010. **30**(20): p. 6838-51.

316. Decressac, M., et al., *TFEB-mediated autophagy rescues midbrain dopamine neurons from alpha-synuclein toxicity.* Proc Natl Acad Sci U S A, 2013. **110**(19): p. E1817-26.

317. Kilpatrick, K., et al., *Genetic and chemical activation of TFEB mediates clearance of aggregated alpha-synuclein.* PLoS One, 2015. **10**(3): p. e0120819.

318. Perucho, J., et al., *Trehalose protects from aggravation of amyloid pathology induced by isoflurane anesthesia in APP(swe) mutant mice.* Curr Alzheimer Res, 2012. **9**(3): p. 334-43.

319. Du, J., et al., *Trehalose rescues Alzheimer's disease phenotypes in APP/PS1 transgenic mice.* J Pharm Pharmacol, 2013. **65**(12): p. 1753-6.

320. Ding, K., et al., *Rapamycin protects against apoptotic neuronal death and improves neurologic function after traumatic brain injury in mice via modulation of the mTOR-p53-Bax axis.* J Surg Res, 2015. **194**(1): p. 239-47.

321. Liu, K., et al., *Therapeutic effects of rapamycin on MPTP-induced Parkinsonism in mice.* Neurochem Res, 2013. **38**(1): p. 201-7.

322. Jo, E., et al., *alpha-Synuclein-synaptosomal membrane interactions: implications for fibrillogenesis.* Eur J Biochem, 2004. **271**(15): p. 3180-9.

323. Jao, C.C., et al., *Structure of membrane-bound alpha-synuclein from site-directed spin labeling and computational refinement.* Proc Natl Acad Sci U S A, 2008. **105**(50): p. 19666-71.

324. Nath, S., et al., *Lipidation of the LC3/GABARAP family of autophagy proteins relies on a membrane-curvature-sensing domain in Atg3.* Nat Cell Biol, 2014. **16**(5): p. 415-24.

325. Burre, J., et al., *Alpha-synuclein promotes SNARE-complex assembly in vivo and in vitro.* Science, 2010. **329**(5999): p. 1663-7.

326. Freeman, D., et al., *Alpha-synuclein induces lysosomal rupture and cathepsin dependent reactive oxygen species following endocytosis.* PLoS One, 2013. **8**(4): p. e62143.

327. Kawai, A., et al., *Autophagosome-lysosome fusion depends on the pH in acidic compartments in CHO cells.* Autophagy, 2007. **3**(2): p. 154-7.

328. Boland, B., et al., *Autophagy induction and autophagosome clearance in neurons: relationship to autophagic pathology in Alzheimer's disease.* J Neurosci, 2008. **28**(27): p. 6926-37.

APPENDEX A

IACUC APPROVAL FORMS

UAB THE UNIVERSITY OF ALABAMA AT BIRMINGHAM
Institutional Animal Care and Use Committee (IACUC)

MEMORANDUM

DATE: 15-Feb-2016

TO: Zhang, Jianhua

FROM: *[signature]*

Robert A. Kesterson, Ph.D., Chair

Institutional Animal Care and Use Committee (IACUC)

SUBJECT: **NOTICE OF APPROVAL**

The following application was approved by the University of Alabama at Birmingham Institutional Animal Care and Use Committee (IACUC) on 15-Feb-2016.

Protocol PI: Zhang, Jianhua

Title: Alpha-Synuclein Degradation Mechanisms

Sponsor: National Institute of Neurological Disorders and Stroke/NIH/DHHS

Animal Project Number (APN): IACUC-09019

This institution has an Animal Welfare Assurance on file with the Office of Laboratory Animal Welfare (OLAW), is registered as a Research Facility with the USDA, and is accredited by the Association for Assessment and Accreditation of Laboratory Animal Care International (AAALAC).

Institutional Animal Care and Use Committee (IACUC)		Mailing Address:
CH19 Suite 403	|	CH19 Suite 403
933 19th Street South	|	1530 3rd Ave S
(205) 934-7692	|	Birmingham, AL 35294-0019
FAX (205) 934-1188	|	

UAB THE UNIVERSITY OF ALABAMA AT BIRMINGHAM
Institutional Animal Care and Use Committee (IACUC)

MEMORANDUM

DATE: 10-May-2016

TO: Zhang, Jianhua

FROM:

Robert A. Kesterson, Ph.D., Chair

Institutional Animal Care and Use Committee (IACUC)

SUBJECT: **NOTICE OF APPROVAL**

The following application was approved by the University of Alabama at Birmingham Institutional Animal Care and Use Committee (IACUC) on 10-May-2016.

Protocol PI: Zhang, Jianhua

Title: Validation of Cathepsins as Targets for Huntington's Disease Therapy

Sponsor: UAB DEPARTMENT

Animal Project Number (APN): IACUC-08786

This institution has an Animal Welfare Assurance on file with the Office of Laboratory Animal Welfare (OLAW), is registered as a Research Facility with the USDA, and is accredited by the Association for Assessment and Accreditation of Laboratory Animal Care International (AAALAC).

Institutional Animal Care and Use Committee (IACUC) | Mailing Address:
CH19 Suite 403 | CH19 Suite 403
933 19th Street South | 1530 3rd Ave S
(205) 934-7692 | Birmingham, AL 35294-0019
FAX (205) 934-1188 |

146